Cellular functions of VASP phosphorylations

Dissertation zur Erlangung des

naturwissenschaftlichen Doktorgrades

der Bayerischen Julius-Maximilians-Universität Würzburg

vorgelegt von

Constanze Blume

aus Leipzig

Würzburg 2009

Eingereicht am: ....

Mitglieder der Promotionskommission:

Vorsitzender: ....

Gutachter: Prof. Dr. Dr. Thomas Renné

Gutachter: Prof. Dr. Dr. h.c. Roland Benz

Tag des Promotionskolloquiums: ....

Doktorurkunde ausgehändigt am: ....

The present study was performed under the supervision of Prof. Dr. Dr. Thomas Renné in the Juniorgroup of the SFB355 at the Institut of Clinical Biochemistry and Pathobio-chemistry (Director: Prof. Dr. Ulrich Walter), Julius-Maximilians-University of Würzburg.

Erklärung gemäß § 4 Abs. 3 Promotionsordnung:

Hiermit erkläre ich ehrenwörtlich, dass ich die vorliegende Arbeit selbständig angefertigt und keine anderen als die angegebenen Quellen und Hilfsmittel benutzt habe.

Die Dissertation hat weder in gleicher noch in ähnlicher Form in einem anderen Prüfungs-verfahren vorgelegen.

Ich habe bisher außer den mit dem Zulassungsgesuch urkundlich vorgelegten Graden keine weiteren akademischen Grade erworben oder zu erwerben versucht.

Würzburg, den

(Constanze Blume)

TABLE OF CONTENTS

1 Summary

Members of the enabled/vasodilator-stimulated phosphoprotein (Ena/VASP) family are important regulators of the actin cytoskeleton dynamics. VASP functions as well as its interactions with other proteins are regulated by phosphorylation at three sites - serine157 (S157), serine239 (S239), and threonine278 (T278) in humans. cAMP- and cGMP-dependent protein kinases phosphorylate S157 and S239, respectively. In contrast, the kinase responsible for T278 was as yet unknown and identified in the first part of this thesis. In a screen for T278 phosphorylating kinases using a phospho-specific antibody against phosphorylated T278 AMP-activated protein kinase (AMPK) was identified in endothelial cells. Mutants of AMPK with altered kinase-activity modulate T278-phosphorylation levels in cells. AMPK-driven T278-phosphorylation impaired stress fiber formation and changed cell morphology in living cells. AMPK is a fundamental sensor of cellular and whole body energy homeostasis. Zucker Diabetic Fatty (ZDF) rats, which are an animal model for type II diabetes mellitus, were used to analyze the impact of phosphorylated T278 *in vivo*. AMPK-activity and T278-phosphorylation were substantially reduced in arterial vessel walls of ZDF rats in comparison to control animals. These findings demonstrate that VASP is a new AMPK substrate, that VASP phosphorylation mediates the effects of metabolic regulation on actin cytoskeleton rearrangements, and that this signaling system becomes down-regulated in diabetic vessel disorders in rats.

In the second part of this thesis, a functional analysis of differential VASP phosphorylations was performed. To systematically address VASP phosphorylation patterns, a set of VASP phosphomimetic mutants was cloned. These mutants enable the mimicking of defined phosphorylation patterns and the specific analysis of single kinase-mediated phosphorylations. VASP localization to the cell periphery was increased by S157-phosphorylation and modulated by phosphorylation at S239 and T278. Latter phosphorylations synergistically reduced actin polymerization. In contrast, S157-phosphorylation had no effect on actin-dynamics. Taken together, the results of the second part show that phosphorylation of VASP serves as a fine regulator of localization and actin polymerization activity.

In summary, this study revealed the functions of VASP phosphorylations and established novel links between signaling pathways and actin cytoskeleton rearrangement.

2 Zusammenfassung

Die Mitglieder der Enabled/Vasodilator-stimulated phosphoprotein (Ena/VASP) Familie sind bedeutende Regulatoren der Aktinzytoskelettdynamik. Die Funktionen und die Protein-Protein-Wechselwirkungen von VASP werden durch Phosphorylierungen an drei Aminosäureresten reguliert. Im Fall von humanem VASP sind dies Serin157 (S157), Serin239 (S239) und Threonin278 (T278). S157 und S239 sind Substrate der cAMP- und cGMP-abhängigen Proteinkinasen. Die Kinase, die T278-Phosphorylierung vermittelt, ist nicht bekannt.

Der erste Teil der Arbeit beschäftigt sich mit der Identifizierung der T278-phosphorylierenden Kinase. Mit Hilfe eines phospho-spezifischen Antikörpers gegen das phosphorylierte T278 (pT278) wurde in Endothelzellen eine systematischen Suche nach T278-phosphorylierenden Kinasen durchgeführt. Dabei wurde die AMP-aktivierte Proteinkinase (AMPK) entdeckt. Mutanten der AMPK, welche eine veränderte Kinaseaktivität besitzen, erhöhten bzw. reduzierenten das Niveau der pT278. Die T278-Phosphorylierung durch die AMPK reduzierte die Stressfaserbildung und führt zu einer veränderten Zellmorphologie. Die AMPK ist ein fundamentaler Sensor des zellulären und Organismus-umfassenden Energiehaushalts. Zur Analyse der Funktion der pT278 *in vivo* wurden Zucker Diabetic Fatty (ZDF) Ratten, ein Tiermodell für den Diabetes mellitus Typ II, verwendet. Die AMPK-Aktivität und die pT278 waren in arteriellen Gefäßwänden von ZDF-Ratten im Vergleich zu Kontrolltieren deutlich reduziert. Diese Ergebnisse zeigen, dass VASP ein neues Substrat der AMPK ist, dass die T278-Phosphorylierung metabolische Signale an das Aktin-Zytoskelett koppelt und, dass bei diabetischen Ratten dieser Signaltransduktionsweg supprimiert ist.

Im zweiten Teil wurde die Bedeutung der VASP-Phosphorylierungsmuster für die Aktin-bildung und die VASP-Lokalisation untersucht. Hierzu wurden systematisch VASP-Phoshorylierungsmutanten generiert. Diese Mutanten imitieren fixierte Phosphorylierungen oder erlauben einzelne Phosphorylierungen durch die jeweilige Kinase. Die Untersuchungen zeigten, dass S157-phosphoryliertes VASP (pS157) sich an der Zellperipherie anreichert, wobei die S239- und T278-Phosphorylierungen diesen Lokalisationseffekt modulieren. Phosphoryliertes S239 und T278 reduzierten synergistisch die Aktinpolymerisation. Im Gegensatz hierzu beeinflusste pS157 die Aktindynamik nicht. Dies zeigt, dass die VASP-Phosphorylierungen als Feinregulator für die Lokalisation und die Aktinpolymerisationsaktivität fungierten.

Zusammenfassend identifiziert diese Studie die Funktionen der einzelnen VASP-Phosphorylierungen und deckt neue Verbindungen von Signalwegen zur Aktinzytoskelett-Reorganisation auf.

3 Introduction

3.1 Actin cytoskeleton

The actin cytoskeleton is essential for the generation and maintenance of cell morphology and polarity, for endocytosis and intercellular trafficking, for contractility, motility, and cell division (Winder and Ayscough, 2005; Gourlay and Ayscough, 2005). Actin filaments together with microtubules and intermediate filaments, are the three types of filaments, which together form the cytoskeleton that extends from the plasma membrane to the nuclear envelope, and even to the interior of the nucleus in all eukaryotic cells (Lodish *et al*., 2000; Ramaekers and Bosman, 2004). The actin cytoskeleton consists of a network of actin filaments. The dynamics of the actin cytoskeleton are determined by the assembly of actin filaments, via nucleation and polymerization, or by the disassembling of existing filaments. All these processes are tightly regulated by a plethora of actin-binding proteins (Winder and Ayscough, 2005).

3.1.1 Actin dynamics

Actin is the most abundant intracellular protein in eukaryotic cells (10% or 1-5% by weight of total cellular proteins of muscle or non-muscle cells, respectively). It exists in two forms: the globular, monomeric actin (G-actin) and the filamentous polymeric actin (F-actin) (Lodish *et al*., 2000). F-actin is a thin, flexible and helical actin homopolymer. The actin fiber is polarized, as characterized by a fast-growing (barbed) end and a slow-growing (pointed) end. Actin filaments extend when ATP-actin monomers are incorporated at the barbed end (Winder and Ayscough, 2005). Actin also displays ATPase activity. As the filament matures, ATP bound in the central cleft of actin is hydrolyzed, phosphate is released and the resulting ADP-actin filament is disassembled by loss of monomers from the pointed end. ADP-actin monomers are recycled by nucleotide exchange from ADP to ATP. The ATP-hydrolysis-driven, directional filament-growth is crucial in actin motility. Filaments are oriented in such a way that the growing barbed ends are near the plasma membrane, whereas the disassembling pointed ends face away from the cell periphery (Disanza *et al*., 2005). The assembly and disassembly of actin filaments and also the organization into functional higher order networks is regulated by a number of actin-binding proteins. These proteins promote a large number of processes, including nucleation, polymerization, capping, depolymerization, nucleotide exchange, branching, and bundling. The activities of

the actin-binding proteins are in turn under the control of specific signaling pathways, which allow the cell to respond to its environment (Winder and Ayscough, 2005).

3.2 Ena/VASP proteins

3.2.1 Domain structures of Ena/VASP proteins

The Ena/VASP protein family has been implicated in the regulation of actin-based motility, playing an important role in cell adhesion and migration, which are required for axon guidance (Dent *et al*., 2007; Bear *et al*., 2000; Gertler *et al*., 1996; Holt *et al*., 1998). In vertebrates, this family consists of three members: Mena (mammalian Enabled), VASP (vasodilator-stimulated phosphoprotein), and Evl (Ena-VASP-like). Another family member in Drosophila is Ena (Enabled) (for a review see Sechi and Wehland, 2004). All family members share a conserved domain structure comprised of an N-terminal Ena/VASP homology 1 (EVH1) domain, a central poly-proline region (PPR) and a C-terminal Ena/ VASP homology 2 (EVH2) domain (Fig. 1).
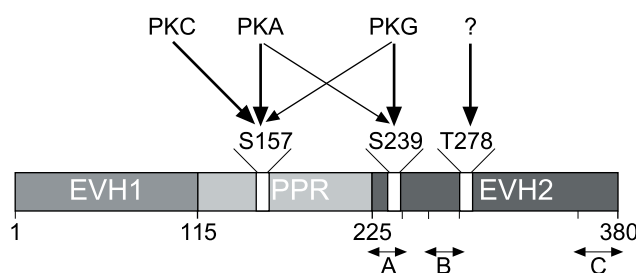
Figure 1: Schematic representation of the domain structure and phosphorylation sites of human VASP. VASP comprises a central poly-proline region (PPR) flanked by two Ena/VASP homology domains (EVH1, 2). Protein kinase C (PKC) and cAMP-dependent protein kinase (PKA) preferentially phosphorylate VASP at S157, which is located within the PPR. cGMP-dependent protein kinase (PKG) mediates phosphorylation at S239 within the A-Block of the EVH2 domain. The T278 phosphorylation site adjacent to the B-Block of the EVH2 domain and the kinase responsible for T278 phosphorylation is yet unknown.

The EVH1 domain (residue 1-115 in human VASP) serves as a binding site for proteins containing proline-rich motifs (FP$_5$) such as vinculin, zyxin, lamellipodin, and migfilin (Krause *et al*., 2003; Krause *et al*., 2004; Zhang *et al*., 2006). The central PPR (115-225) contains proline-rich stretches and interacts with the G-actin binding protein profilin (Reinhard *et al*., 1995), and with proteins that harbor SH3- or WW-domains, like the non-receptor Abelson tyrosine kinases (Abl; Howe *et al*., 2002) and the neuronal protein FE65 (Ermekova *et al*., 1997). The EVH2 domain (225-380) mediates tetramerization of Ena/VASP proteins and binds monomeric and filamentous actin. Functionally, the EHV2 domain is divided into three blocks: the A-block (225-245), harboring the KLRK-binding motif at residues 169-186 for G-actin binding (Walders-Harbeck *et al*., 2002), the B-block (259-276), containing the

binding motif for F-actin, and the C-block (343-377), responsible for tetramerization via coiled-coil structure-mediated interactions (Bachmann *et al*., 1999; Kuhnel *et al*., 2004).

3.2.2 Functions of Ena/VASP proteins

EVH1 domain-mediated interactions are important for subcellular localization and for Ena/ VASP recruitment to receptor/signaling complexes. Localization of Ena/VASP proteins at focal adhesions is attributed to interactions of the EVH1 domain with vinculin, zyxin, and migfilin (Hoffman *et al*., 2006; Zhang *et al*., 2006), whereas localization at the leading edge is associated with EVH1-binding to lamellipodin (Krause *et al*., 2004). Therefore, the EVH1 domain recruits Ena/VASP proteins to specific sites of high actin motility within the cell. Previous studies reported that in different cell lines (epithelial cells or fibroblasts) reduced interaction of Ena/VASP proteins with migfilin and zyxin impaired cell migration (Zhang *et al*., 2006; Drees *et al*., 1999), whereas diminished binding to lamellipodin reduced lamellipodia protrusion (Krause *et al*., 2003). The PPR of VASP contributes to filament elongation by recruiting profilin-actin complexes and directing the transition of profilin-actin to the EVH2 domain from where the actin monomer can join the growing filament (Ferron *et al*., 2007). The PPR-mediated recruiting of multiple actin-profilin complexes may serve to increase the local concentration of actin monomers, further promoting the F-actin elongation process (Reinhard *et al*., 1995; Chereau *et al*., 2006; Krause *et al*., 2003; Sechi and Wehland, 2004; Ferron *et al*., 2007). The Ena/VASP proteins modulate actin-based processes via EVH2 domain-mediated interactions. The EVH2 domain influences actin-polymerization and organization by binding to G- and F-actin, and by complex formation with other Ena/ VASP family members (Bachmann *et al*., 1999; Walders-Harbeck *et al*., 2002; Loureiro *et al*., 2002; Grosse *et al*., 2003).

Several studies investigated the effect of VASP on actin assembly and organization *in vitro* and revealed that VASP, or the isolated EVH2 domain induces bundling of actin filaments, and increases actin polymerization (Bachmann *et al*., 1999; Laurent *et al*., 1999; Huttelmaier *et al*., 1999). Barzik and co-workers demonstrated that VASP and the EVH2 domain have anti-capping activity by competition with capping proteins, which resulted in an increased actin-polymerization *in vitro* (Barzik *et al*., 2005). However, the anti-capping activity of VASP is still under discussion, since *Dictyostelium* VASP does not compete with capping proteins or block depolymerization *in vitro* (Schirenbeck *et al*., 2006). A later study demonstrated that anti-capping activity of VASP, which is reflected in enhanced actin-

polymerization, is due to an increased filament length and elongated time of polymerization *in vitro* (Pasic *et al*., 2008). It is likely that species-specific mechanisms give rise to anti-capping processes. The EVH2 domain of VASP captures free and growing barbed ends of actin filaments in preference to capped ends (Pasic *et al*., 2008). The bundling activity of VASP is required for filopodial formation in murine fibroblasts and *Dictyostelium* cells. Besides bundling activity, Ena/VASP proteins reduce branching of actin filaments *in vitro* (Skoble *et al*., 2001) and in living cells (Bear *et al*., 2002).

To date, the detailed molecular mechanism of how VASP promotes actin motility has yet to be elucidated. One reason for this is the considerable controversy concerning the effects of VASP as summarized by Trichet and co-workers (Trichet *et al*., 2008). Ena/VASP proteins are present at actin stress fibers and the tips of lamellipodia and filopodia. At these sites, where actin polymerization occurs, Ena/VASP promotes lamellipodial protrusion, filopodia formation, as well as filopodial protrusion (Rottner *et al*., 1999; Vitriol *et al*., 2007; Applewhite *et al*., 2007). Expression of VASP or the EVH2 domain increases F-actin assembly (Grosse *et al*., 2003) and filopodia formation (Applewhite *et al*., 2007). Mislocalization of VASP results in an increased actin polymerization (Fradelizi *et al*., 2001) and altered actin organization with respect to filament length and frequency of branching (Bear *et al*., 2002) at the artificially targeted site. All these EVH1-, PPR-, and EVH2-mediated protein-protein interactions, which are likely to be spatially and temporally defined, contribute to the regulation of the actin cytoskeleton via Ena/VASP proteins.

3.3 VASP phosphorylation

The functions of Ena/VASP proteins are regulated by phosphorylation of serine/threonine and tyrosine kinases (Sechi and Wehland, 2004). Recently, VASP was identified as a substrate of tyrosine kinases, but it remain unknow if this tyrosine phosphorylation has regulatory infuence on VASP functions (Rikova *et al*., 2007). Therefore this studies focuses on serine/theorine phosphorylation of VASP. All vertebrate Ena/VASP proteins are phosphorylated by serine/threonine kinases, at least at the conserved phosphorylation site adjacent to the PPR (corresponding to S157 in human VASP; Kwiatkowski *et al*., 2003). VASP was originally discovered in platelets as a substrate of cAMP- and cGMP-dependent protein kinases (PKA and PKG; Butt *et al*., 1994). In these early studies, VASP phosphorylation was induced by vasodilators such as prostaglandin E_1 and sodium nitroprusside. These substances raise intracellular cAMP and cGMP levels and inhibit platelet aggregation

(Horstrup *et al*., 1994). In a later study, protein kinase C (PKC) was found to phosphorylate VASP in vascular smooth muscle cells (Chitaley *et al*., 2004). Human VASP harbors three phosphorylation sites: serine157 (S157), serine239 (S239), and threonine278 (T278; Butt *et al*., 1994). PKA and PKC preferentially phosphorylate S157. S157-phosphorylated VASP (pS157) migrates with a higher apparent molecular weight in SDS-PAGE (50 kDa), while S157-unphosphorylated VASP migrates at 45 kDa. PKG predominantly phosphorylates S239. Phosphorylation at S239 (pS239) and T278 (pT278) does not alter VASP motility in SDS-PAGE. PKA and PKG have overlapping substrate specificities. Although PKA preferentially phosphorylates S157, the kinase also mediates S239 phosphorylation, but with lower preference (Fig. 1). PKG initially phosphorylates S239 and then S157. PKA and PKG may phosphorylate VASP at T278 to a small extent *in vitro* (Butt *et al*., 1994; Harbeck *et al*., 2000), but to date the significance of cyclic nucleotide-dependent protein kinase driven phosphorylation of T278 *in vivo* has not yet been demonstrated convincingly.

All three phosphorylation sites are located within the VASP sequence close to ligand-binding motifs such as GP_5 ligands and actins. The S157 phosphorylation site is situated within the PPR upstream of the $(GP_5)_3$-motif. In the EVH2 domain, S239 is adjacent to the G-actin binding motif and T278 flanks the F-actin binding residues (Bachmann *et al*., 1999; Walders-Harbeck *et al*., 2002; Chereau *et al*., 2006) (Fig. 1). Previous studies have shown that VASP functions are regulated by phosphorylation, but a systematic analysis of phosphorylation-dependent functions is lacking.

Phosphorylation at S157 affects a broad range of functions, for example, pS157 blocks VASP interaction with Abl (Howe *et al*., 2002). The dissociation of the VASP/Abl complex seems to play a role during cell detachment (Howe *et al*., 2002). In detached cells, PKA activity is high and S157 is phosphorylated, whereas S157 is not phosphorylated in the re-attachment phase (Howe *et al*., 2002). In addition, inhibition of platelet aggregation and integrin activation appears to correlate with PKA-mediated VASP phosphorylation (Horstrop *et al*., 1994). Different studies reported that stimulation of PKA or PKC leads to VASP phosphorylation at S157 and translocation to the cell periphery in endothelial cells, platelets, and prostate cancer cells (Comerford *et al*., 2002; Profirovic *et al*., 2005; Wentworth *et al*., 2006; Hasegawa *et al*., 2008). Whether VASP phosphorylation is required for this targeting process or whether phosphorylation occurs at the cell periphery is still a matter of debate. The interaction of VASP with the G-actin-binding protein profilin is not affected by S157 phosphorylation *in vitro* (Harbeck *et al*., 2000). S157 phosphorylation does not influence F-actin formation *in*

vitro (Barzik *et al*., 2005; Harbeck *et al*., 2000). In contrast to pS157, S239 phosphorylation negatively regulates actin polymerization, F-actin binding and anti-capping activity of VASP *in vitro* (Barzik *et al*., 2005; Harbeck *et al*., 2000). In living cells, the influence of pS239 on actin dynamics is still controversial: Zhuang and co-workers reported that pS239 interfered with actin assembly (Zhuang *et al*., 2004). In contrast, Grosse and co-workers reported that S239 phosphorylation did not alter actin-based processes (Grosse *et al*., 2003).

To identify the physiological relevance of VASP *in vivo*, two independent groups generated VASP-deficient mice (Hauser *et al*., 1999; Aszodi *et al*., 1999). In contrast to the embryo-lethal phenotype of Ena-deficient flies (*Drosophila melanogaster*), VASP gene deficient (VASP $^{-/-}$) mice showed a mild phenotype. VASP $^{-/-}$ mice are viable and fertile. Since VASP is involved in cyclic nucleotide signaling cascade processes, it was assumed that smooth muscle relaxation and platelet aggregation would be altered. However, intestinal and vascular smooth muscles of adult VASP $^{-/-}$ mice had normal agonist-induced contraction and normal cAMP- and cGMP-dependent relaxation (Aszodi *et al*., 1999). Animals showed a mild platelet dysfunction, e. g., cAMP- and cGMP-mediated inhibition of platelet aggregation was reduced. The explanation of the mild phenotype of VASP-deficient mice is likely to be due to compensation by other family members of the Ena/VASP family, such as Mena and Evl (Hauser *et al*., 1999; Aszodi *et al*., 1999). Notably, platelets predominantly express VASP, although stomach, intestine, spleen, lung, and blood vessels are also rich sources of VASP (Hauser *et al*., 1999; Gambaryan *et al*., 2001). The important role of VASP in platelets was reflected by increased platelet adhesion to vessel walls in VASP $^{-/-}$ mice, as compared to the wild-type controls (Massberg *et al*., 2004). Increased platelet adhesion appears to be due to the loss of VASP in endothelial and smooth muscle cells rather than due to the deficiency in platelets (Massberg *et al*., 2004).

The broad and overlapping expression patterns of Mena, Evl, and VASP require combined deletions to reveal their functions. Mice deficient in Mena and VASP die perinatally and display defects in neurulation, craniofacial structures, and in the formation of several fiber tracts in the central and the peripheral nervous system (Menzies *et al*., 2004). These neural defects were not exhibit in mice deficient in Mena or VASP alone, indicating the compensatory function of both genes for development of these structures. However, deletion of VASP enhances many Mena-dependent axon guidance phenotypes in the forebrain. Mice deficient in all Ena/VASP proteins were lethal at an early embryonic stage

due to a number of neuronal defects, including cobblestone cortex, exencephaly, and lack of cortical fiber tract formation (Kwiatkowski *et al.*, 2007). In addition, these mice displayed severe vascular defects, e.g. hemorrhagia and edema due to an impaired endothelial barrier function (Furman *et al.*, 2007). A single allele of Mena was sufficient to produce viable and fertile mice, albeit at a significantly reduced frequency. Interestingly, mice possessing one allele of Mena and one of VASP or Evl were viable, and showed no obvious defects in brain morphology. However, neither two alleles of VASP, nor two of Evl alone were sufficient for viability (Kwiatkowski *et al.*, 2007).

Since the nitric oxide (NO)/cGMP/PKG signaling pathway is critical in various vascular functions, VASP phosphorylation at S239 is used to monitor endothelial dysfunction in rats, rabbits, and in humans (Mulsch *et al.*, 2001; Oelze *et al.*, 2000; Schulz *et al.*, 2002). Endothelial dysfunction has been demonstrated in conditions of atherosclerosis, hypercholesterolemia, diabetes mellitus, hypertension, and nitrate tolerance. These studies show reduced pS239 in various vascular beds from several animal models of vascular dysfunction (Wistar rats, New Zealand White Rabbits and hyperlipidemic Watanabe rabbits) and patients with coronary arterial disease. Endothelial dysfunction is defined by impaired vascular relaxation due to reduced NO/cGMP/PKG signaling. Superoxides impair the NO/cGMP/PKG signaling pathway by the uncoupling of eNOS and the subsequent decrease in vascular bioavailability of NO (Munzel *et al.*, 2005; Munzel *et al.*, 2003).

3.4 AMP-activated protein kinase

The AMP-activated protein kinase (AMPK) is a major regulator of metabolism not only at the cellular, but also at the whole organism level (Carling, 2004; Kahn *et al.*, 2005). The evolutionary conserved AMPK is an ubiquitously expressed serine/threonine kinase. AMPK is a heterotrimeric complex composed of a catalytic α-subunit harboring a serine/threonine kinase domain and two regulatory $\beta-$ and $\gamma-$ subunits (Carling, 2004; Hardie, 2003). AMPK is activated on one hand by metabolic stress and ATP depletion, which elevates the cellular AMP:ATP ratio, and on the other hand by phosphorylation at T172 within the catalytic subunit by upstream kinases (Fig. 2).

Until now, two AMPK-regulatory kinases have been identified: (i) the calmodulin-dependent protein kinase kinase (CaMKK) and (ii) the tumor suppressor LKB1 (also known as STK11).

Phosphorylation of AMPK links CaMKK and LKB1 signaling pathways to AMPK-mediated regulation of the metabolism (Hong *et al*., 2005; Hurley *et al*., 2005; Woods *et al*., 2005). Once activated, AMPK phosphorylates several downstream substrates, thereby switching off energy-consuming biosynthetic pathways and switching on energy-generating biosynthetic pathways. The AMPK activation conserves cellular ATP pools and preserves energy homeostasis (Carling, 2004). Substrates of AMPK include key enzymes of fatty acid and sterol synthesis, like acetyl-CoA carboxylase (ACC) and 3-hydroxy-3-methylglutaryl-CoA reductase. Furthermore, AMPK phosphorylates key enzymes of fatty acid oxidation and glycolysis, like malonyl-CoA decarboxylase and 6-phosphofructo-2-kinase (substrates are reviewed by Foretz *et al*., 2005; Hardie, 2004; Kemp *et al*., 2003). Therefore, disturbance of AMPK activity has been linked to the pathogenesis of diabetes mellitus type II and obesity (Minokoshi *et al*., 2002; Zhou *et al*., 2001). Modulation of AMPK may offer novel therapeutic options for treatment of these diseases.
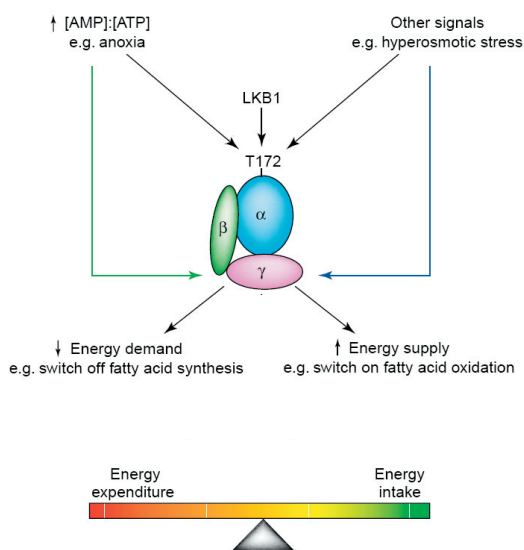
Figure 2: Schematic representation of AMPK domain structure, its activation and function. AMPK is a heterotrimeric S/T kinase comprising a catalytic α-subunit and two regulatory subunits β and γ. AMPK is involved in maintaining the intercellular energy balance. Conditions that cause an increase in the AMP:ATP ratio lead to allosterical activation of AMPK by AMP (green arrow). AMPK is activated by increased phosphorylation at T172 mediated by upstream kinases. Once activated AMPK switches on energy-generating pathways and switchs off energy-consuming pathways by phosphorylation of several downstream substrates. Figure is taken from Carling, 2004.

3.5 Aim of the present study

Regulation of cytoskeletal dynamics is required for a huge number of cellular processes including cell movement, adhesion, and shape change. The actin-binding protein VASP is regarded as an important regulator of cytoskeletal remodulation since VASP is localized to cytoskeleton hot spots in the cells and is involved in a variety of actin-remodeling processes including F-actin elongation, filament branch formation, F-actin nucleation, and filament capping. It is likely that different VASP-functions in distinct subcellular locations, are subject to spatial and temporal regulation either by VASP modification or by VASP distribution. VASP harbors three phosphorylation sites and is a substrate for PKA and PKG. VASP phosphorylations are involved in regulation and subcellular targeting of the protein.

In order to obtain a better understanding of how signaling pathways regulate actin cytoskeleton rearrangement via differential VASP phosphorylations this work had two aims: (i) the identification of the kinase responsible for VASP T278 phosphorylation *in vivo* and (ii) the systematic investigation of phosphorylation-regulated cellular VASP functions.

i) In order to identify the kinase responsible for T278 VASP phosphorylation *in vitro*, in living cells, and *in vivo*, the following steps were planned and performed:

　　1) Generation of a phospho-specific antibody against T278

　　2) A systematic screening for S/T kinases using the phospho-specific

　　　　antibody against T278 to identify T278-phosphorylating kinases

　　3) Investigation of the specificity of VASP T278 phosphorylation

After identification of the kinase, this study should unravel the function of T278 phosphorylation in living cells and *in vivo*.

ii) In order to investigate the VASP functions that are regulated by phosphorylation, the effects of VASP phosphorylation on VASP subcellular localization and actin polymerization were determined. The latter was determined by the alteration of the F- and G-actin equilibrium. A systematic set of VASP point mutants were generated in order to mimic defined phosphorylation patterns and to allow the investigation of the effects of specific kinase-mediated single phosphorylations. This combined approach allowed the investigation of VASP functions regulated by VASP phosphorylation and also the comparison of mimicked phosphorylation by acidic amino acids with kinase-mediated phosphorylation.

4 Materials and Methods

4.1 Materials

4.1.1 Animals

Four to seven-month-old male Zucker Diabetic Fatty (ZDF) rats (615.0 ± 24.9 g, n= 5) and their lean controls (392.4 ± 35.2 g, n= 5) were from Harlan Winkelmann (Borchen, Germany). All procedures and animal studies were approved by the local government.

4.1.2 Cell culture

Human umbilical vein endothelial cells (HUVEC, Cambrex Bioproducts) of passages 2-7 were cultivated in endothelial cell basal medium supplemented with endothelial growth factors (Cambrex Bioproducts). Immortalized endothelial cells from myocardial microvessels were generated from wild-type mice and cultured as described (Schlegel *et al*., 2008). VASP-deficient immortalized endothelial cells from myocardial microvessels were generated from VASP-deficient mice using the procedure as described for wild-type mice (Schlegel *et al*., 2008). ECV304, HEK293, and HeLa cells were grown in Dulbecco´s modified Eagle´s medium containing 4.5 g/l glucose supplemented with 10% fetal bovine serum, 100 U/ml sodium-pyruvate, 100 U/ml penicillin, and 100 μg/ml streptomycin as described (Benz *et al*., 2008; Renne *et al*., 2005; Hurley *et al*.,2005). All cells were maintained at 37°C in a humidified atmosphere containing 5% CO_2.

4.1.3 Plasmids

A wild-type (wt) and a catalytic inactive (CI) form of the human PKGIβ (cGMP-dependent protein kinase Iβ; Sandberg *et al*., 1989; Smolenski *et al*., 2000) was cloned into the pcDNA3 vector using the enzymes Not I/Xho I and Xho I/Xba I for the wild-type and catalytic inactive forms, respectively. C-terminal myc-tagged constitutively active (CAα), dominant negative (DNα) and wild-type (wtα) forms of AMPK α-subunit were cloned into the pcDNA3 vector (Hwang *et al*., 2004). For the SRE assays, the following plasmids were used: plasmid pSRE (Stratagene) encoding the firefly luciferase, under transcriptional control of the serum response element, and the plasmid phRL-TK (Promega) coding for the *Renilla* luciferase, which was used for transfection control.

4.2 Generation and purification of anti-pT278 antibody

To generate antibodies that specifically recognize phospho-T278 (pT278)-VASP, rabbits were immunized with the following phospho-peptide coupled to keyhole limpet hemocyanin: C^{273}RRKApTQVGE^{282}. For immunopurification of phospho-specific anti-T278 VASP antibodies, the serum was first passaged across a phosphopeptide-coupled affinity column (CNBr-activated Sepharose, Affigel10, Amersham). The column was washed with PBS. Thereafter, 1 ml fractions were eluted with 0.1 M glycine (pH 2.8) and immediately neutralized with 1 M Tris (pH 8.1). Eluted fractions were then passaged over a column with unphosphorylated VASP peptides to remove antibodies recognizing the non-phosphorylated epitope. Unbound fractions, which contained phospho-specific anti-pT278 VASP (anti-pT278) antibodies were concentrated and stored at –80°C. The specificity of the anti-pT278 antibody for the T278-phosphorylated VASP was verified using recombinant VASP. Hexahistidine-tagged VASP was expressed in *E.coli* and purified as described (Reinhard *et al.*, 1992). In Western blot analysis, the anti-pT278 antibody did not cross-react with non-T278 phosphorylated VASP (loaded 2 μg/lane). Following *in vitro* phosphorylation with an equimolar mixture of the α-subunit of PKA or PKG for 60 min (Smolenski *et al.*, 1998), pT278-VASP was readily detectable with anti-pT278 down to a minimum of 50 ng protein per lane. As expected, *in vitro* phosphorylated VASP could also be detected by the phospho-specific anti-VASP antibodies 5C6 (anti-pS157; NanoTools) and 16C2 (anti-pS239; NanoTools).

4.3 Cloning of VASP mutants

VASP mutants were generated by site-directed mutagenesis using the "QuikChange Multi" kit according to the manufacturer´s instructions (Stratagene). Human VASP cDNA cloned into the EcoRI site of the pcDNA3 vector (Invitrogen) and the following primers were used to exchange S157, S239 and T278 with alanines, aspartic acid or glutamic acid, respectively: 5´- CG GAG CAC ATA GAG CGC CGG GTC GCC AAT GCA GGA GGC CCA CC-3´ (S157A); 5´- CG GAG CAC ATA GAG CGC CGG GTC GAC AAT GCA GGA GGC CCA CC-3´ (S157D); 5´-GGA GCC AAA CTC AGG AAA GTC GCC AAG CAG GAG GAG GCC TCA GGG-3´(S239A); 5´-GGA GCC AAA CTC AGG AAA GTC GAC AAG CAG GAG GAG GCC TCA GGG-3´(S239D); 5´- G CTG GCC CGG AGA AGG AAA GCC GCG CAA GTT GGG GAG AAA ACC-3´(T278A); 5´-G CTG GCC CGG AGA AGG AAA GCC GAG CAA GTT GGG GAG AAA ACC-3´(T278E).

Truncated EGFP-VASP mutants were generated by cloning human VASP sequence into Xho I/Hind III sites of the EGFP-C1 vector (BD Bioscience). VASP cDNA was cut after the base pair 588 at the endogenous Pst I site in order to remove the VASP sequence of the EVH2 domain and the C-terminal part of the PPR. After truncation, the VASP mutant spans the N-terminal 196 amino acids of VASP, which includes the S157 phosphorylation site. Thereafter the truncated VASP construct was cut at the PflM I and Pst I sites in order to exchange the corresponding cDNA coding for S157 with the fragment coding for S157A or S157D, which allows the generation of truncated VASP point mutants. All constructs were confirmed by DNA sequence analyses.

4.4 Nomenclature of VASP mutants

All full-length VASP mutants were named using one-letter amino acid code based on the amino acids present at positions 157, 239 and 278: AAA, DAA, ADA, DDA, AAE, DAE, ADE, DDE, SAA, ASA and AAT. According to their phosphorylation patterns, full-length VASP mutants were separated into two groups: first, arrested mutants, which cannot be phosphorylated at all three phosphorylation sites and second, partially arrested mutants, which can be phosphorylated at one of the three phosphorylation sites.

Truncated VASP mutants were named according to their N-terminal tag fusion protein and their amino acid present at position 157. The length of contructs was indicated by the first and last amino acid number: EGFP-S$_{1-196}$, EGFP-A$_{1-196}$ and EGFP-D$_{1-196}$.

4.5 Methods

4.5.1 Analysis of T278 phosphorylation status in cells

To screen for kinases that may phosphorylate the VASP T278 residue, confluent HUVEC, ECV304, or HEK293 cells, which were transiently transfected with cDNAs coding for the human VASP in the pcDNA3 vector, were treated with protein kinase activators or inhibitors. Following incubation, the relative amount of pT278 in inhibitor- or activator-treated cells was quantified by Western blot analysis with anti-T278 antibody. PKA inhibitors used were H89 (N-[2-((p-Bromocinnamyl)amino)ethyl]-5-isoquinolinesulfonamide, 0.5-5 μM for 10-60 min, Sigma) and Rp-8Br-cAMPS (8-Bromoadenosine-3´,5´-cyclic monophosphorothioate, Rp-isomer, 50-500 μM for 10-60 min, BioLog). PKA activators used were Forskolin (1-10 μM for 0.5-60 min, Sigma) and 8-Br-cAMP (8-Bromoadenosine-3´,5´-cyclic monophosphorothioate, 50-200 μM for 0.5-60 min, BioLog). PKG effects on T278

phosphorylation were analyzed with the inhibitor Rp-8-Br-cGMPS (8-Bromoguanosine-3´,5´-cyclic monophosphorothioate, Rp-isomer, 50-500 μM for 10-60 min, BioLog), and with the activators SNP (sodium nitroprusside, 0.5-20 μM for 1-60 min, Sigma) and 8-Br-cGMP (8-Bromoguanosine-3´,5´-cyclic monophosphorothioate, 50-200 μM, 0.5-60 min, BioLog). PKC was analyzed using the inhibitors Bis I (2-[1-(3-Dimethylaminopropyl)-1H-indol-3-yl]-3-(1H-indol-3-yl)-maleimide, 0.5-50 μM for 0.5-8 h, Calbiochem) and Rottlerin (1-[6-[(3-Acetyl-2,4,6-trihydroxy-5-methylphenyl)methyl]-5,7-dihydroxy-2,2-dimethyl-2H-1-benzopyran-8-yl]-3-phenyl-2-propen-1-one, 1-10 μM for 0.5-8 h, Sigma), and the activator PMA (Phorbol-12-myristate-13-acetate, 0.1-10 μM for 2-30 min, Sigma). For CaM kinase, KN93 (N-[2-[[[3-(4'-Chlorophenyl)-2-propenyl]methylamino]methyl]phenyl]-N-(2-hydroxyethyl)-4'-methoxy-benzenesulfonamide phosphate salt, 0.5-5 μM for 0.5-8 h, Sigma), CaMKII peptide (CaM Kinase II Inhibitor 281-301, 0.5-5 μM for 0.5-8 h, Calbiochem), and Calcimycin (Ca^{2+}-Ionophor A23187, 1-10 μM for 10-30 min, Sigma) were utilized. PKB activity was investigated by Wortmannin (0.1-10 μM for 0.5-8 h, Calbiochem) and FCS (0.5-20% for 0.5-3 h, Gibco). AMPK-driven T278 phosphorylation was assessed using the AMPK activators Metformin (1,1-dimethylbiguanide, 0.5-8 mM for 10-60 min, Sigma), Phenformin (Phenethylbiguanide, 0.5-8 mM for 10-60 min, Sigma) and AICAR (5-Aminoimidazole-4-carboxamide-1ß-riboside, 0.5-2.5 mM for 10-30 min, Calbiochem), and AMPK inhibitors Compound C (2-20 μM for 0.5-8 h, Calbiochem) and Indirubine (Indirubine-3-oxime, 0.5-20 μM for 0.5-8 h, Tocris).

4.5.2 Analysis of VASP phosphorylation by Western blotting

For Western blot analyzes, cells were washed two times with ice-cold PBS. Afterwards 3x SDS sample buffer (200 mM Tris-HCl pH 6.7; 6% SDS; 15% glycerine; 0.003% bromphenole-blue; 10% β-mercaptoethanol) was added, samples were immediately boiled at 90°C for 10 minutes, and stored at - 20°C. The tissue lysates were prepared using mortar and pestle. Tissue was homogenized in the mortar under liquid nitrogen, afterwards 3x SDS buffer was added and boiled at 95°C for 15 minutes. Cell lysates or tissue lysates were separated by 8% SDS PAGE under reducing conditions and electro-transferred onto a nitrocellulose membrane (Schleicher&Schüll). Proteins on blots were probed using antibodies against AMPKα (1:1000, Cell Signaling Technology), phospho-AMPKα (1:1000, Cell Signaling Technology), and phospho-ACC (1:1000, Cell Signaling Technology), GAPDH (1:5000, Chemicon), myc-tag (1:500, Santa Cruz Biotechnology), VASP (1:4000, M4, Halbrugge et

al., 1990), and pT278-VASP (1:500, Blume *et al*., 2007), as well as horseradish peroxidase-conjugated secondary antibodies (1:5000). Signal detection was performed using a chemiluminescence technique (ECL Plus, Amersham Pharmacia Biotech.). The intensity (area) of the individual bands on the x-ray films (XBA, Fotochemische Werke Berlin) was quantified via densitometric scans using the software Scan Pack 3.0 from Biometra.

4.5.3 Immunohistochemistry of aortic tissue

Excised aortic rat tissue was immediately rinsed with PBS transferred into isopentane and frozen in liquid nitrogen. Isopentane was evaporated from the frozen tissue and samples were stored at –80°C. For cryosections, the frozen tissue was embedded in OCT compound (Sakura Finetek), then cut into 7 μm slices that were immediately fixed in 3.7% paraformaldehyde/PBS for 5 min, permeabilized with 0.1% Triton X100/PBS for 20 min, and finally blocked in 5% goat serum/PBS for 1 h. Sections were incubated overnight with primary antibodies against VASP (1:250, M4), IE273 (1:200, Abel *et al*., 1995), and phospho-VASP (anti-pS157 1:250, anti-pS239 1:250, and anti-pT278 1:200), followed by secondary anti-mouse and anti-rabbit antibodies conjugated to Alexa-fluor 488 or 594 (1:1000, Invitrogen) for 1 h. All incubations were performed in 5% goat serum/PBS at room temperature.

4.5.4 Immunocytochemistry

For co-localization of AMPK α-subunits and F-actin, HeLa cells were cultivated in 60 mm plastic dishes to 70% confluence, before co-transfection (GenePorter 2 and Booster Reagent 2, Peqlab) with pcDNA3 vectors coding for VASP mutants (AAA, AAE, AAT; 1.0 μg each), or myc-tagged AMPK α-subunits (wtα, CAα,DNα; 2.0 μg each; Hwang *et al*., 2004). The cells were cultured in DMEM with all supplements for 24 h.

For localization of endogenous VASP, wild-type endothelial cells from myocardial vessels were cultivated on 2-well chamberslides (Nunc). For phosphorylation studies, cells were incubated with 5 μM Forskolin for 15 min.

For localization of truncated mutants, VASP-deficient endothelial cells from myocardial vessels were transiently transfected with 400 ng cDNA coding for EGFP truncated VASP mutants. 6 h after transfection, cells were trypsinized, seeded on 2-well chamberslides and cultured for a further 16 h.

For localization of arrested VASP mutants and co-localization with wild-type VASP,

VASP-deficient endothelial cells were cultivated in 6-well plates to 70% confluence and transfected or co-transfected (GenePorter2 and Booster2, Peqlab) with 400-800 ng of plasmids coding for the arrested VASP mutants and/or the wild-type. 6 h after transfection, cells were trypsinized, seeded on 2-well chamberslides (Nunc) and cultivated for a further 16 h. Phosphorylation at S157 was increased by PKA stimulated using incubation with 5 μM Forskolin for 15 min.

All cells were washed with PBS and immediately fixed with 3.7% paraformaldehyde/PBS for 5 min, permeabilized with 0.1% Triton X100/PBS for 5 min and finally blocked in 5% goat serum/PBS for 1 h. Sections were incubated overnight with primary antibodies against myc-tagged AMPK α-subunits (anti-myc 1:250), His-tagged arrested VASP mutants (anti-His 1:1000, Novagen), VSV-tagged wild-type VASP (anti-VSV, 1:500, Sigma), VASP (M4, 1:1000) and phospho-VASP (anti-pS157, 1:250), followed by secondary anti-mouse and anti-rabbit antibodies conjugated to Alexa-fluor 488 or 594 (1:1000, Molecular Probes) for 1 h. F-actin fibers were stained using TRITC-conjugated Phalloidin (Sigma) diluted 1:250 in PBS and incubated for 45 min. All incubation with antibodies was performed in 5% goat serum/PBS at room temperature. Staining sections were investigated using a NIKON Eclipse E600 microscope equipped with a C1 confocal scanning head and a 100x oil immersion objective. Images were acquired using the EZ-C1 2.10 software from Nikon.

4.5.5 SRE assay

HEK293 cells were grown on 6-well plates to 70% confluence before transient transfection was performed using Rotifect (Roth). Each transfection mix (2 μg total plasmid DNA) consisted of 0.1 μg of arrested VASP mutants, 0.5 μg of SRE reporter vector (pSRE), 0.25 μg of Renilla luciferase transfection control vector (phRL-TK) and 1.15 μg pcDNA3 vector without insert (Invitrogen). For phosphorylation studies, instead of the arrested mutants, partially arrested VASP mutants were transfected with or without the addition of cDNA coding for PKGI (different amounts of wild-type and catalytic inactive form), or for mutants of the AMPK α-subunit (different amounts of constitutive active and dominant negative form). In all SRE assay transfections, the pcDNA3 vector without an insert was added to bring the total amount of cDNA to 2 μg. After transfection, cells were cultivated in DMEM with sodium pyruvate and antibiotics in the absence of serum for 26 h. For the S157-phosphorylation study, transfected cells were incubated with 5 μM Forskolin for 5, 20, 40, and 80 min in serum-free medium. Cells were washed with PBS and lysed using 100 μl of

Passive Lysis Buffer (Dual Luciferase Reporter Assay System from Promega) for each well. Cell lysates were centrifuged (10000xg for 10 min at 4°C) and luciferase activities of 20 µl from the supernatant were measured using the Dual Luciferase Reporter Assay System, including substrates for firefly- and *Renilla*-luciferase (each 100 µl per reaction) according to the manufacturer´s protocol. Luminescence of each single reaction was measured by a luminometer (Lumat, Berthold). To normalize the luciferase activity to the transfection efficiency, firefly luciferase activity was related to the activity of *Renilla* luciferase. The *Renilla* luciferase is constitutively expressed and therefore correlated to the transfection efficiency. For phosphorylation studies cell lysates were analyzed by Western blotting (described in detail in section 4.5.2.) using antibodies against PKGI (1:5000, Markert *et al.*, 1995), myc (1:500), VASP (1:4000, M4) and VASP phospho-specific antibodies against pS157 (1:500, 5C6), pS239 (1:1000, 16C2), and pT278.

4.5.6 Quantification of cellular F-actin content by FACS analysis

In order to investigate the effect of AMPK activity on F-actin accumulation, HeLa cells were cultivated in 100 mm dishes to 70% confluence and co-transfected (GenePorter 2 and Booster Reagent 2, Peqlab) with pcDNA3 vectors coding for VASP mutants (AAA, AAE, AAT; 2.5 µg each), or myc-tagged AMPK α-subunits corresponding to the wild-type, a constitutively active mutant or a dominant negative mutant (5 µg each) (Hwang *et al.*, 2004). The cells were cultured in DMEM with all supplements for 24 h. For analysis of the effects of VASP phosphorylation on F-actin accumulation, HEK293 cells were grown on 6-well plates to 60% confluence and transiently co-transfected using Metafectene (Biontex) with cDNAs (in total 1.0 µg) encoding the arrested VASP mutants (AAA, DAA, ADA, DDA, AAE, DAE, ADE, DDE; 0.25 µg each) and the pcDNA3 vector without an insert (0.75 µg). Transfected cells were maintained in DMEM with all supplements, including FCS for 26 h. To stain F-actin in the cell for FACS analysis, cells were washed with ice-cold PBS and trypsinized at room temperature with ice-cold trypsin/EDTA solution. Cells in suspension were transferred into ice-cold DMEM-medium with 10% FCS to inactivate trypsin/EDTA. After centrifugation (1000xg, 3 min, 4°C), the supernatant was removed and cells were resuspended in ice-cold PBS. After a further centrifugation step, cells were fixed in 3.7% paraformaldehyde/PBS (5 min at 4°C), then permeabilized with 0.1% Triton X100/PBS (5 min, 4°C) and again fixed in 3.7% paraformaldehyde/PBS (5 min at 4°C). To exchange solutions cells were pelleted (1000xg, 3 min, 4°C) . Cells were washed twice by resuspension

in PBS (5 min, 4°C) and centrifugation (1000xg, 3 min, 4°C). Afterwards, cells were co-stained for F-actin using Cy5-conjugated Phalloidin (1:250 diluted in 5% goat serum/PBS; Molecular Probes), and for myc-tagged AMPK α-subunit using anti-myc antibody (1:250 diluted in 5% goat serum/PBS) or for His-tagged VASP mutants using anti-His antibody (1:500 diluted in 5% goat serum/PBS), followed by FITC-conjugated anti-mouse antibody (1:500 diluted in 5% goat serum/PBS; Sigma). All incubations were performed in darkness at room temperature for 1 h. The mean cellular F-actin content determined by Phalloidin staining of cells overexpressing AMPK mutant or arrested VASP mutant was quantified using FACScan (Becton-Dickinson). FACScan was performed using FACSCalibur equipped with two lasers and the CellQest-software. FACS-data was analyzed by software WinMDi 2.8.

4.5.7 *In vitro* VASP phosphorylation with purified AMPK

AMPK-phosphorylation assays were performed at 30°C in 40 μl reaction mixtures containing 80 ng of the purified recombinant human VASP and 100 mU of purified AMPK (Upstate Inc.) in reaction buffer (5 mM Hepes, pH 7.5, 0.1 mM DTT, 0.25% NP40, 7.5 mM MgCl$_2$, 50 μM ATP, 300 μM AMP). Reactions were stopped at different time points by addition of SDS-sample buffer and heating at 90°C for 10 min.

4.5.8 Analysis of T278 phosphorylation modified by AMPK mutants in cells

ECV304 and HeLa cells were cultivated in 6-well plates to 70% confluence and transiently transfected using GenePorter 2 with Booster Reagent 2 (Peqlab) with 1.0 μg of cDNA coding for wtα, CAα or DNα, respectively (Hwang *et al*., 2004). Alternatively, HEK293 were transiently co-transfected using Metafectene (Biotex) with 0.25-2 μg of cDNA coding for the human protein phosphatase 2B (clone IRATp970H0549D, RZPD, Berlin) and 1.0 μg of cDNA coding for the human VASP in the pcDNA3 vector. The cDNA amount was then supplemented with empty vector up to a total of 3.0 μg. After 24h expression, washed cells were lysed and the relative degree of pT278 was quantified by Western blot analysis with anti-T278 antibody.

4.6 Statistics

Results were expressed as means ± SD. Comparisons between 2 groups were analyzed using Student´s t-tests (Microsoft Office Excel). The significant difference was defined as indicated in the legends.

5 Results

5.1 Identification of AMPK as a kinase responsible for T278 phosphorylation

5.1.1 AMPK phosphorylates VASP at position T278

To detect VASP T278 phosphorylation and to identify the kinase that phosphorylates residue T278, a phospho-specific antibody against phosphorylated T278 was raised. Rabbits were immunized with the phosphopeptide representing T278 and flanking residues (amino acid residues 273-282). The hyperimmune serum was immunoselected by a two-step affinity chromatography using a column coupled with phosphopeptide first and then a second column coupled with unphosphorylated peptide. As demonstrated by Western blotting, anti-pT278 specifically detects T278 only in the phoshorylated state and does not cross-react with the non-phosphorylated VASP site (Fig. 3).

Protein phosphatase 2B (PP2B) has been shown to dephosphorylate VASP at T278 *in vitro* (Abel *et al*., 1995). PP2B were transiently overexpressed in HEK293 cells and the lysates were analyzed by Western blotting using the new phospho-specific antibody. As shown in figure 3, anti-pT278 specifically detects T278-phosphorylated VASP in cell lysates.
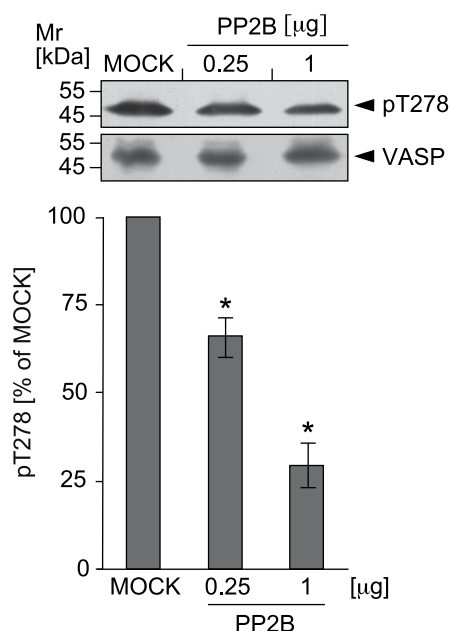
Figure 3: Anti-pT278 specifically detects pT278 levels in cell lysates. The specificity of anti-pT278 antibodies for T278-phosphorylated VASP was analyzed using protein phosphatase 2B (PP2B), which dephosphorylates pT278. HEK293 cells were co-transfected with 1.0 µg human VASP in pcDNA3 vector and 0.25 or 1 µg cDNA coding for PP2B or vector without insert (MOCK). After 24h cells were lysed and analyzed for pT278 (anti-pT278) and total VASP (anti-VASP antibody M4) by Western blot.

To identify the kinase responsible for T278 phosphorylation, a systematical screen for serine/threonine kinases in intact cells was performed using anti-pT278. The kinases were first selected according to their consensus sequences that matched the residues flanking

T278. As a second step, endothelial cell lines (ECV304 and HUVEC), which express a high amount of endogenous VASP (Smolenski *et al*., 2000), as well as HEK293 cells, which transiently overexpressed VASP, were incubated with specific activators or inhibitors of the selected kinases. As a third step, treated cells were then analyzed for pT278 and total VASP by Western blotting. Incubation with the PKA activators Forskolin (1-10 μM) or 8-Br-cAMP (50-200 μM) for up to 60 min did not increase pT278 levels in ECV304 cells (Fig. 4) or HUVEC (not shown). Consistently, treatment with PKA inhibitors H89 (applied up to 5 μM for 60 min) or Rp-8Br-cAMPS (up to 500 μM for 60 min) did not alter pT278 levels (not shown), confirming that PKA does not phosphorylate T278 in living cells. PKA phosphorylates VASP at S157, thus phosphorylation levels were used as a control for PKA activity. Cells treated with PKA activators (Forskolin or 8-Br-cAMP) and an inhibitor (H89) showed increased and decreased pS157 levels, respectively, which indicates modulation of PKA activity (Fig. 4, lower panel at the left side). Similarly, PKG activators SNP (0.5-20 μM) and 8-Br-cGMP (50-200 μM) or inhibitors, such as Rp-8-Br-cGMPS (50-500 μM) incubated for up to 60 min, failed to change T278 phosphorylation in cells (shown for 8-Br-cGMP in ECV304, Fig. 4, right side). Under these conditions, the tested inhibitors and activators clearly altered PKG activity as indicated by modulated S239 phosphorylation levels. Next, PKB activity was targeted using the inhibitor Wortmannin (up to 10 μM for 8 h), or activator FCS (up to 20% for 3 h). However, these treatments did not change pT278 levels in ECV304, HUVEC or HEK239 cells (not shown).
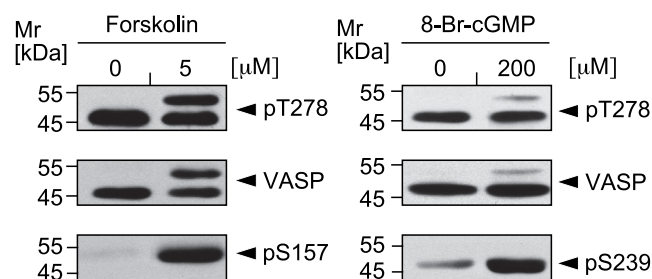
Figure 4: PKA and PKG do not phosphorylate T278 in endothelial cells. ECV304 cells were treated with the PKA or PKG activators Forskolin (10 μM, 10 min) or 8-Br-cGMP (200 μM, 15 min), respectively. Phosphorylations at the sites T278, S157, and S239 were analyzed and compared to untreated cells by Western blotting using phospho-specific antibodies (anti-pT278, anti-pS157 and anti-pS239).

Further, the contribution of PKC for pT278 was analyzed. This kinase phosphorylates S157 in vascular smooth muscle cells (Chitaley *et al*., 2004). PKC inhibitors Bis I (up to 50 μM for 30 min) or Rottlerin (up to 10 μM for 8 h), or stimulators such as PMA (up to 10 μM for

30 min) did not affect pT278 levels (not shown). Additionally, pT278 was independent of CaMK activity as indicated by kinase inhibitors (KN93 or CaMKII peptide) and activators (Ca^{2+}-Ionophor A23187, data not shown).

Next, the AMPK was tested for phosphorylation of VASP at T278 and HUVECs were incubated with AMPK inhibitors Indirubine (5-20 μM for 0.5-8 h) or Compound C (2-20 μM for 0.5-8 h). Western blot analysis of cell lysates revealed that AMPK inhibitors significantly decreased pT278 by up to 45% relative to the basal pT278 level of untreated cells in a concentration- and time-dependent manner (Fig. 5A and B).
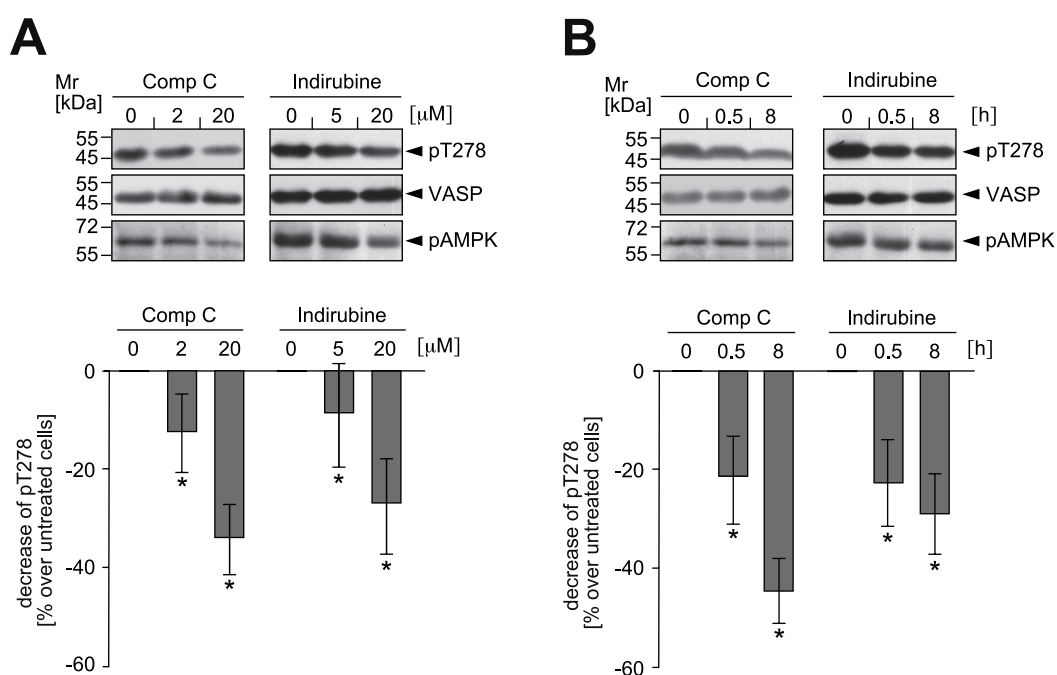
Figure 5: AMPK inhibition reduces VASP phosphorylation at residue T278 in endothelial cells.

To test the effect of AMPK activity for T278 phosphorylation, confluent HUVECs were incubated with AMPK inhibitors Indirubine (5, 20 μM for 4h or 10 μM for 0.5 and 8h) and Compound C (2, 20 μM for 4h; 10 μM for 0.5 and 8 h). Washed cells were lysed and analyzed by Western blotting using antibodies against pT278, VASP, and phosphorylated activated AMPK (anti-pAMPK). Changes in pT278 were quantified from Western blots and are blotted relative to basal pT278 levels in untreated cells (0% value). The columns give means ± SD (n=4; p<0.05, treated *vs.* untreated). A: pT278 was dose-dependently reduced by the AMPK inhibitors Indirubine (5, 20 μM) or Compound C (2, 20 μM) incubated for 4 h. B: Time dependent decrease of AMPK activity and pT278 in cells incubated with Indirubine or Compound C (10 μM for 0.5 and 8h).

Consistently, increased AMPK activity induced by AMPK activating agents such as Metformin (0.5-2 mM for 30-60 min), Phenformin (0.5-2 mM for 30-60 min), or AICAR (0.5-2.5 mM for 10-30 min) led to increased pT278 in a concentration- and time-dependent manner up to maximally 56%, 72%, and 73% over initial levels, respectively (Fig. 6A and B). As a control

for increased AMPK activity, phosphorylation of AMPK at residue T172, which correlates with the kinase activity (Stein *et al.*, 2000), was analyzed in parallel. Phosphorylation of AMPK at T172 coincided with the magnitude of pT278 (Fig. 5 and 6), supporting the hypothesis that AMPK phosphorylates VASP. Modulation of AMPK activity using inhibitors and activators (conditions as used for HUVECs) was also applied to HEK293 and ECV304 cells. In these cells, pT278 levels were changed in a similar manner compared to HUVECs (data not shown). The results indicate that the modulation of AMPK activity is parallel to the phosphorylation levels at T278 in different cell lines, suggesting that VASP might be a novel AMPK substrate *in vivo*.

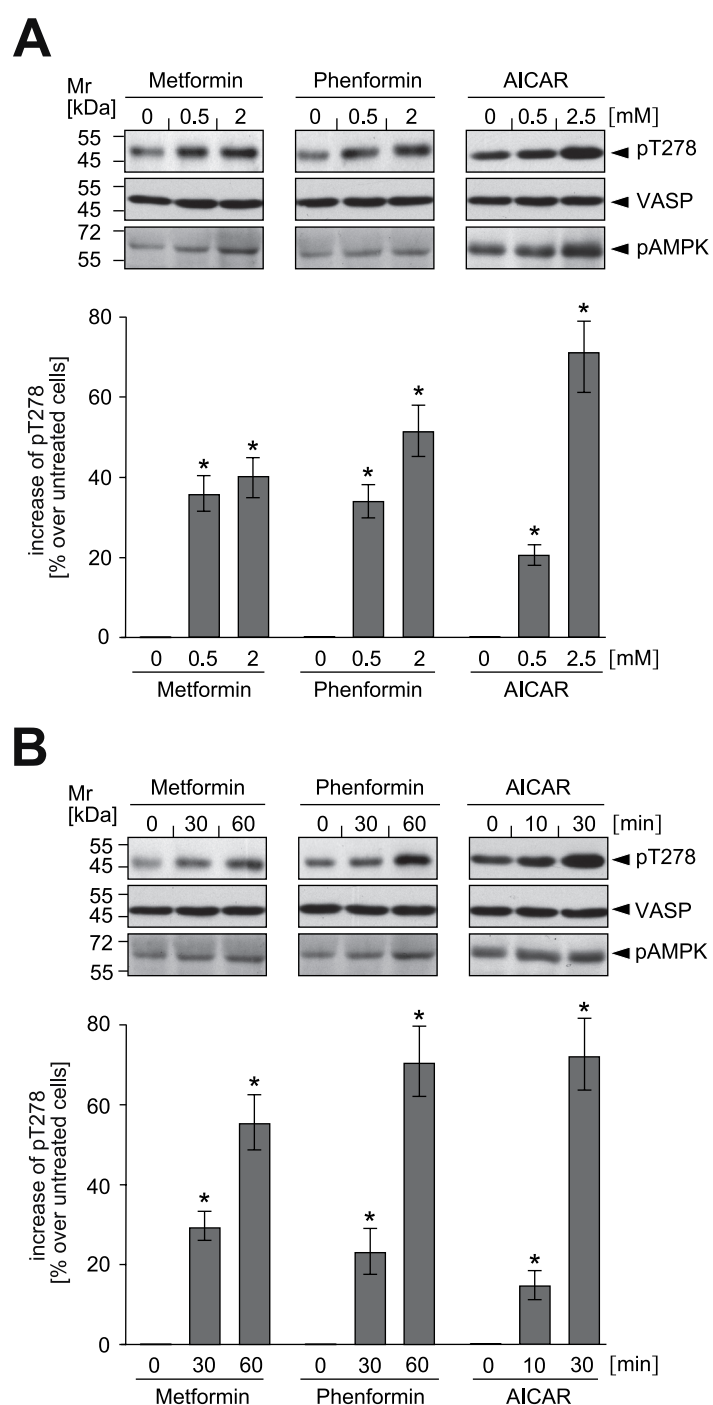**Figure 6: AMPK stimulation increases VASP phosphorylation at residue T278 in cells.**
To test the effect of AMPK activity on T278 phosphorylation, confluent HUVECs were incubated with AMPK activators. Washed cells were lysed and analyzed by Western blot using antibodies against pT278, VASP and phosphorylated activated AMPK (anti-pAMPK). Changes in pT278 were quantified from Western blots and are blotted relative to basal pT278 levels in untreated cells (0% value). The columns give means ± SD (n=4; p<0.05, treated *vs.* untreated). A: pT278 and AMPK activity were stimulated with Metformin (0.5, 2 mM) or Phenformin (0.5, 2 mM) for 1 h or with AICAR (0.5, 2.5 mM) for 30 min. B: Time dependence of pT278 and AMPK activation following stimulation with Metformin (2 mM), Phenformin (2 mM) for 30 and 60 min or AICAR (2.5 mM) for 10 and 30 min.

5.1.2 AMPK specifically targets the VASP residue T278 *in vitro*

To confirm that AMPK mediates phosphorylation of VASP at T278 and to examine the specificity of AMPK for any of the three VASP phosphorylation sites, an *in vitro* phosphorylation assay was performed. For this purpose, *E.coli*-expressed purified VASP was incubated with purified active AMPK at 30°C. After 0.5, 2, 8, and 30 min incubation, aliquots from the reaction mixture were collected and analyzed for total VASP (anti-VASP, M4) and its phosphorylations at residues S157, S239, and T278 using the phospho-specific anti-VASP antibodies 5C6 (detects pS157), 16C2 (detects pS239), and anti-pT278. Western blot analysis revealed that phosphorylation at T278 occurred rapidly within 2 min and increased for 30 min. The results are blotted relative to total VASP. In contrast, residues S157 or S239 were not phosphorylated by AMPK within the incubation period (Fig. 7). Taken together, these data indicate that AMPK specifically targets the VASP T278 phosphorylation site *in vitro*.
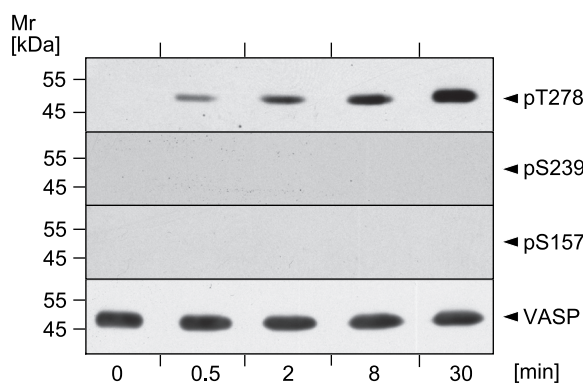
Figure 7: AMPK specifically targets VASP residue T278 *in vitro*.
Purified recombinant human VASP (80 ng) was incubated with active AMPK (100 mU) at 30°C. At different time points (0.5, 2, 8, 30 min) aliquots were collected, separated by SDS-PAGE, and analyzed for phosphorylation by immunoblotting using phospho-specific antibodies directed against the VASP phosphorylation sites T278 (anti-pT278), S157 (anti-pS157), or S239 (anti-pS239). Polyclonal anti-VASP antibodies quantified total VASP in the samples. The blot is representative for a series of four independent experiments.

5.1.3 AMPK activity mutants modulate VASP T278 phosphorylation

In order to confirm the effects of AMPK inhibitors and activators on T278 phosphorylation levels, an independent approach employing AMPK mutants was performed. ECV304 and HeLa cells were transiently transfected with cDNAs encoding a constitutively active mutant of the AMPK α-subunit (CAα), a dominant negative variant (DNα), the wild-type α-subunit (wtα), or an empty vector (MOCK). These mutants are C-terminal myc-tagged and differ in their enzymatic activity. After 24 h of expression, cells were lysed. Lysates were analyzed by Western blotting for pT278 levels, total VASP amount and expression

of the constructs. As a control for AMPK activity, phosphorylation of the established AMPK substrate acetyl-coenzyme A carboxylase (ACC) was examined (Davies *et al.*, 1989). Compared to MOCK-transfected cells (set to 100%), overexpression of CAα increased pT278 levels to 123% and 129% in ECV304 and HeLa cells, respectively (Fig. 8, upper lanes of A and B). Consistently, blocking of AMPK activity by overexpression of the mutant DNα in ECV304 or HeLa cells reduced pT278 down to 60% and 88%, respectively. In contrast, wtα overexpression did not significantly affect pT278 levels (104% in both cell lines; Fig 8, lower graphs of A and B). Correlation of phosphorylation of ACC and VASP T278 suggest that AMPK mutants may mimic the activation state of AMPK. The modulation of T278-phosphorylation by overexpression of AMPK mutants is in accordance with the previous findings using pharmacological AMPK inhibitors and activators (Fig. 5 and 6). These findings support the hypothesis that AMPK phosphorylates VASP T278 *in vivo*.
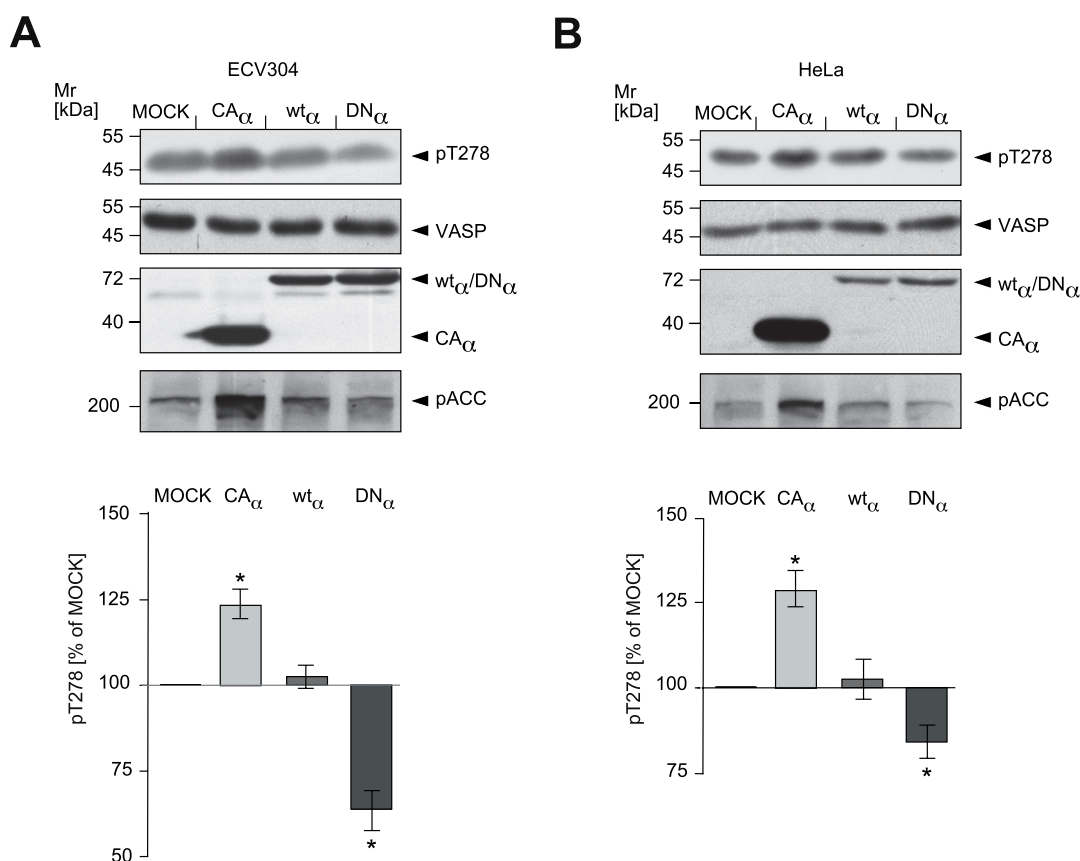
Figure 8: AMPK mutants modulate VASP T278 phosphorylation in cells.
(A) ECV304 or (B) HeLa cells were transiently transfected with cDNAs coding for myc-tagged wild-type (wtα), dominant-negative (DNα) and constitutively active (CAα) AMPK α subunit or with empty vector (MOCK). After 24 h cells were lysed, separated by SDS-PAGE and analyzed by immunoblotting using antibodies against pT278 (anti-pT278), total VASP (anti-VASP), myc-tag (anti-myc), and the S79-phosphorylated AMPK substrate acetyl-CoA carboxylase (anti-pACC). The blot is representative for a series of four independent experiments. VASP phosphorylation at T278 was quantified using Densitometric analysis (Scan pack 3.0) and is normalized to total VASP protein (n=4; $p < 0.05$, AMPK activity mutants *vs.* MOCK).

5.1.4 AMPK-mediated VASP T278 phosphorylation decreases the cellular F-actin content

VASP is an actin-binding protein that regulates different processes of actin assembly and organization. Phosphorylation of VASP impairs F-actin formation *in vitro* (Harbeck *et al.*, 2000). To analyze the effects of pT278 on actin polymerization independently of phosphorylation at S157 and S239, three VASP mutants were generated. In all constructs serine residues of phosphorylation sites at positions 157 and 239 were exchanged with alanine residues. Then T278 was either mutated to a glutamic acid residue, which mimics a constitutive phosphorylated threonine residue (mutant AAE: S157A, S239A, T278E), or replaced by an alanine (AAA), which cannot be phosphorylated, or left unchanged to allow AMPK-mediated phosphorylation (AAT; Fig. 9). These mutants were utilized to specifically analyze the effects of T278 phosphorylation mediated by AMPK on cellular actin dynamics.
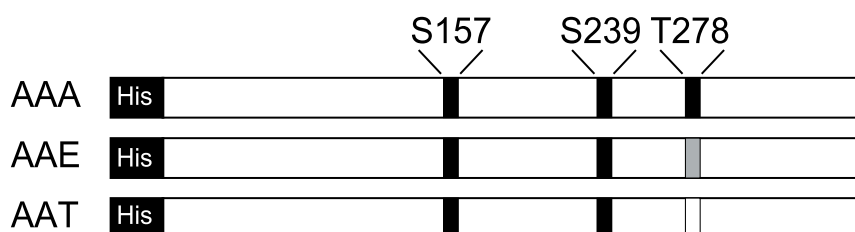
Figure 9: Scheme of arrested and partially arrested VASP mutants.
Schematic representation of N-terminal His-tagged VASP mutants AAT, AAA, or AAE. To block VASP phosphorylation at positions S157 and S239, these residues were replaced by alanines. Additionally, to imitate a defined phosphorylation status at position 278 the residue was either mutated into alanine (A), into glutamic acid (D) or left unchanged to allow AMPK-phosphorylation specifically at this residue. In the scheme dark, grey, or open boxes represent an alanine, glutamic acid, or threonine residue at the indicated positions, respectively.

Initially, the mutant AAT was tested for its ability to serve as a substrate for AMPK. For that purpose, AAT was transiently co-expressed with AMPK mutants (CAα, DNα, wtα) in HeLa cells. Western blot analysis with anti-pT278 antibody indicated that CAα increased, whereas DNα decreased T278 phosphorylation of AAT when compared to wtα-transfected cells (Fig. 10A).

FACS analysis using an F-actin specific dye (Cy5-conjugated Phalloidin) determined the consequences for the cellular F-actin content induced by T278 phosphorylation. This FACS assay quantifies the mean F-actin content of cells co-expressing AMPK mutants and VASP-AAT. F-actin content was measured relative to that of MOCK transfected cells (0% value).

Signals of the cellular F-actin were normalized to cells that express phosphorylation-resistant VASP-AAA (100%). The mutant AAE without any AMPK variant served as an internal control for the negative effect of phosphorylation on F-actin formation. The cellular level of F-actin in AAE-overexpressing cells was reduced to 57% (Fig. 10B). Consistently, co-expression of the VASP-mutant AAT with wtα-AMPK or CAα-AMPK diminished F-actin content to 64% or 46%, respectively, of the VASP-AAA value. In contrast, in DNα-AMPK- and VASP-AAT-overexpressing cells, the F-actin amount was only slightly reduced (91%). Together the data indicate that AMPK-driven VASP phosphorylation at the third site negatively interferes with F-actin assembly.
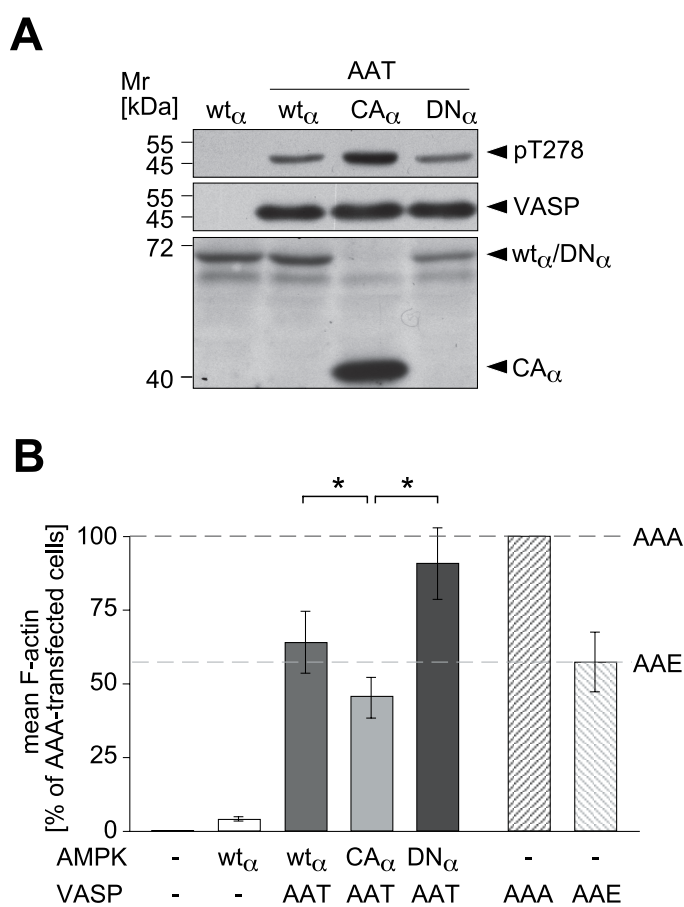
Figure 10: AMPK-mediated VASP T278 phosphorylation decreases actin assembly.
HeLa cells were transiently co-transfected with cDNAs coding for wild-type (wtα), a dominant negative (DNα), or a constitutively active (CAα) form of the AMPK α-subunit and the VASP-mutant AAT. A: After 24 h, overexpressing cells were lysed and probed for VASP phosphorylation at T278 (anti-pT278), total VASP (anti-VASP), or for AMPK-mutants using the myc-tag (anti-myc) by Western blotting. Blots show representative experiments of a series of 7. B: After 24 h AMPK- and VASP-mutants overexpressing cells were fixed and F-actin was stained using Alexa-fluor 647-Phalloidin and quantified by FACS-analysis. F-actin content of VASP AAA overexpressing cells and MOCK-transfected cells was set to 100% and 0%, respectively. Column bars represent means ± SD (n=7; *p<0.007).

To confirm the results of the FACS analyses that pT278 decreases F-actin content, the actin cytoskeleton of AMPK- and VASP-mutants expressing cells were investigated by immunofluorescence microscopy. HeLa cells were transfected with AMPK and VASP mutants. F-actin and AMPK mutants were then stained using TRITC-conjugated Phalloidin

and anti-myc antibody, respectively (Fig. 11). Consistent with the localization of endogenous AMPK α-subunit (da Silva Xavier *et al.*, 2000), the overexpressed myc-tagged AMPK α-subunit mutants (wtα, CAα, DNα) were found to be diffusely distributed in the cytoplasm. In agreement with the FACS data, cells transfected with wtα presented few actin stress fibers. Co-expression of the VASP mutant AAT with AMPK mutant wtα strongly increased stress fiber formation. Importantly, stress fiber formation was further enhanced in cells which expressed the DNα variant instead of wtα and was dramatically diminished in cells which expressed the CAα variant instead of wtα. The reduced stress fiber formation in cells that co-expressed the CAα mutant and AAT is in line with the hypothesis that AMPK activity negatively regulates F-actin content and stress fiber formation. These data demonstrate that AMPK activity impairs F-actin assembly via VASP T278 phosphorylation, resulting in defective stress fiber formation and altered cell morphology.

AMPK	wt$_\alpha$	wt$_\alpha$	CA$_\alpha$	DN$_\alpha$
AAT	-	+	+	+

Figure 11: AMPK-mediated VASP T278 phosphorylation decreases stress fiber formation.
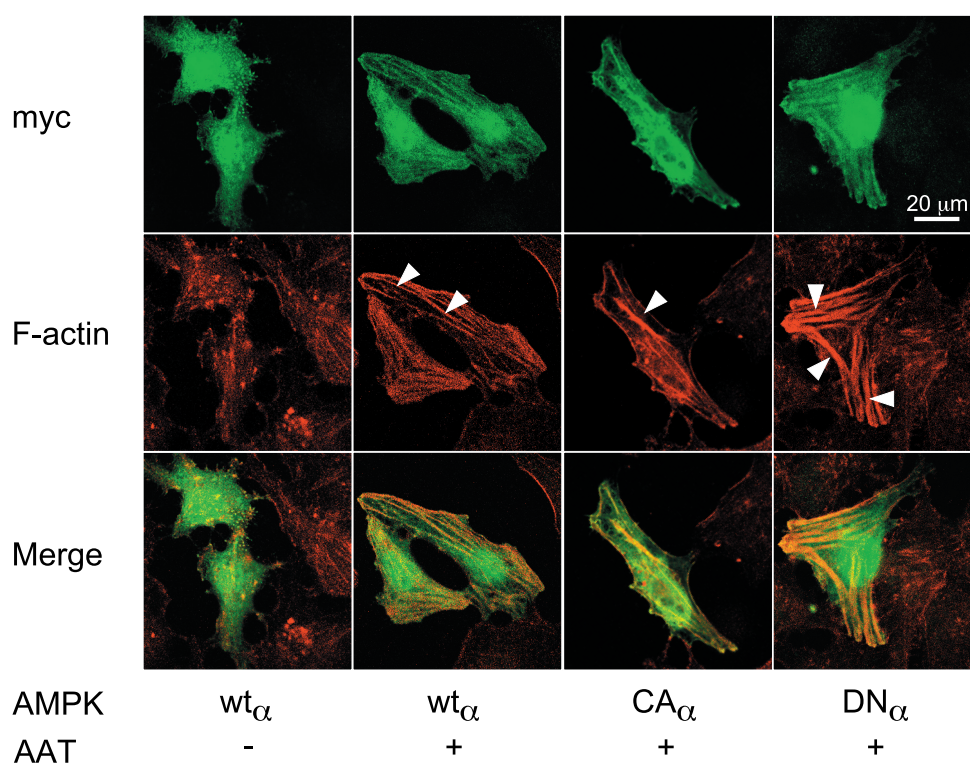HeLa cells were transiently co-transfected with cDNAs coding for wild-type (wtα), a dominant negative (DNα), or a constitutively active (CAα) form of the AMPK α-subunit and VASP mutant AAT. For immunofluorescence stainings, cells transfected with AAT and AMPK-mutants were fixed, permeabilized, and stained using antibodies against the myc-tag (anti-myc) of the AMPK-mutants. TRITC-conjugated Phalloidin was used to stain actin fibers. The white arrowheads indicate stress fibers. Pictures were taken using a NIKON Eclipse E600 microscope equipped with a 100x objective. The pictures are representative of a series of 5 independent experiments.

5.1.5 AMPK-mediated VASP-phosphorylation is reduced in the aorta of diabetic rats

AMPK is a metabolic master switch and AMPK signaling cascades are involved in many of the metabolic perturbations observed in type II diabetes mellitus (reviewed in Winder and Hardie, 1999). To analyze the relevance of AMPK-mediated VASP phosphorylation for vascular diseases, a well-characterized rat model of diabetes mellitus type II (ZDF rats) with endothelial dysfunction was utilized (Unger and Orci, 2001; Oltman *et al.*, 2006; Schafer *et al.*, 2004). The level of VASP phosphorylation at any of the three sites and localization of differentially phosphorylated VASP were investigated in the aorta of diabetic animals. The phosphorylation sites of human VASP S157, S239, and T278 correspond, in rats, to positions S154, S236, and T275, respectively.

For the investigation of T278 VASP phosphorylation in diabetic rats, phosphorylation levels of T275 and AMPK controls were analyzed by Western blotting. Notably, phospho-specific antibodies raised against phosphorylated peptides derived from the human VASP sequence cross-react with the rat homologs (not shown). Western blot analysis revealed that phosphorylation levels of T275 in aortic tissue from ZDF rats were greatly reduced to 30% when compared to control animals (lean, 100%; Fig. 12A, B). In contrast, the total amount of VASP protein in ZDF rat aortas was indistinguishable from controls (Fig. 12A, lower panel). As controls, phosphorylations of AMPK at T172 and of AMPK substrate ACC, which indicates enzymatic activity, were analyzed by Western blotting. The amount of phosphorylated AMPK (pAMPK) coincided with pT275 levels and was greatly reduced in the vessels of diabetic animals (Fig. 12D). Consistent with earlier reports (Chen *et al.*, 2005; Wang and Unger, 2005; Oltman *et al.*, 2006), the expression of AMPK was not altered in diabetic animals as compared to lean controls (Fig. 12C). In line with the reduced phosphorylation of AMPK, the phosphorylation level of the AMPK-substrate ACC (pACC) was diminished in the vessels of ZDF rats (Fig. 12E). For the comparison of phosphorylation levels, all samples were normalized to content of the housekeeping protein glyceraldehyde-3-phosphate dehydrogenase (GAPDH; Fig. 12F).
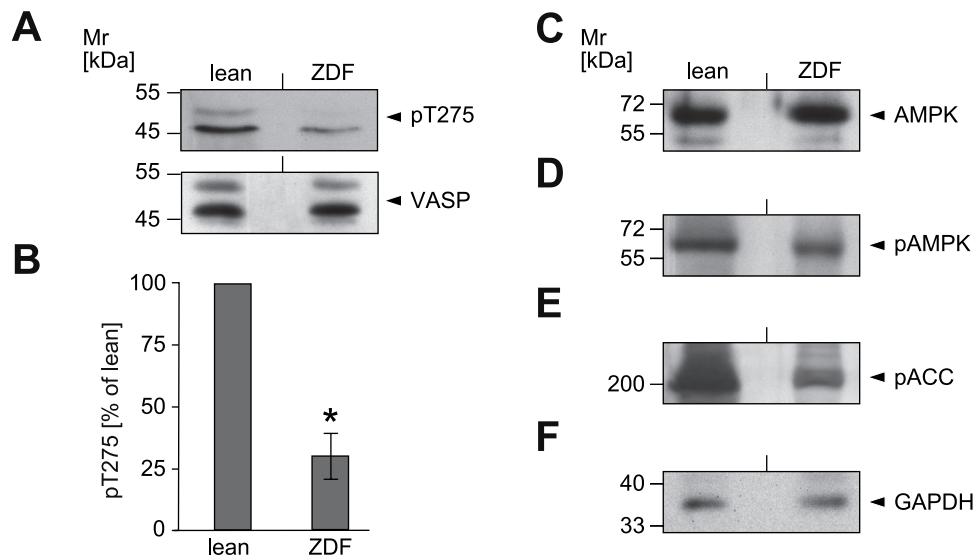
Figure 12: AMPK-mediated VASP phosphorylation is decreased in aortic tissue in a rat model of type II diabetes mellitus.

Aortas were isolated from ZDF and lean rats, rinsed, and tissue lysates were prepared immediately. Proteins were separated by SDS-PAGE and analyzed by Western blotting. A: Aortic tissues were probed using antibodies against VASP phosphorylated at T275 (anti-pT278) or polyclonal anti-VASP antibodies, which quantified total VASP. B: pT275 levels were quantified from Western blot signals using densitometric analysis. Blotted values are normalized to total VASP. Columns give means ± SD (n=4; *p<0.05, lean *vs.* ZDF). C-F: Aortas from ZDF *vs.* Lean controls were probed for C: AMPK (anti-AMPK), D: active AMPK phosphorylated at T172 (anti-pAMPK), E: the AMPK substrate acetyl-CoA carboxylase phosphorylated at S79 (anti-pACC), or F: GAPDH (anti-GAPDH). The blots give representative results, n=6 per group.

To further dissect the consequences of VASP phosphorylation at any of the three phosphorylation sites, distribution of pS154, pS236, and pT275 were analyzed by immunohistochemistry staining on the aortic ring sections with phospho-specific antibodies (Fig. 13). Phosphorylation at T275 was severely diminished in vessels of ZDF rats as compared to lean controls, while the total VASP amounts were indistinguishable in both groups as indicated by the fluorescence intensities. The reduced pT275 levels were observed most conspicuously in the endothelial and sub-endothelial smooth muscle cell layers (Fig. 13A to F). In contrast, the amount of pS154 in aortas of ZDF rats was not altered in comparison to the controls. These findings were in line with the results of the Western blot analyses (Fig. 12A, lower panel). VASP phosphorylated at S154 was almost completely localized to the luminal plasma membrane of the endothelial layer (Fig. 13G to M). In endothelial and smooth muscle cells of the aortas of ZDF rats, VASP phosphorylation at the PKG-preferred site, S236, was greatly reduced (Fig. 13N to S). This is consistent with the data from the models of defective vascular NO/cGMP signaling in rabbits and rats (Mulsch *et al*., 2001). In accordance with the Western blot analyses, immunohistochemistry

revealed reduced phosphorylation levels of ACC and AMPK, while expression of AMPK in the aortas of ZDF rats was comparable to control rats (Fig. 13T to Y). These results demonstrate that AMPK-mediated pT275 is largely decreased in the aorta of diabetic rats and establish VASP T275-phosphorylation as a vascular marker for pathological glucose metabolism.
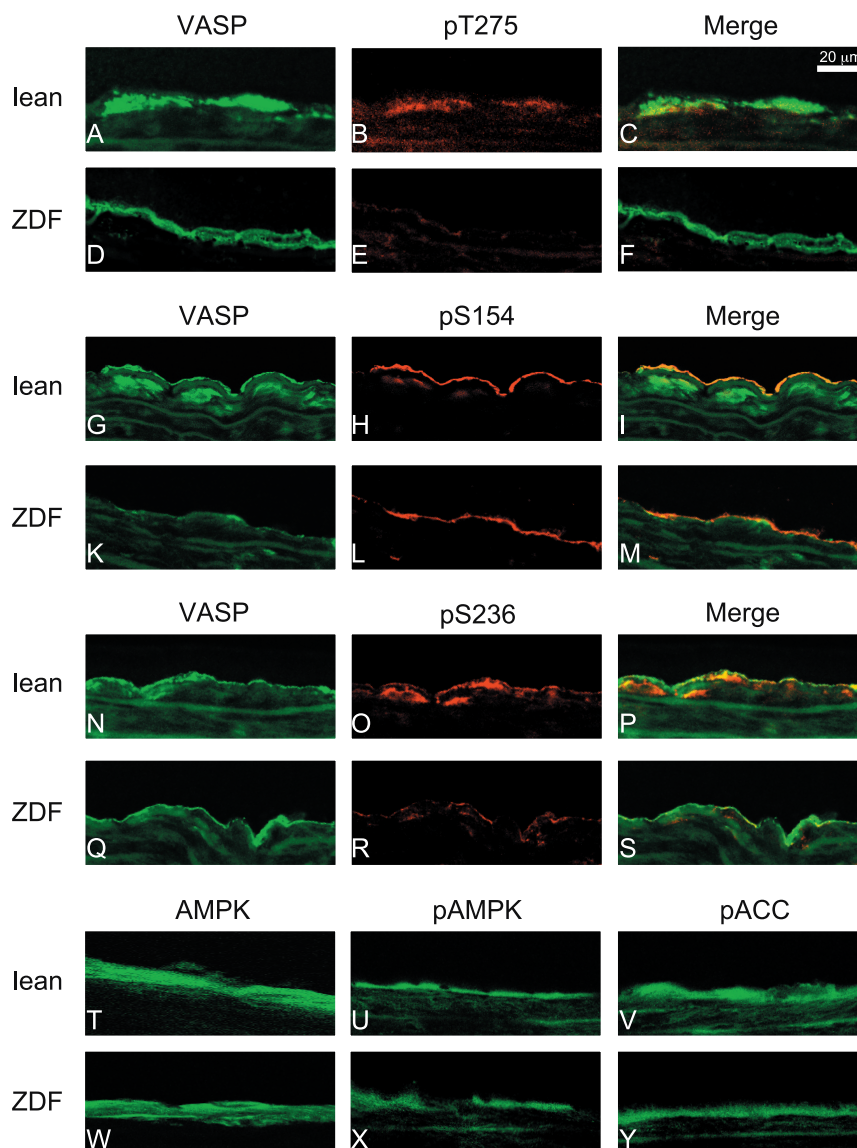
Figure 13: Immunolocalization of differentially phosphorylated VASP in aortic tissue of diabetic type II rats.

Aortic tissues were isolated from male ZDF and lean rats. Cryosections were stained using antibodies against total VASP (anti-VASP), followed by Alexa488-conjugated secondary antibody (A, D, G, K, N, Q), or with phospho-specific antibodies, which detect rat VASP phosphorylated at S154 (anti-pS157) (H and L), at S236 (anti-pS239) (O and R), or at the site T275 (anti-pT278) (B and E), followed by Alexa594-coupled secondary antibodies. As controls, sections were stained using antibodies against total AMPK (anti-AMPK) (T and W), against the active AMPK enzyme phosphorylated at T172 (anti-pAMPK) (U and X), or against the AMPK substrate acetyl-CoA carboxylase, which is phosphorylated by AMPK at S79 (anti-pACC) (V and Y), followed by Alexa488-conjugated secondary antibody. Pictures were taken using the NIKON microscope equipped with a 100x objective. The pictures give representative results, n=5 animals per group.

5.2 Investigation of VASP functions regulated by differential VASP phosphorylations

5.2.1 Experimental strategy

In mammals, protein phosphorylation is the addition of a phosphoryl group (PO_4^{2-}) to a serine, threonine, or tyrosine residue. This introduces two negative charges into the protein. Phosphorylations are catalyzed by protein kinases. Since VASP harbors three phosphorylation sites, eight phosphorylation patterns are possible due to the combination of the phosphorylation status at each site. In order to investigate the phosphorylation-regulated functions of a defined phosphorylation state, several approaches were used in this study:

1) Phosphorylation of endogenous VASP, mediated by kinase, was investigated using specific activators

2) Investigation of pS157-regulated functions using truncated VASP mutants, which span N-terminal 196 amino acids to limit the influence of EVH2 and pS239 as well as pT278. Phosphorylation state at S157 was modulated according to one of the following points:

   a) phosphorylation by endogenous kinase

   b) phosphorylation was mimicked by acidic amino acid at position 157

   c) non-phosphorylated state was mimicked by alanine residue at position 157

3) Investigation of the eight phosphorylation patterns was performed using VASP phosphomimetic mutants. These mutants imitate "locked" phosphorylation status and were generated by systematically exchange of phosphorylation sites to acidic amino acids, which imitate a constitutively phosphorylated residue. Substitution with alanine arrested the remaining phosphorylation sites into a non-phosphorylated state.

4) The function of defined kinase-mediated phosphorylations was investigated using phosphomimetric mutants, which have a partly "unlocked" phosphorylation pattern that allows one single phosphorylation only.

5.2.2 VASP S157-phosphorylation targets VASP to focal adhesions and the plasma membrane

VASP forms hetero- or homotetramers with its family members or with itself in cells. In order to investigate phosphorylation-regulated functions of defined VASP phosphorylation

patterns in the presence or absence of endogenous VASP, two immortalized murine endothelial cell lines were utilized. These cell lines were derived from myocardial vessels of VASP-deficient (VASP$^{-/-}$) and wild-type mice (VASP$^{+/+}$; Schlegel *et al*., 2008) and enable the investigation of VASP localization with or without the influence of endogenous VASP by homotetramerization. To control the expression level of VASP and its family member Mena, lysates of VASP$^{-/-}$ and VASP$^{+/+}$ cell lines were analyzed by Western blotting. The expression level of Mena was indistinguishable between VASP$^{+/+}$ and VASP$^{-/-}$ cells (Fig. 14A). Expression of VASP was not detected in endothelial cells derived from VASP-deficient mice in contrast to cells generated from wild-type mice.
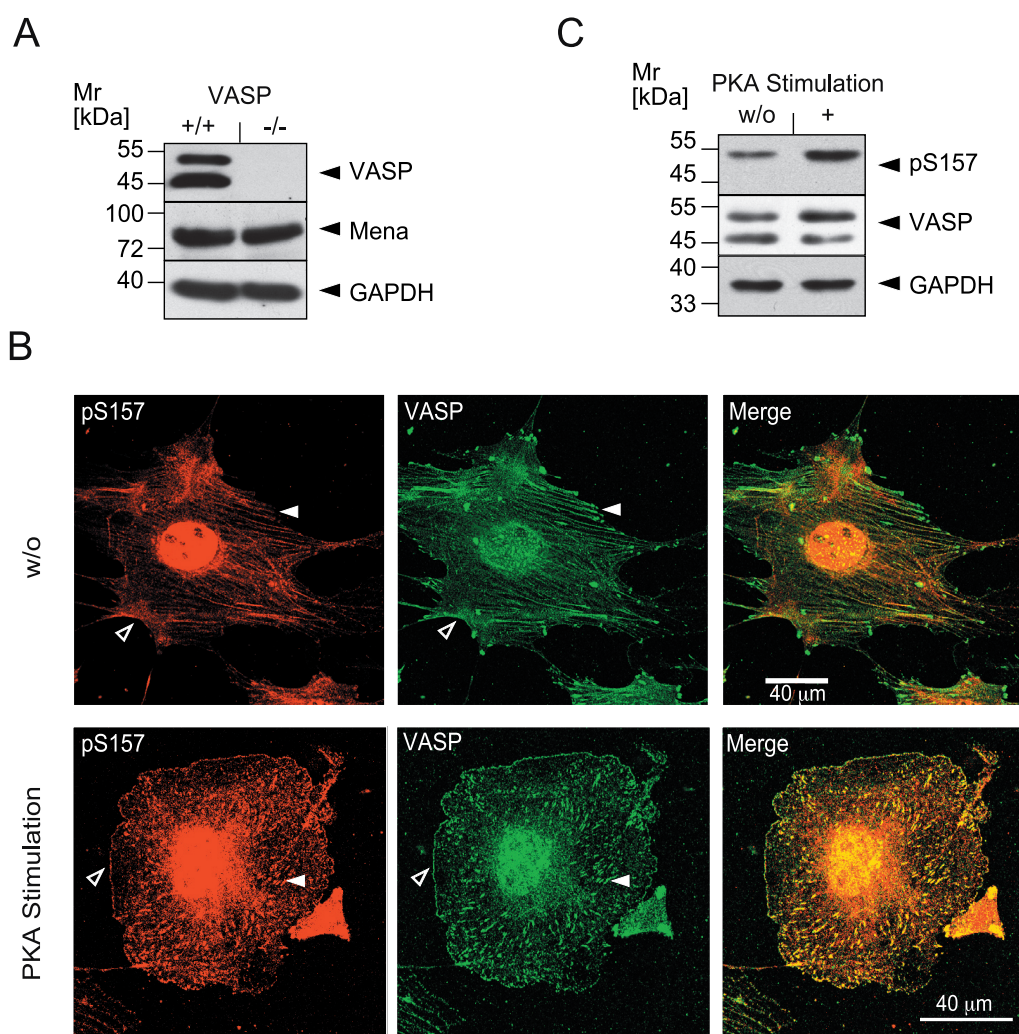
Figure 14. S157 phosphorylated VASP predominantly localizes to focal adhesions and to the plasma membrane

A: Mena/VASP protein expression of immortalized endothelial cell lines of wild-type or VASP-deficient mice. Cell lysates were analyzed by Western blotting using antibodies against VASP, Mena and GAPDH.

B, C: Localization and Western blot analysis of endogenous S157 phosphorylated VASP in endothelial cells. Cells were cultured in chamberslides for 24 h and subsequently incubated with 5 µM Forskolin for 15 min to stimulate PKA. For the localization, cells were fixed, permeabilized and stained using antibodies against VASP and pS157 followed by Alexa488-

or Alexa594-conjugated secondary antibodies. White arrowheads indicate focal adhesions and black filled arrowheads mark the plasma membrane. Pictures were taken using the Nikon Eclipse E600 microscope equipped with a 100x objective. The pictures are representative of a series of 4 independent experiments. For Western blotting, proteins of cell lysates were separated by SDS-PAGE and analyzed by immunoblotting using antibodies against pT278, total VASP and GAPDH.

Initially, S157-phosphorylated VASP was analyzed. In VASP-expressing endothelial cells, pS157 antigen was immunolocalized using the phospho-specific antibody. As a control, cell lysates were analyzed by Western blotting using the same antibody. To analyze the basal S157 phosphorylation levels and pS157 localization, cells were investigated in unstimulated conditions. Immunofluorescence analysis of untreated cells revealed that VASP phosphorylated at S157 was found at the cell periphery, i.e., at focal adhesions and the plasma membrane. A second VASP pool, which was non-phosphorylated at S157, was localized to actin filaments. To increase pS157 levels, cells were incubated with the PKA-activator Forskolin (5 μM for 15 min). In stimulated cells, pS157-VASP was found at the cell periphery (Fig. 14B). To confirm the efficiency of PKA stimulation, endothelial cell lysates were analyzed by Western blotting using antibodies against pS157, VASP, and housekeeping protein GAPDH as a loading control. Compared to untreated cells, incubation with Forskolin increased S157 phosphorylation (Fig. 14C). The results indicate that phosphorylation at S157 increases VASP localization to focal adhesions and the plasma membrane.

To address the importance of pS157-regulated VASP localization more precisely, the contribution of the EVH2 domain was investigated. EVH2 mediates interaction with G- and F-actin, which contributes to cellular localization of VASP at actin cytoskeletal structures. VASP localization at the plasma membrane and focal adhesions is attributed to EVH1 domain-mediated interactions (Huttelmaier *et al*., 1999; Bear *et al*., 2002). To distinguish the influence of EVH1 and pS157 from EVH2, pS239, and pT278, in terms of their contributions to VASP localization, truncated N-terminal EGFP-tagged VASP mutants were generated (Fig. 15). These mutants span the N-terminal 196 amino acids of VASP but lack the actin binding sites. They also differ at position S157, which was either mutated into an alanine residue (EGFP-A$_{1-196}$), or replaced by a glutamic acid (EGFP-D$_{1-196}$). A third variant was left unchanged at position S157 (EGFP-S$_{1-196}$). All three variants are shown in Figure 15A.
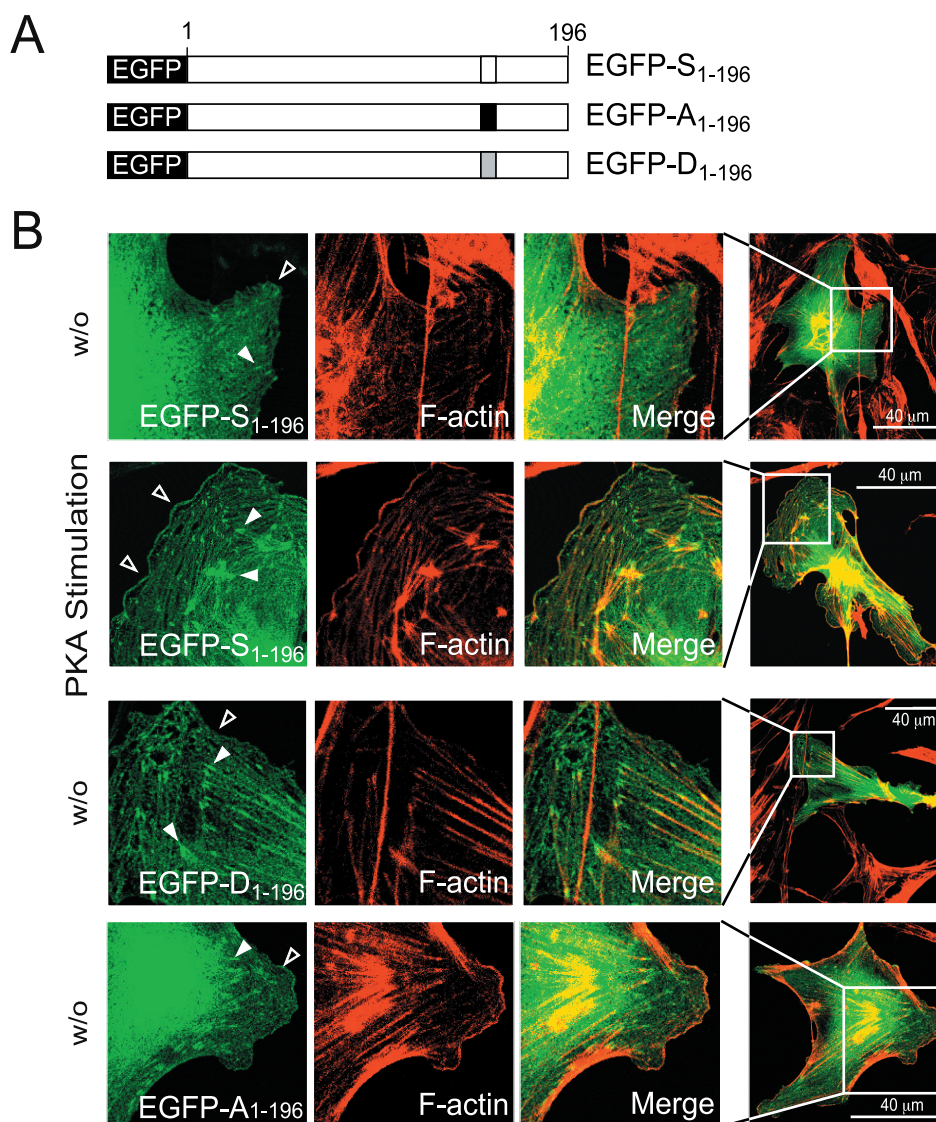
Figure 15. Residues 1-196 are sufficient to enrich S157 phosphorylated VASP at the focal adhesions and at the plasma membrane.

A: Schematic representation of the truncated VASP mutants, which span the N-terminal 196 amino acids of VASP (the EVH1 domain and N-terminal part of PPR). In order to mimic defined phosphorylation patterns of VASP, S157 was either replaced by an alanine residue (EGFP-A$_{1-196}$), or a glutamic acid (EGFP-D$_{1-196}$) residue. A third variant, EGFP-S$_{1-196}$, was left unchanged at this site to allow the specific phosphorylation at S157. B: Truncated mutants localize at focal adhesions (white arrowheads) and the plasma membrane (black filled arrowheads). Localization of EGFP-S$_{1-196}$ in untreated (first lane) and Forskolin-treated VASP $^{-/-}$ cells (second lane). Phosphorylation at S157 was increased by PKA stimulation using incubation with 5 μM Forskolin for 15 min (second lane). EGFP-D$_{1-196}$ and EGFP-A$_{1-196}$were localized in untreated cells (third and fourth lane). Cells were fixed, permeabilized and actin fibers were stained using TRITC-conjugated Phalloidin. Pictures were taken using the Nikon Eclipse E600 microscope equipped with a 100x objective. The pictures are representative of a series of 4 independent experiments.

Immunofluorescence of transiently transfected VASP-deficient endothelial cells with these truncated VASP mutants showed two different pools of mutants independent of the amino acid at position 157. The first pool of mutants was found to be diffusely distributed

throughout the cytoplasm and the nucleus (Fig. 15B, right pictures) whereas the second pool was enriched at the cell periphery (Fig. 15B, left pictures). Localization of each of the three VASP mutants in the cytoplasm and the nucleus was comparable. Phosphorylation-dependent localization of truncated mutants affected the second pool located at the cell periphery.

In non-stimulated cells, EGFP-S$_{1-196}$ was less prominent at the cell periphery (Fig. 15B, first lane). In contrast, in cells treated with Forskolin (5 μM for 5 min), EGFP-S$_{1-196}$ was enriched at focal adhesions (white arrowheads) and at the plasma membrane (black filled arrowheads). To verify the results of PKA-mediated effects on the localization of mutant EGFP-S$_{1-196}$, mutants EGFP-A$_{1-196}$ and EGFP-D$_{1-196}$ were immunolocalized in non-stimulated cells. EGFP-A$_{1-196}$ was found less at the cell periphery as compared to EGFP-D$_{1-196}$ (Fig. 15B, third and fourth lane). In summary, the localization of truncated VASP mutants indicates that the EVH1 domain and the N-terminal part of the PPR (residues 1-196) are sufficient to target VASP to focal adhesions and to the plasma membrane. The localization at the cell periphery is increased by PKA-mediated S157 phosphorylation or by mimicked phosphorylation at position 157.

5.2.3 VASP localization to the cell periphery is increased by S157D substitution and enhanced by acidic residues at S239 and T278

To examine the influence of the phosphorylation status of S239 and T278 on S157 phosphorylation-dependent VASP localization, four arrested mutants (DDE, ADE, DAA, AAA) were used. Phosphorylation sites at positions 239 and 278 were exchanged either to acidic amino acid (D239/E278) or to an alanine residue (A239/A278). These two variants (D239/E278 or A239/A278) were combined with either a mimicked phosphorylation state or blocked phosphorylation at position 157 (A157 or D157) (Fig. 16).
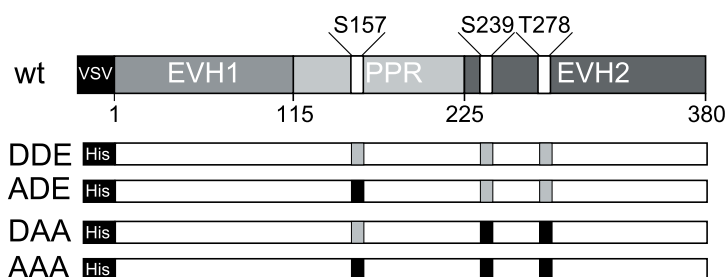
Figure 16. Schematic representation of wild-type VASP and the arrested VASP mutants DDE, ADE, DAA, and AAA in the VASP domain structure.
Wild-type VASP was N-terminally VSV-tagged and arrested VASP mutants were N-terminally His-tagged. To mimic fixed non-phosphorylated or phosphorylated states in these constructs, the phosphorylation sites S157, S239, and T278 were systematically replaced by an alanine (black), acidic (grey) residue, or a combination of both.

VASP-deficient endothelial cells were transiently transfected with these arrested mutants and wild-type VASP. Co-localization of mutated and wild-type VASP was performed using tag-specific antibodies: the antibody against His-tag detects arrested VASP mutants, and the antibody against VSV-tag detects wild-type VASP. Immunolocalizations of the four arrested mutants showed that all four mutants largely co-localized with wild-type VASP (Fig. 17A). VASP mutants bearing an acidic amino acid residue at position 157 (DDE and DAA) enriched at the cell periphery in contrast to mutants harboring an alanine at this position (ADE and AAA). Localization at focal adhesions and the plasma membrane was pronounced by mimicked phosphorylations at S239 and T278 (DDE) compared to non-phosphorylation state within the EVH2 domain (DAA). The results of a complementary localization study using DDE, ADE, DAA, and AAA mutants in absence of wild-type VASP confirmed the findings of studies with the presence of VASP, that mimicked phosphorylation at S157 targets VASP to focal adhesions and the plasma membrane. The comparable localization of VASP mutants in presents or absence of endogenous VASP indicates that arrested mutants localize independently of wild-type VASP. Notably, pS157-mediated VASP targeting to the cell periphery was enhanced in absence of wild-type VASP (Fig. 17B).

Figure 17. VASP localization to the cell periphery is increased by S157D substitution and enhanced by acidic residues at S239 and T278
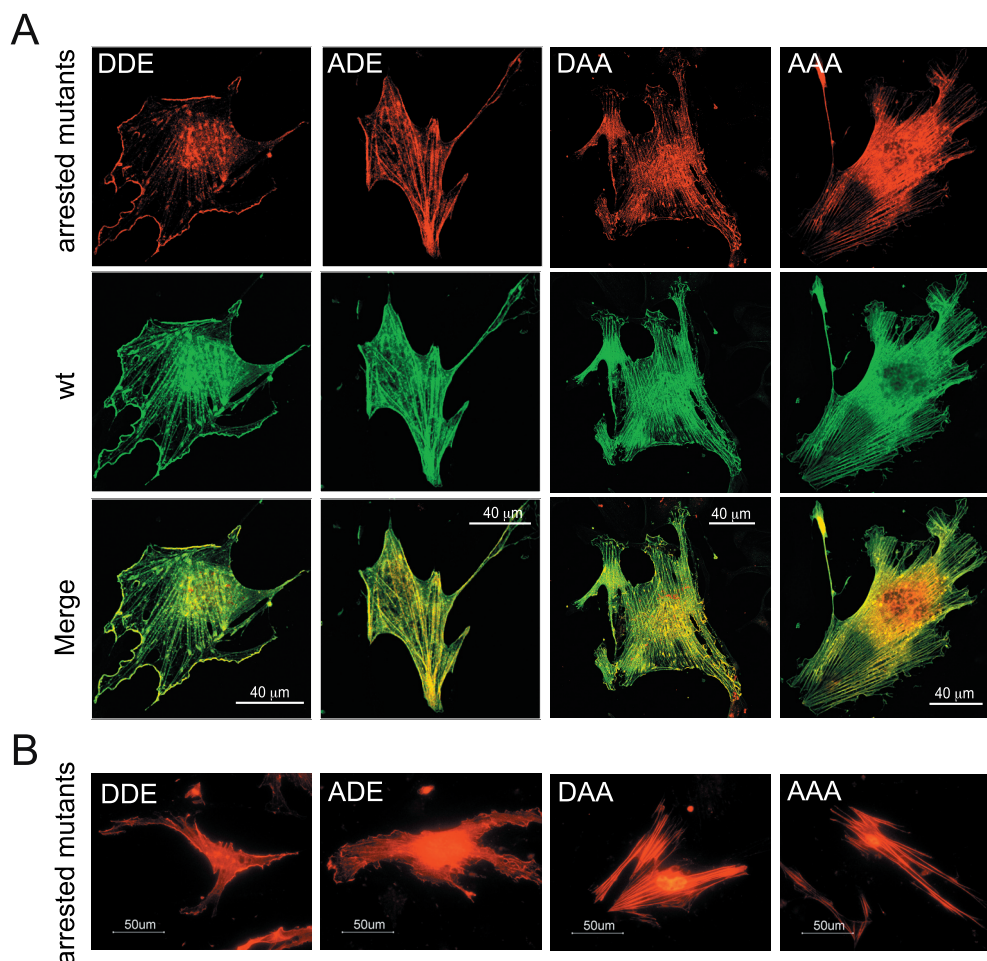
A: VASP-deficient endothelial cells transiently transfected with 400 ng cDNA coding for arrested His-tagged VASP mutants and 400 ng cDNA coding for VSV-tagged wild-type VASP. 8 h after transfection, cells were trysinized, placed on 2-well chamberslides and cultured for afurther 16 h. Washed cells were fixed, permeabilized, and stained using tag-specific antibodies against His and VSV, followed by Alexa594- or Alexa488-conjugated secondary antibodies. B: VASP-deficient endothelial cells were grown on glas-cover slips in 6-well plates and transiently transfected with 400 ng cDNA coding for arrested His-tagged VASP mutants. After expression for 24 h, washed cells were fixed, permeabilized and stained using an antibody against His-tag followed by an Alexa594-conjugated secondary antibody. A and B: Pictures were taken using the Nikon Eclipse E600 microscope equipped with a 100x objective. The pictures are representative of a series of 5 independent experiments.

The localization of DDE and DAA at the cell periphery confirmed previous findings using endogenous VASP and truncated VASP mutants (Fig. 14 and 15). All data strongly suggest that S157 phosphorylation mediated by PKA enhances VASP localization to focal adhesions and to the plasma membrane (Fig. 14 and 15) and that pS239 and pT278 contribute to cell periphery targeting.

5.2.4 Mimicked pS239 and pT278 promote pS157-dependent VASP localization

To investigate the specific influence of S239 or T278 phosphorylation on VASP localization, another four arrested VASP mutants (ADA, AAE, DDA, DAE) were generated, which mimic all possible phosphorylation patterns at S239 and T278 (Fig. 18A).

Consistent with the previous findings, where arrested mutants co-localize with wild-type VASP (Fig. 17A), the mutants ADA, AAE, DDA, and DAE also showed almost 100% co-localization with wild-type VASP (Fig. 18B). Mutants with an acidic amino acid residue at position 157 (DAE and DDA) localized to the cell periphery, in contrast to mutants with alanine at this site (ADA and AAE). Subcellular localization was independent of an acidic amino acid residue at S239 or T278 (ADA versus AAE; DDA versus DAE). Complementary localizations of ADA, AAE, DDA, and DAE in the absence instead of presents of wild-type VASP revealed that mimicked phosphorylation at S157 enriched mutants at the cell periphery. Mimicked phosphorylations at S239 and T278 reduced the pool of VASP constructs associated with actin filaments (Fig. 18C). Membrane enrichment and detachment from actin fibers of VASP mutants was increased in the absence of wild-type VASP. Collectively, the results of the localization study indicate that mimicked phosphorylations at S157, S239, and T278 regulate VASP subcellular localization. An acidic residue at S157 enriches

VASP localization at the cell periphery and mimicked phosphorylations at S239 and T278 promote VASP membrane targeting. Both phosphorylation sites have similar effects on this promotion.
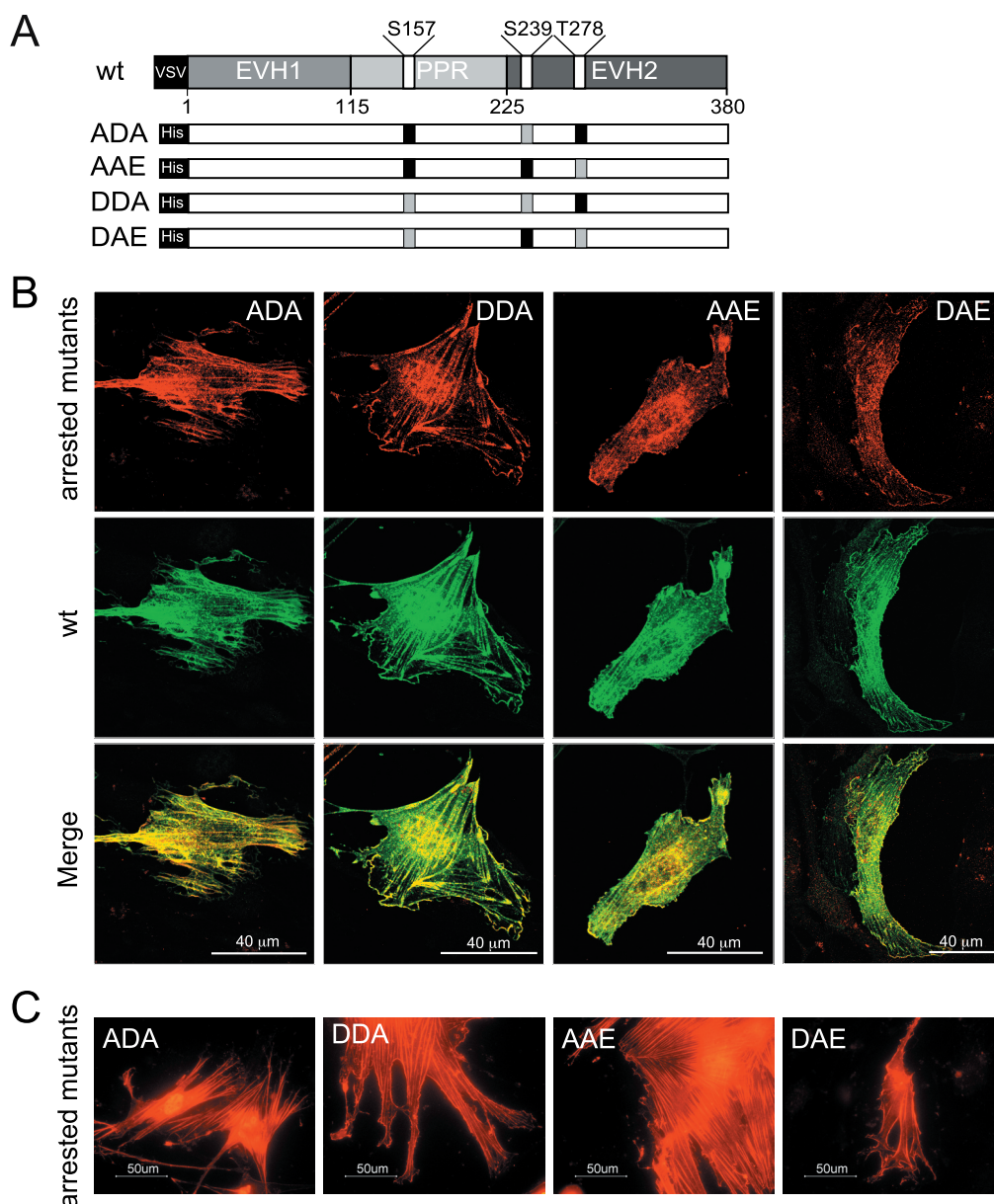
Figure 18. Mimicked phosphorylations at S239 and T278 promote pS157-dependent VASP localization at the cell periphery.

A: Schematic representation of wild-type VASP and the arrested VASP mutants ADA, AAE, DDA, and DAE in the VASP domain structure. His-tagged arrested VASP mutants simulated different arrested phosphorylation patterns at these sites. Phosphorylation states were mimicked using an alanine (black) and/or an acidic (grey) residue at each of the phosphorylation sites. B: Immunofluorescence co-localization of arrested mutants and wild-type VASP in VASP-deficient endothelial cells was performed as described in figure 17A. C: Localization of arrested His-tagged VASP mutants by immunofluorescence in VASP-deficient endothelial cells was peformed as described in figure 17B. B and C: Pictures were taken using the Nikon Eclipse E600 microscope equipped with a 100x objective. The pictures are representative of a series of 5 independent experiments.

5.2.5 Mimicked pS239 and pT278 increase the cellular G-actin pool

Several previous studies reported that VASP phosphorylation reduced actin polymerization *in vitro* and in living cells (Harbeck *et al*., 2000; Barzik *et al*., 2005; Zhuang *et al*., 2004). To examine the effect of different VASP phosphorylation patterns on actin polymerization, the set of arrested VASP mutants (AAA, ADA, AAE, ADE, DDA, DAE, DDE, and DAA) were tested by a serum response element (SRE)-controlled reporter assay. This assay allows the quantification of the cellular G-actin pool depletion by the observance of a rise of SRE-binding serum response factor (SRF) expression (Grosse *et al*., 2003). Increased SRF was measured indirectly using a reporter vector encoding a luciferase gene under the control of the SRE promoter, which binds SRF. In the nucleus, SRF binding enhances SRE promoter activity. Hence, high SRE activity indicates G-actin pool depletion and increased actin polymerization.

Initially, the expression of the arrested mutants was investigated. For that purpose, VASP-deficient endothelial cells were transiently transfected with cDNA encoding the constructs. Immunoblot analysis, using an antibody against His-tag, revealed that all mutants bearing an acidic residue at position 157 (DDE, DDA, DAE, and DAA) migrated with a higher apparent molecular mass of approximately 48 kDa in SDS-PAGE. In contrast to wild-type VASP, which is unphosphorylated at S157 and migrates at 46 kDa, VASP phosphorylated at S157 showed an electromobility shift from 46 to 50 kDa (Fig. 19). Mutants bearing an alanine residue at position 157 (AAA, ADA, AAE, and ADE) migrated as non-phosphorylated wild-type VASP did. The apparent molecular mass of the arrested mutants suggests that replacement with acidic amino acid residues and/or alanine residues at each phosphorylation site is an appropriate tool to analyze phosphorylation patterns.
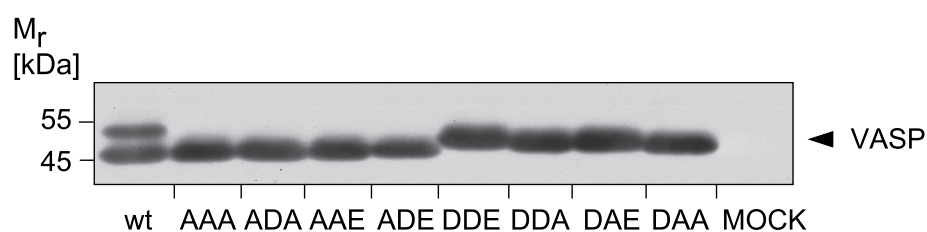
Figure 19. VASP mutants bearing an acidic amino acid residue at position 157 show an increased apparent molecular mass in SDS-PAGE.
VASP-deficient endothelial cells were grown on 6-well plates and transiently transfected with 500 ng of cDNA coding for arrested mutants, wild-type VASP or vector without insert (MOCK). After 24 h of expression, cells were lysed and lysates were separated by SDS-PAGE and analyzed for expression of arrested VASP mutants and wild-type VASP using antibody against His-tag.

To examine the effect of mimicked VASP phosphorylations on actin polymerization in living cells, arrested mutants and SRE-Assay was utilized. Cells were transiently transfected with plasmids coding for the arrested mutants and for the luciferase under control of a SRE-promoter. The SRE activity of mutants can be classified in three groups, corresponding to significant differences in SRE values (Fig. 20). The mutants AAA (set to 100%) and DAA (92%) showed the highest SRE-activities and are grouped together. The second group, with significantly diminished SRE activities as compared to AAA/DAA, comprises mutants DDA, ADA, DAE, and AAE. The SRE activities of these mutants were reduced down to 60%, 72%, 61%, and 68%, respectively. The third group consists of mutants DDE and ADE, which showed further decreased SRE activities down to 33% and 40%. SRE activities of all three groups were significantly different to each other ($p < 0.00001$). Interestingly, SRE activities of mutants within each group did not differ significantly.
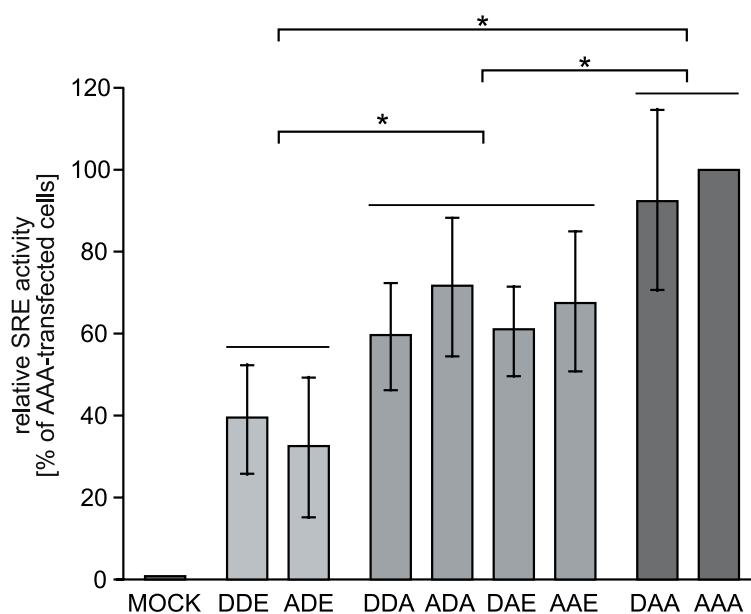
Figure 20. Mimicked phosphorylations at S239 and T278 increase cellular G-actin pool. HEK293 were transiently transfected with arrested VASP mutants (100ng cDNA), SRF reporter (500ng cDNA) and Renilla luciferase (250ng cDNA) as a transfection control. After 26 h of expression, the luciferase activity of cell lysates was measured. Three groups can be classified by SRE-activities of arrested mutants. SRE-activities of the three groups compared to each other were significantly different (n=7, *p<0.00001). In contrast, SRE-activities of VASP mutants within each group did not differ significantly. Arrested mutants, which mimic phosphorylated S239 and/or T278, increased the cellular amount of G-actin. Increase of SRE activity was dependent on the number of negative charges at S239 and T278. All SRE signals are given relative to AAA, which was set to 100%.

Grouping of arrested VASP mutants according to their SRE-activities parallels the number of acidic amino acid residues at S239 and T278: Group one bearing no acidic residues, group two with one acidic residue and group three with two acidic residues at these positions. The comparable SRE activities of AAA with DAA and DDE with ADE suggest that

VASP-mediated actin polymerization activity is independent of the phosphorylation state at position S157. Mutants of the second group showed no significantly different SRE activities despite differences in phosphorylation states. This indicates that mimicked phosphorylation at S239 or T278 makes an equal contribution to actin filament formation. Finally, the decreased SRE activity from the first to the third group of arrested mutants indicates that the amount of negative charge at S239 and/or T278 is critical for F-actin formation.

5.2.6 Mimicked pS239 and pT278 reduce cellular F-actin content

To confirm that mimicked phosphorylations at S239 and T278 interfere with actin polymerization, an independent approach that measures the F-actin content by FACS analysis was performed. Arrested VASP mutants were overexpressed in HEK293 cells. Mutants were immunofluorescence labeled using antibody against His-tag and FITC-conjugated secondary antibody. F-actin of the overexpressing cells was stained with Cy5-conjugated Phalloidin. Double labeling allowed the measurement of cellular F-actin content in overexpressing cells by FACS analysis. The F-actin contents of the transfected cells allowed for the formation of three groups, based on their significantly different F-actin values (Fig. 21A). In the first group, the highest F-actin amount was observed in cells transfected with AAA (set to 100%) or DAA (99%). In the second group, in comparison to AAA and DAA, F-actin content of cells overexpressing mutants DDA, ADA, DAE, or AAE was significantly decreased down to 76%, 80%, 79%, and 83%, respectively. In the third group, further diminished F-actin content down to 70% and 71% was observed in cells transfected with DDE or ADE. F-actin contents of the first ($p<0.0001$), the second ($p<0.005$) and third group were significantly different from each other (Fig. 21). Notably, the cellular F-actin content of the mutants within each group did not significantly differ. Representative F-actin measurements are shown in figure 21B. The F-actin contents of ADE and AAA overexpressing cells differed largely, whereas the F-actin contents of cells that overexpress ADE and DDE were similar. F-actin contents of cells overexpressing arrested mutants confirmed the data of the SRE-assay, and arranged arrested mutants into three groups corresponding to the number of acidic amino acid residues at S239 and T278. In summary, the effects of arrested VASP mutants on F-actin content indicate that actin polymerization is independent of the negative charge at S157 and is synergistically impaired by mimicked phosphorylation at S239 and T278.
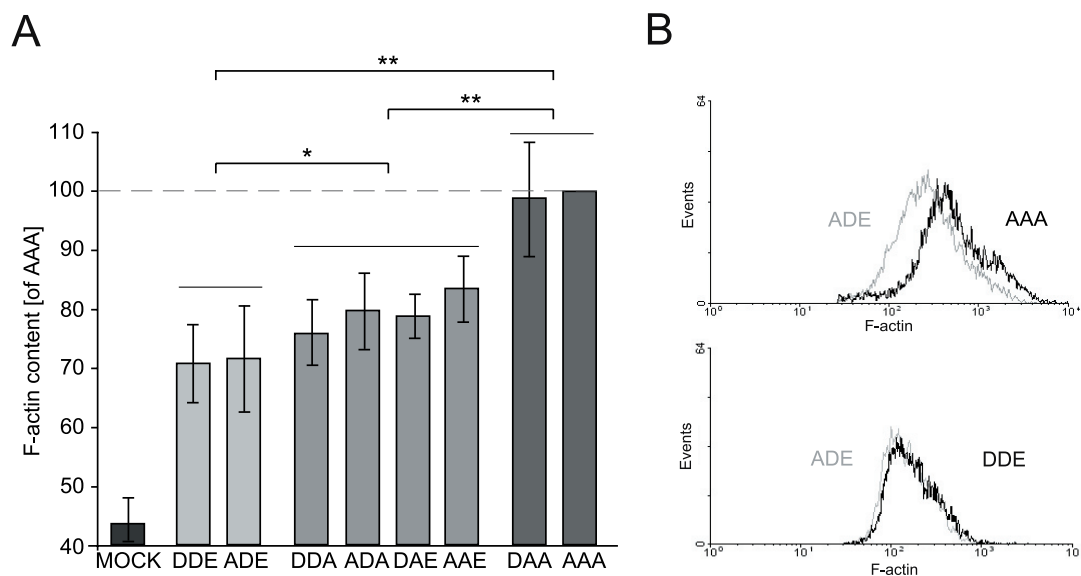
Figure 21. Mimicked phosphorylations at S239 and T278 reduce the cellular F-actin content.

A: HEK293 cells grown on 6-well plates were transiently transfected with 250 ng cDNA coding for His-tagged arrested mutants. After 48 h of expression, cells were trypsinized, fixed, permeabilized and immunoflourescence labeled with antibody against His, and F-actin was stained with Cy5-conjugated Phalloidin. The amount of F-actin in the overexpressing cells was measured by FACS analysis. Expression of arrested mutants, which mimic phosphorylation at S239 and/or T278, decreases the cellular amount of F-actin. The F-actin content of AAA-VASP mutant overexpressing cells was set to 100% (n=6, *p<0.005, **p<0.0001). B: Mimicked phosphorylation at S239 and T278 reduced the cellular amount of F-actin in contrast to S157D. F-actin contents of ADE expressing cells (gray curve) and DDE or AAA (black curve) expressing cells are compared in a histogram.

5.2.7 Phosphorylation at S239 and T278, mediated by PKG and AMPK, respectively, reduces actin polymerization

To confirm that mimicked phosphorylations at S239 and T278 but not at S157 impair actin polymerization, an independent approach using kinases-mediated phosphorylation was performed. Three partially arrested VASP mutants were generated. These mutants can be phosphorylated at only one of the three sites, whereas the other two phosphorylation sites were substituted by an alanine residue (SAA, ASA, and AAT; Fig. 22).
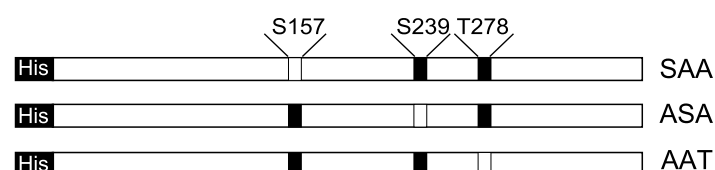
Figure 22. Schematic representation of the partially arrested VASP mutants.

The N-terminal His-tagged partially arrested VASP mutants, allowed only a single phosphorylation at one of three phosphorylation sites, whereas the other sites are mutated into alanine residues, which can not be phosphorylated.

Firstly, the effect of PKA-mediated phosphorylation on actin polymerization was examined. HEK293 cells were transiently transfected with cDNA coding for mutant SAA and SRE-controlled luciferase gene (Fig. 23). To stimulate S157 phosphorylation, PKA was activated in overexpressing cells by incubation with Forskolin (5 μM) for different time periods (0, 5, 20, 40, and 80 min). As controls, the SRE activity of the completely arrested mutants AAA and AAE was analyzed. The SRE activity of AAA-transfected cells was set to 100%. As a positive control, SRE activity of AAE-transfected cells was measured (46%). Under unstimulated conditions, SRE activities of SAA-overexpressing cells were 102%. Following PKA-stimulation SRE activities were largely unaltered (100%, 110%, 104%, and 99%, respectively). SRE activities of SAA-overexpressing cells before stimulation did not significantly differ to cells after treatment. To control the success of the PKA stimulation, pS157 was analyzed. Western blotting revealed an increasing S157 phosphorylation with a maximum after 20 min. In accordance with results of arrested mutants, SRE-assay of the partially arrested mutant SAA indicates that phosphorylation at S157, mediated by PKA, did not affect F-actin formation.
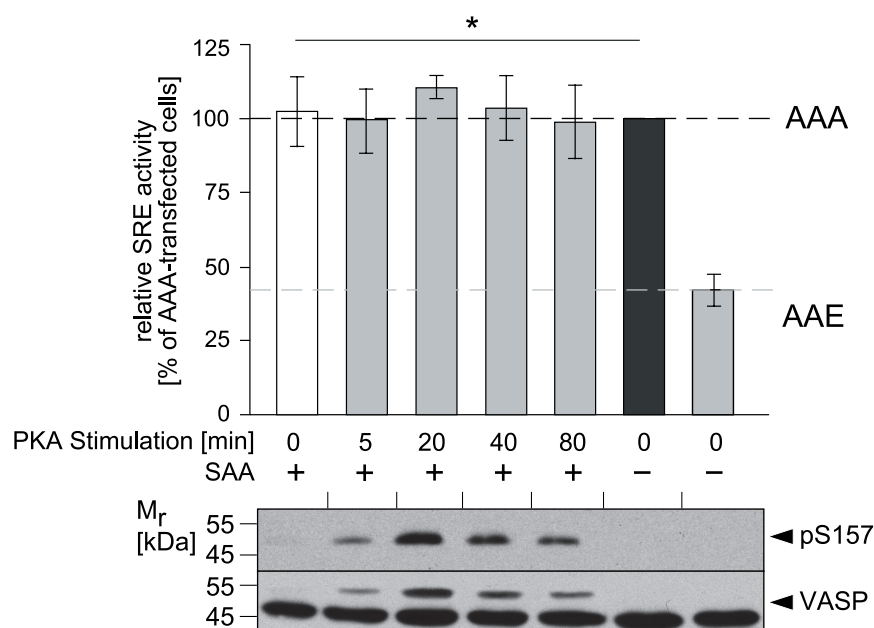
Figure 23. PKA-mediated phosphorylation at S157 does not influence actin polymerization.
HEK239 cells were transiently transfected with 100 ng cDNA coding for SAA, which allows phosphorylation at S157 and with reporter genes as described above. As a control, mutants AAA and AAE were analyzed. After 26 h of expression, cells were incubated with, or as a control without, 5 μM Forskolin for 5, 20, 40, and 80 min. Afterwards, luciferase activity of cell lysates was measured. Phosphorylation at S157 by PKA does not influence SRE-activities. All SRE signals are given relative to AAA-transfected cells (n=4, *p=ns). pS157 phosphorylation and VASP expression were confirmed by immunoblotting using antibodies against pS157 and VASP.

Secondly, the effect of PKG-mediated phosphorylation at S239 on actin dynamics was investigated using plasmids coding for PKG a wild-type (PKG$_{wt}$), or a catalytic inactive (PKG$_{CI}$) form. The catalytic inactive form of PKG was generated by an amino acid residue substitution (A405L; Smolenski *et al.*, 2000). HEK293 cells were transiently transfected with cDNAs coding for the VASP mutant ASA, the SRE-controlled luciferase gene, and either PKG$_{wt}$ or PKG$_{CI}$ (Fig. 24). As a control, SRE activities of cells transfected with arrested mutants AAA and ADA were analyzed. SRE-activity of AAA was set to 100%. ADA-overexpressing cells showed SRE-activity of 33%. Cells overexpressing the partially arrested mutant ASA without PKG showed SRE-activity of 116%. SRE activities of cells transfected with ASA and different amounts of PKG$_{wt}$ (0.01, 0.1 and 1.0 μg) were reduced down to 111%, 95%, and 76%, respectively. In contrast, SRE activities of cells transfected with ASA and different amounts of PKG$_{CI}$ (0.01 or 0.1 μg) were almost unaltered (113% and 121%). Western blot analysis of cell lysates using antibodies against pS239, VASP, and PKG (detecting both forms) revealed an increased S239 phosphorylation by overexpressing PKG$_{wt}$. In contrast, cells overexpressing PKG$_{CI}$ at comparable expression levels to PKG$_{wt}$ showed no detectable phosphorylation at this site. Taken together, an increase of VASP phosphorylation at S239 inverse correlates with SRE activity reflecting diminished actin polymerization.
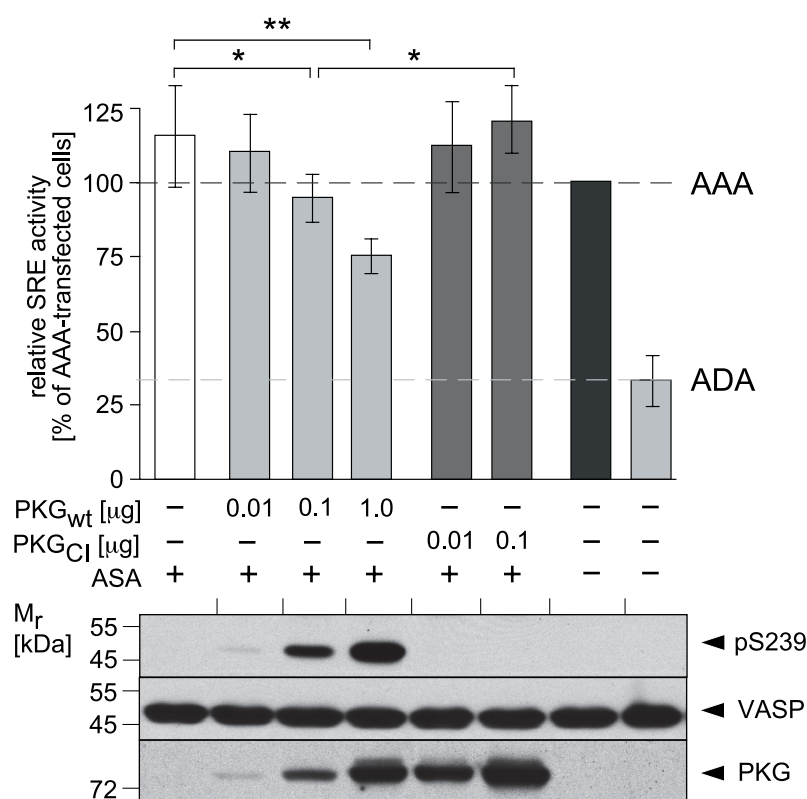
Figure 24. Phosphorylation at S239 mediated by PKG reduces actin polymerization. HEK239 cells were transiently transfected with 100 ng cDNA encoding for mutant ASA, which allows phosphorylation at S239, and with reporter constructs as described above. As a control, cells over-expressing arrested mutants AAA and ADA were measured. To induce S239 phosphorylation, cells were additionally transiently transfected

with different amounts of cDNA coding for PKG_{wt} or PKG_{Cl}. After 26 h of expression, cells were lysed and luciferase activity was measured. Phosphorylation at S239 mediated by PKG reduces SRE-activity. All SRE signals are given relative to the AAA-transfected cells (n=8; *p<0.05; **p<0.0001). S239 phosphorylation and expression of VASP mutants and PKG forms were confirmed by immunoblotting using antibodies against pS239, VASP and PKG.

Thirdly, the effect of AMPK-mediated T278 phosphorylation (Fig. 10) on actin dynamics was examined more precisely in an experiment using different amounts of cDNA of constitutively active or dominant negative forms of the AMPK α-subunit. HEK293 cells were transiently transfected with plasmids coding for the VASP mutant AAT, the SRE-reporter, and AMPK mutants (Fig. 25). The SRE activity of cells overexpressing arrested mutants AAA (set to 100%) and AAE (42%) was utilized as control. Cells overexpressing the partially arrested mutant AAT but not AMPK mutants showed a SRE activity of 93%. SRE activities of cells transfected with AAT and different amounts of CAα-encoding cDNA (0.5, 1.0, and 2.0 μg) were reduced down to 77%, 72%, and 64%, respectively, whereas transfection with DNα instead of CAα increase SRE-activities up to 103%, 107%, and 133%, respectively. Western blot analysis of the cell lysates using antibodies against pT278, VASP, and myc (detecting myc-tagged AMPK mutants) revealed an increased phosphorylation at T278 by overexpressing CAα. In contrast, phosphorylation at T278 by overexpressing DNα was decreased. The increase and decrease of pT278 therefore reflect the amount of CAα and DNα.

Taken together, VASP phosphorylation at T278 reduced SRE activity, correlating with the diminished actin polymerization. In contrast, actin polymerization was increased by reduced T278 phosphorylation due to the expression of dominant negative AMPK. These results indicate that AMPK-mediated T278 phosphorylation reduces actin polymerization and support the findings obtained with arrested mutants.
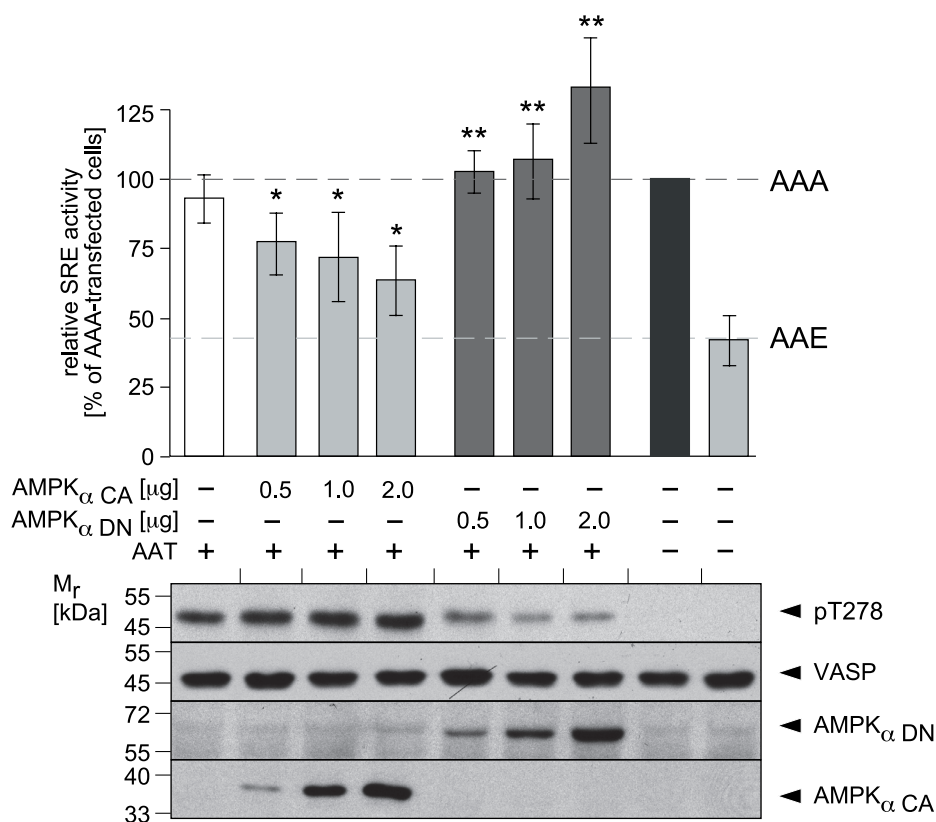
Figure 25. Phosphorylation at T278 mediated by AMPK reduces actin polymerization.
HEK239 cells were transiently transfected with 100 ng coding for mutant AAT, which allows phosphorylation at T278, and with reporter genes as described above. As a control, cells overexpressing the arrested mutants AAA and AAE were measured. To modulate phosphorylation at T278, cells were transiently transfected with cDNA coding for CAα or DNα and with mutant AAT. After 26 h, cells were lysed and luciferase activity was measured. All SRE signals are given relative to the AAA-transfected cells, which was set to 100% (n=6; *p<0.001; **p<0,05). T278 phosphorylation and expression of VASP and AMPK mutants were confirmed by Western blot using antibodies against pT278, VASP and against myc to detect tagged AMPK mutants.

To sum up the findings of the kinase-mediated effects on actin polymerization: VASP phosphorylation at S239 and T278 mediated by PKG and AMPK, respectively, reduced actin polymerization. In contrast, S157 phosphorylation by PKA did not modulate F-actin assembly.

The investigation of phosphorylation-regulated functions of VASP demonstrates that S157 phosphorylation enriches VASP at the cell periphery and that phosphorylations at S239 and T278 reduce actin polymerization. These results suggest that the differential regulation of VASP functions by phosphorylation, whereby pS157 regulates VASP targeting, and pS239 and pT278 determines the level of actin polymerization.

6 Discussion

6.1 AMPK phosphorylates VASP T278 and links metabolism to the cytoskeleton

Defective cytoskeleton organization has important implications for a variety of actin-based processes such as changes of cellular morphology and cell-cell or cell-matrix adhesion is suspected to be important for endothelial dysfunction in diabetic vessel disorders (Brownlee, 2001; Frank, 2004; Ruderman and Prentki, 2004). The first part of this work identified AMPK as a kinase responsible for VASP phosphorylation at T278 *in vitro*, in living cells, and in a rat model for diabetes mellitus typ II (Fig. 5, 6, 7, 12). AMPK-mediated T278 phosphorylation reduces VASP F-actin accumulation activity and thereby impairs stress fiber formation (Fig. 10, 11). Therefore, VASP phosphorylation at the T278 site mediated by AMPK directly links the regulation of metabolic energy to cytoskeletal control. A schematic model of the new proposed mechanism is given in figure 26.
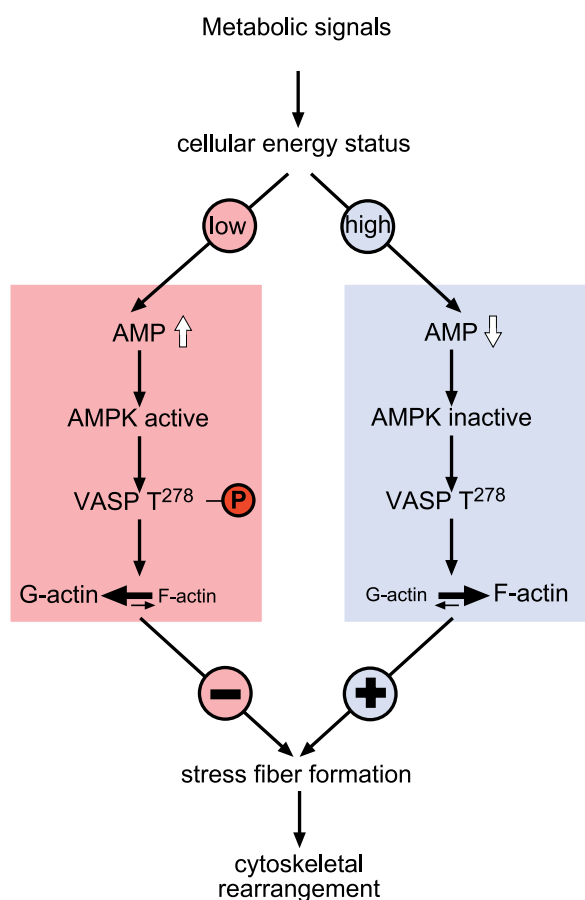
Figure 26: Proposed mechanism of AMPK-mediated cytoskeletal rearrangements driven by VASP T278-phosphorylation.
ATP consumption with concomitant increased AMP levels activates AMPK, which phosphorylates VASP at T278. T278-phosphorylation inhibits VASP actin polymerization activity and shifts the cellular G-/F-actin equilibrium towards the monomeric actin form. Impaired F-actin assembly results in morphological changes and cytoskeletal rearrangements. In contrast, high energy situations with full ATP stores and reduced AMP levels result in low AMPK activity and non-phosphorylated VASP T278. VASP-driven actin polymerization persists in the presence of non-phosphorylated T278. Actin stress fibers are formed, inducing changes in the cytoskeletal and cellular morphology.

6.1.1 Cellular function of AMPK-mediated T278 phosphorylation

Historically, AMPK was regarded as a sensor and regulator of the energy balance on the cellular level. AMPK was found to inhibit anabolic and initiate catabolic pathways by rapid, direct phosphorylation of rate-limiting enzymes. Different key enzymes of such metabolic pathways are substrates of the AMPK, for example, the AMPK-mediated phosphorylation of glycogen synthase (Carling and Hardie, 1989) and 6-phosphofructo-2-kinase (Marsin *et al.*, 2002), which preserves glucose homeostasis. Furthermore, AMPK switches off ATP-consuming enzymes of anabolic lipid metabolism pathways, for example, it phosphorylates acetyl-CoA carboxylase (Davies *et al.*, 1989) and HMG-CoA reductase (for a complete list of AMPK substrates, see Kahn *et al.*, 2005). In the last years, AMPK was reported to regulate the energy balance at the whole body level in response to hormone and nutrient signals in mammals. The modulation of hypothalamic AMPK activity was shown to alter food intake and body weight in transgenic mice (Minokoshi *et al.*, 2004) indicating that AMPK regulates appetite stimulation and inhibition (Kahn *et al.*, 2005). Furthermore, AMPK activity has been demonstrated to be important in the cardiovascular system. Mutations in the gene encoding for the regulatory γ2-subunit cause a hereditary heart disease, the Wolff-Parkinson-White syndrome (WPWS), in humans (Arad *et al.*, 2002). The important role of AMPK expands by the discovery of VASP as a substrate of AMPK in this study. AMPK specifically targets the VASP T278 site, but not S157 and S239, and the phosphorylation status of T278 seems to be independent of PKA- and PKG-mediated phosphorylations at S157 and S239 (Fig. 7 and 13). Despite T278 being specifically phosphorylated by AMPK, the amino acid sequence flanking T278 in human VASP (G-L-M-E-E-M-N-A-M-L-A-R-R-R-K-A-T278-Q-V-G-E-K-T-P) does partially match to the proposed consensus AMPK recognition motif, which harbors the core motif Hyd-(Basic, X)-X-X-Ser/Thr-X-X-X-Hyd (Hardie, 2003). What could be the functional consequence of AMPK-mediated VASP phosphorylation? The AMPK-site is located close to the C-terminal end of the B-block (positions 259-276) within the VASP EVH2 domain. The B-block of the EVH2 domain mediates binding to filamentous actin, and is critically involved in actin polymerization *in vitro* (Bachmann *et al.*, 1999) and in living cells (Grosse *et al.*, 2003). In this complex process of VASP-promoted actin polymerization, the two VASP domains EVH2 and PPR are involved (Ferron *et al.*, 2007).

The findings of this study, i.e. F-actin accumulation and stress fiber formation is impaired by AMPK-mediated T278 phosphorylation (Fig. 10, 11 and 25), is in accordance to previous studies (Harbeck *et al.*, 2000; Barzik *et al.*, 2005). In these *in vitro* assays, T278 phosphory-

lation impaired F-actin formation. The mechanistical rationale could be that AMPK-mediat-ed VASP T278 phosphorylation modulate the electrostatic interactions between the nearby arginine residues (R273, R274, R275) of the B-block and the negatively charged actin filament. Indeed, PKG- and PKA-mediated phosphorylation of S239 within the A-block, another motif important for VASP-mediated F-actin formation, supports the concept that phosphorylations of sites within EVH2 inhibit actin polymerization *in vitro* (Harbeck *et al.*, 2000) and in living cells (Zhuang *et al.*, 2004). The functions of T278 phosphorylation are not easily deducible by comparison to other Ena/VASP family members, because within the protein family the T278 site is unique to VASP. This phosphorylation site may have evolved late in evolution, and may allow a more complex regulation of VASP in comparison to Ena and Mena/Evl (Han *et al.*, 2002; Kwiatkowski *et al.*, 2003). In future investigations, one challenge would be to understand why this additional regulation of VASP is required.

6.1.2 PKA and PKG do not phosphorylate T278

One of the surprising findings of this study was that the cyclic nucleotide-dependent protein kinases, PKA and PKG, do not phosphorylate VASP at the T278 residue in living cells. Pre-vious data, based on *in vitro* experiments using the purified PKA catalytic-subunit and PKG, suggested that T278 might be targeted by these kinases (Butt *et al.*, 1994). However, even following long-term incubation with PKA, the magnitude of pT278 was minor as compared to S157 and S239 phosphorylation *in vitro* (Butt *et al.*, 1994). PKA has a low preference for T278 (Harbeck *et al.*, 2000). Indeed, in an attempt to reproduce T278 phosphorylation by PKA and PKG *in vitro*, according to the study of Butt and co-workers, T278-phosphorylation was detected using Western blot analysis. However, pT278 VASP migrated with an appa-rent molecular weight of 50-60 kDa in the SDS-PAGE. In contrast, phospho-VASP purified from PKA-stimulated cells migrates as a doublet of 46 and 50 kDa (Halbrugge *et al.*, 1990), with the upper band representing the S157-phosphorylated protein. This discrepancy might indicate that pT278-positive VASP, which is excessively phosphorylated *in vitro* by PKA and PKG, is not likely to be found under physiological conditions. In endothelial cells, even un-der maximal stimulation, PKA- and PKG-mediated T278 phosphorylation was not increased (Fig. 4). These findings are supported by data from Butt and co-workers. They reported that pT278 was not increased after stimulation of PKA and PKG in human platelets (Butt *et al.*, 1994). Under basal conditions, T278 in endothelial cells was considerably phosphorylated, in contrast to minor basal phosphorylation of S157 and S239 (Fig. 4). This basal constituti-

ve T278 phosphorylation is consistent with basal pT278 levels observed in human platelets (Butt *et al*., 1994). Taken together, the present study demonstrates that AMPK specifically phosphorylates T278 *in vitro*, in primary and stable cell lines and animal models.

6.1.3 Function of VASP phosphorylation for diabetic vessel disorder

The first part (section 5.1) of this work focused on AMPK-mediated VASP phosphorylation in endothelial cells and vascular walls. These cells and tissue were chosen because AMPK signaling pathway is implicated in defective glucose metabolism (Lage *et al*., 2008) and has an importance in diabetic vessel disorders, such as diabetic retinopathy (Kim *et al*., 2007; Yu *et al*., 2005), or microvascular leakage (Yu *et al*., 2005). One of the important findings of this study was that pT278 is decreased and accompanied by reduced pS239, in contrast to the unaltered pS157 levels, in vessels of diabetic animals (Fig. 13). The parallel decrease of pS239 and pT278 levels suggests the existence of a crosstalk between NO/cGMP/PKG signaling, which regulates S239-phosphorylation in the endothelium (Smolenski *et al*., 2000) and AMPK-mediated pathways in diabetic conditions. Several mechanisms might explain the co-regulation of PKG-dependent S239 phosphorylation with AMPK-mediated pT278. Recently, a direct link between AMPK and NO/cGMP/PKG signaling has been established. Endothelial nitric oxide synthase (eNOS) can be directly phosphorylated by AMPK at S633 and S1179 (Chen *et al*., 2009; Davis *et al*., 2006). This induced eNOS-phosphorylation at both phosphorylation sites results in an increased eNOS activity and NO bioactivity (Chen *et al*., 2009; Davis *et al*., 2006). Stimulated eNOS increases PKG activity, resulting in an increased VASP phosphorylation at S239 (Schmidt and Walter, 1994). Conversely, diminished AMPK-activity reduces induced eNOS-phosphorylation (Davis *et al*., 2006; Chen *et al*., 2009) and, in turn, decreases VASP phosphorylation at S239 via the NO/cGMP/PKG pathway. Under pathological glucose conditions, the NO/cGMP/PKG signaling pathway is impaired and AMPK activity as well as reactive oxygen species (ROS) are increased. The uncoupling of eNOS by ROS and the subsequent decrease in vascular bioavailability of NO are critical for the development of endothelial dysfunction (reviewed by Munzel *et al*., 2005). Increased oxidative stress due to increased ROS production have been shown to activate AMPK (Zou *et al*., 2004). AMPK activation in response to oxidative stress may be implicated in an anti-oxidative role in endothelial cells (Zou and Wu 2008), because several studies reported that activated AMPK reduces ROS production (as reviewed by Zou and Wu, 2008). These findings support the notion that AMPK has a beneficial effect on endothelial

function by suppressing oxidative stress in endothelial cells. Future studies would provide new insights into the coupling of AMPK and NO/cGMP/PKG signaling pathways, and the role of pS239 and pT278 in the development of endothelial dysfunction.

Data of the present study demonstrate that VASP phosphorylations at S239 and T278 impair F-actin formation, and influence cytoskeletal rearrangement (Fig. 20, 21, 24 and 25). Previous data support these findings, they showed that pS239 and pT278 inhibit actin polymerization *in vitro* (Harbeck *et al*., 2000). Less is known about the influence of metabolism on actin reorganization in living cells or *in vivo*. A previous study reported that the actin cytoskeleton is expanded in retinal endothelial cells of diabetic rats and is associated with diabetic retinopathy (Yu *et al*., 2005). It will be interesting to determine the phosphorylation states of the three VASP phosphorylation sites in this diabetic model using phospho-specific antibodies, which are valuable tools. These antibodies (anti-pS157, -pS239, and -pT278) offer the opportunity to quantify and to dissect PKA, PKG, and AMPK-mediated signaling via differential VASP phosphorylations *in vivo* and may help to answer questions such as: how these signaling pathways crosstalk and what their implication for endothelial dysfunction via VASP phosphorylation is.

6.2 VASP phosphorylations regulate the subcellular localization and the actin dynamics

In section 5.2, differential VASP phosphorylations were shown to modulate VASP functions in living cells. Firstly, phosphorylation at S157 enriches VASP at focal adhesions and the plasma membrane, but does not influence actin polymerization. Secondly, phosphorylations at S239 and T278 diminish VASP localization at actin filaments and decrease actin polymerization. A summary of VASP phosphorylations and the physiological consequences are shown in figure 27.
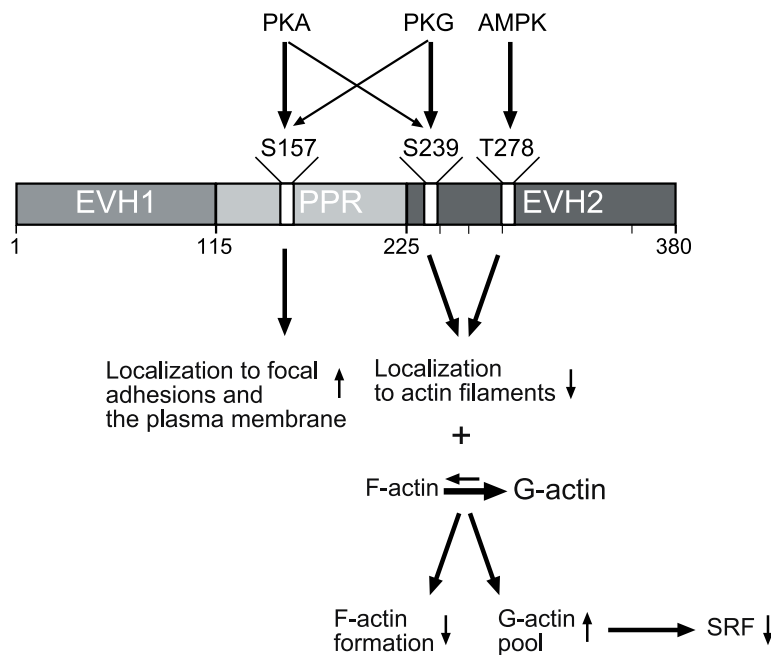
Figure 27. Scheme of phosphorylation-regulated VASP functions
VASP functions are regulated by phosphorylation at the three residues S157, S239 and T278. VASP is predominantly phosphorylated at S157 by PKA and at S239 by PKG. This study shows that T278 is phosphorylated by AMP-activated protein kinase. S157 phosphorylation is important for VASP subcellular localization. pS157 enriches VASP at focal adhesions and the plasma membrane. Phosphorylations at S239 and T278 impair actin polymerization, as indicated by reduced F-actin formation, and increased G-actin pool, which leads to an enhanced serum response element activity. pS239 and pT278 seem to detach VASP from actin structures.

6.2.1 Function of VASP S157 phosphorylation

The present study demonstrated that S157-phosphorylation enriches VASP at focal adhesions and the plasma membrane of murine endothelial cells (Fig. 14, 15, and 17). This data is in line with several previous studies in various other endothelial cells (Comerford et al., 2002; Profirovic et al., 2005), platelets (Wentworth et al., 2006), and prostate cancer cells (Hasegawa et al., 2008), which reported that pS157, mediated by PKA and PKC, increases VASP localization to the cell periphery, which includes cell-cell junctions, the plasma membrane and focal adhesions. Even more noteworthy, S157-phosphorylated VASP enriches at the luminal plasma membrane of endothelial cells in intact vessels (Fig. 13). The present results suggest that S157 phosphorylation is primarily a switch to target VASP to the subcellular site, where VASP is needed.

The pS157-dependent localization of VASP is contradictory to the findings by Smolenski and co-workers in HUVECs (Smolenski et al., 2000). They reported that S239 phosphorylation by PKG results in a loss of VASP and zyxin from focal adhesions. Phosphorylation-dependent

subcellular VASP localization was investigated using immunolocalizations in cells, that overexpressed the wild-type form or a catalytic inactive form of PKG with and without stimulation. Western blot analysis showed that treatment of wild-type overexpressing cells with various PKG activators increased VASP phosphorylation at its primary site (S239) and at S157 (Smolenski *et al.*, 2000). Furthermore, these Western blots revealed that wild-type PKG is active at a lower level without stimulation in HUVECs. With regard to the finding of the present study that pS157 enriches VASP at focal adhesions and at the plasma membrane, it can be assumed that PKG overexpression and stimulation would increase VASP targeting to the cell periphery. At present, no obvious explanation for this discrepancy could be found. Differences may be due to the usage of varying cell lines, or to other phosphorylations, apart from VASP by PKG, which are involved in focal adhesion disassembly, for example, p21-activated kinase 1 (Fryer *et al.*, 2006).

As analysis of dynamic phosphorylation mediated by kinases has several disadvantages, for example, the phosphorylation of more than one substrate and the activation of crosslinking pathways, this work intentionally concentrated on the constitutive "stable" phosphorylation states and therefore utilized phospho-substitution and alanine-substitution VASP mutants. pS157 increases VASP localization at the cell periphery, as shown by subcellular localization of endogenous VASP and confirmed by His-tagged arrested full-length VASP mutants (Fig. 14 and 17). However, contrary results were published using phosphomimetic mutants of VASP (Harbeck *et al.*, 2000) and Mena (Loureiro *et al.*, 2002). Immunolocalization studies of VASP and Mena mutants in myoblasts and fibroblasts reported that mimicked phosphorylation did not alter subcellular localization of VASP and Mena, as compared to the wild-type protein. Possible explanations for contradictory results of the phosphormimetic VASP and Mena mutants could be that these proteins were fused to an EGFP-tag in contrast to His-tagged VASP mutants used in the present study. Compared to 45 kDa-VASP-protein the EGFP-protein of 27 kDa increases the size of the fusion protein and may influences interaction and localization. Furthermore, N-terminal GFP- or YFP-tagged VASP was reported to show only a weak effect on actin polymerization, as compared to untagged VASP (Grosse *et al.*, 2003). These findings indicate that large sized protein tags affect VASP functions.

The present study demonstrated that pS157 enriches VASP at the cell periphery and investigated the contribution of VASP domains to the S157-phosphorylation dependent

localization. The EVH1 domain-mediated interactions with zyxin, vinculin, migfilin, and lamellipodin have been implicated in VASP targeting to focal adhesions and the plasma membrane. Besides effects due to the EVH1 domain, VASP localization is influenced by the EVH2-mediated protein-protein interactions. Truncated mutants lacking the EVH2 domain were used to investigate the independence of VASP localization to the cell periphery from the EVH2 domain. The EVH1 domain and the N-terminal part of the PPR are sufficient for cell periphery localization of VASP (Fig. 15). When compared to the full-length VASP, truncated mutants (without EVH2 domain) were found less prominently at the plasma membrane. These findings are consistent with the data from Bear and co-workers, who localized an EVH1 domain of Mena in Mena/VASP-deficient and wild-type fibroblasts (Bear *et al*., 2000). The Mena-EVH1 domain was localized to the leading edge and at focal adhesions, but EVH1 mutants were also found diffusely distributed in the cytoplasm and nucleus. As observed for the Mena EVH1 domain, a comparable targeting was previously reported for the VASP EVH1 domain (Huttelmaier *et al*., 1999). In fibroblasts, only weak localization of VASP EVH1 domain to focal adhesions, but also widespread distribution throughout the cytoplasm and the nucleus was observed. This diffuse localization cannot be due to an effect of overexpression driven by the CMV-promoter since the full-size VASP or Mena overexpressed under same promoter was found at F-actin, the cell periphery and cell-cell-contacts, comparable to the endogenous protein. The data from localization studies suggest that the tetramerization of VASP or Mena, mediated by a coiled-coil motif in the EVH2 domain, contributes to the subcellular targeting of the protein (Bear *et al*., 2002). Ena/VASP family members form homo- and hetero-tetramers (Kuehnel *et al*., 2004). This interaction seems to be involved in a series of VASP functions, including subcellular localization, but detailed investigations are lacking.

Cell periphery localization of S157-phosphorylated VASP is either due to a translocation of pS157 VASP, or to a phosphorylation of S157 at focal adhesions and at the plasma membrane. Until now, this question remains open, albeit various data indicate that VASP is phosphorylated at the cell periphery. S157-phosphorylation levels may be mediated by PKA, but PKC and/or PKG may also contribute. Part of the cellular PKA is targeted to the plasma membrane by binding to A-kinase anchoring proteins (AKAPs; Wong and Scott, 2004). The presence of more than 50 structurally diverse, but functionally similar AKAP family members, each located differently within the cell, facilitates compartmentation of

PKA signaling (Wong and Scott, 2004). Besides PKA localization at the cell periphery, VASP phosphorylation requires PKA activity, which is regulated by cAMP. The spatiotemporal regulation of cAMP signaling involves point sources of cAMP generation within sub-domains of the plasma membrane by adenylate cyclase (AC), and cAMP degradation by spatially segregated, anchored forms of phosphodiesterases (PDE; Willoughby *et al*., 2006). The membrane-associated ACs (mACs) are found in distinct plasma membrane sub-domains held by interactions with PKA, PDE, and AKAPs, thereby generating spatially segregated "clouds" of cAMP (Cooper *et al*., 2005). In these complexes, PDEs play a pivotal role in shaping and controlling the intercellular cAMP-gradient by sole means of degrading cAMP. Interestingly, gravin interacts not only with PKA and PDE, but also with PKC (Willoughby *et al*., 2006), which phosphorylates VASP at S157. This interaction between PKC and gravin, results in the recruitment of PKC to the plasma membrane. In addition, the activation of conventional (α, β, γ) and novel (δ, ε, η, θ) isoforms of PKC involves their recruitment to the plasma membrane (Parker *et al*., 2004). The plasma membrane localization of PKA and PKC by AKAPs and PDEs corroborates the notion that VASP-phosphorylation at S157 occurs in close proximity to the plasma membrane.

Function of S157 phosphorylation in cell migration and adhesion was and is an interesting subject of investigations. At the leading edge, VASP plays an important role for lamellipodia dynamics and cell motility in fibroblasts, melanoma and prostate cancer cells (Bear *et al*., 2000; Rottner *et al*., 1999; Howe *et al*., 2005; Hasegawa *et al*., 2008). The concentration of VASP at the leading edge is proportional to the velocity of protrusion (Rottner *et al*., 1999). Since VASP at the cell periphery is phosphorylated at S157, it is tempting to speculate that the concentration of pS157 is important for protrusion. In prostate cancer cells, S157 phosphorylation was required for cell migration (Hasegawa et al., 2008). In these migrating cells, pS157 was localized to the plasma membrane and focal adhesions. Furthermore, S157-phosphorylation is demonstrated to be involved in cell adhesion and cell spreading of fibroblasts and epithelial cells (Howe *et al*., 2002). After detachment of these adherent cells, pS157 was increased up to 95% of the total VASP. Early after the adhesion of cells, where cells were attached but rounded, pS157 was rapidly and completely dephosphorylated. Later, during cell spreading, pS157 was increased to an intermediate magnitude and afterwards returned to the baseline level. Benz and co-workers confirmed pS157 increase in detached and freshly seeded endothelial cells (Benz *et al*., 2008). The decrease of pS157 was related

to the formation of cell-cell contacts during spreading. In confluent cells, in which cell-cell contacts are formed, only trace amounts of pS157 VASP were detected. In epithelial cells, PKA-mediated VASP phosphorylation at S157 was required for VASP localization at cell-cell contacts during tight junction assembly (Kohler *et al*., 2004). In smooth muscle cells, S157-phosphorylation mediated by PKC promoted cell proliferation (Chen *et al*., 2004).

Since this work demonstrated that pS157 does not directly influence actin-polymerization but does regulate VASP localization, it can be speculated that phosphorylation at S157 indirectly influences actin-based processes of cell migration. This phosphorylation changes VASP localization and in the new environment the F-actin forming activity of S157-phosphorylated VASP is regulated by phosphorylation at the other two sites. Other arguments support the hypothesis that pS157 is not important for the F-actin accumulation. Firstly, *in vitro* investigations of pS157 revealed no influence on actin polymerization and anti-capping activity of VASP (Barzik *et al*., 2005). Secondly, S157-phosphorylation within the PPR does not interfere with VASP binding of profilin *in vitro* (Harbeck *et al*., 2000). Interaction of the PPR and profilin is critical for F-actin formation. The PPR recruits profilin-actin complexes and directs the transition of profilin-actin to the EVH2 domain from where the actin monomer can join the growing filament (Ferron *et al*., 2007). The additional contribution of PPR-profilin binding to filament elongation is probably caused by increasing the local concentration of actin monomers (Reinhard *et al*., 1995; Chereau *et al*., 2006; Krause *et al*., 2003; Sechi and Wehland, 2004; Ferron *et al*., 2007).

Other PPR-mediated VASP interactions are influenced by S157 phosphorylation such as binding to Abl. The Abl kinase relays signals from growth factors and adhesion receptors to the cytoskeleton (Hernández *et al*., 2004). In this process, Abl regulates cytoskeletal rearrangement by phosphorylating several cytoskeletal regulatory proteins, or by direct interaction with F- and G-actin. This may explain why Abl-deficient fibroblasts exhibit a reduced membrane ruffling, while Abl overexpression in fibroblasts inhibits cell migration (Hernández et al., 2004). The interaction of Abl and VASP is inhibited by pS157 and is regulated in cell mobility processes (Howe *et al*., 2002). During cell detachment and spreading, S157-phosphorylation was increased and paralleled by a reduced VASP-Abl interaction (Howe *et al*., 2002). In protrusive cellular structures like pseudopodia, enhanced PKA-activity and VASP S157-phosphorylation was required for efficient chemotactic cell migration (Howe *et al*., 2005). In prostate cancer cells, PKA activity and pS157 were required for random and directional cell migration (Hasegawa *et al*., 2008). Abl phosphorylates

tyrosine residues of Mena and Ena (Tani *et al*., 2003; Comer *et al*., 1998). Recently, tyrosine phosphorylations of VASP was reported (Rikova *et al*., 2007), but the responsible kinase and the functional effects remain unknown. Indeed, the biochemical consequence of the VASP-Abl interaction is currently unknown. It is speculative that Abl-VASP interaction influences the functions of both proteins with an implication for cell motility.

Besides interaction with Abl, VASP binds pS157-dependently to αII-spectrin (SPCN; Benz *el al*., 2008). Spectrins are gaint scaffold proteins, which assemble a multifunctional interface that links membranes to actin filaments of the perijunctional cytoskeleton. VASP phosphorylation at S157 abolished the interaction of the PPR of VASP and the SH3 domain of SPCN. In endothelial cells, VASP and SPCN were co-localized to cell-cell junctions. Analysis of paracellular permeability in VASP $^{+/+}$ and VASP$^{-/-}$ cells, as well as investigations in a skin vascular leakage model, showed that VASP-SPCN complexes stabilize cell contacts with implication for vascular barrier integrity, and this process is regulated by pS157.

From the present data and the relevant literature regarding pS157 subcellular localization (Comerford *et al*., 2002; Profirovic *et al*., 2005; Howe *et al*., 2005; Wentworth *et al*., 2006) and implications of pS157 on actin-based processes (Howe *et al*., 2002; Hasegawa *et al*., 2008), it can be hypothesized that pS157 is necessary for directed cell movement by targeting VASP to defined subcellular sites. Apparently, pS157 influences actin-based processes without direct involvement in actin dynamics, but rather by subcellular targeting of VASP.

6.2.2 Mimicked phosphorylation as a tool to study the effects of phosphorylation

The approach of mimicked phosphorylations by acidic amino acid residues and blocked phosphorylation by alanine residues is well established. Diverse phosphorylation-dependent effects have been investigated using this strategy (Trautwein *et al*., 1993; Engel *et al*., 1995; Gu *et al*., 2006). For example, Trautwein and co-workers investigated the influence of S105 phosphorylation of NF-IL6/LAP, a transcriptional activator of cytokine genes (Trautwein *et al*., 1993). This study convincingly demonstrated that the alanine substitution mutant did not change their activity after stimulation (phorbol 12-myristate 13-acetate), in contrast to the wild-type, which showed an increased activity. Aspartic acid mutant revealed that NF-IL6/LAP phosphorylation enhances their transcriptional efficacy in a comparable manner to that of the wild-type after stimulation. Furthermore, phosphomimetic and alanine mutants were used to investigate the regulation of kinase activity of mitogen-activated protein kinase

activated protein (MAPKAP) kinase 2 (Engel *et al*., 1995). MAPKAP kinase 2 mutants bear an alanine or a glutamic acid at phosphorylation sites at T205 and T317. Investigation of kinase activity of these mutants showed that both phosphorylation sites regulate MAPKAP kinase 2 activity. Mutants showed comparable activity to the wild-type with and without heat shock treatment. Furthermore, in the previous study from Gu and co-workers, phosphomimetic mutants were utilized to investigate the phosphorylation-dependent effect of the 14-3-3 protein, an important regulator of cell signaling components (Gu *et al*., 2006). They examined the influence of PKA-mediated phosphorylation on the dimerization and the interaction of 14-3-3 protein with other proteins using PKA activity modulation, and phosphomimetic mutants. This study demonstrated that the unphosphorylated wild-type protein as well as the alanine mutant showed an enhanced dimerization and interaction with p53. In contrast, the phosphorylated wild-type protein and the phosphomimetic mutant failed to form homodimers and had a reduced interaction with p53. Previous studies showed that the effects of mimicked phosphorylations and kinase-mediated phosphorylations on protein functions are comparable (Gu *et al*., 2006; Trautwein *et al*., 1993). Therefore, phosphomimetic mutants have been demonstrated to be a valuable tool to investigate the effects of phosphorylations and were thus utilized in the present study.

6.2.3 Function of VASP S239 and T278 phosphorylation

Binding of VASP to actin is an electrostatic interaction, which causes charge-sensitivity. The presented immunolocalization data indicate that mimicked phosphorylations at S239 and T278 reduce VASP interaction to actin filaments (Fig. 17), which is in accordance to the reduced VASP F-actin binding *in vitro* (Harbeck *et al*., 2000). Detachment of VASP from actin filaments seem to be beneficial for pS157-induced VASP-targeting to focal adhesions and the plasma membrane (Fig. 17). In contrast, no influence on VASP localization by mimicked phosphorylations at S239 and T278 were observed in myoblasts (Harbeck *et al*., 2000). The reasons for this controversial finding might be due to different experimental settings, like utilization of EGFP-tags instead of His-tags and usage of myoblasts instead of VASP-deficient endothelial cells (see section 6.2.1).

One important finding of the present study was that phosphorylations at S239 and T278 reduce actin polymerization in a similar manner (Fig. 20, 21). The magnitude of decreased F-actin formation was comparable between the arrested mutants, which harbor one acidic amino acid at either S239 or T278. This result suggests that phosphorylation within, or near the G- or F-actin binding region of VASP interferes with the actin polymerization process in a

similar way. It is known from truncated VASP mutants lacking the G- or F-actin binding region that the interaction with actin filaments is necessary for actin polymerization (Bachmann *et al*., 1999). *In vitro* actin polymerization assays with murine VASP mutants, harboring amino acid substitutions within the G-actin binding motif (R232E and K233E or R232G and K233E), revealed that intact G-actin interaction was required for F-actin formation (Walders-Harbeck *et al*., 2002). In consideration of the model of actin filament elongation described by Ferron and co-workers, it can be suggested that pS239 interferes with the transition of profilin-actin from the PPR to the G-actin binding region of EVH2 (Ferron *et al*., 2007). Reduced F-actin formation is further diminished by T278 phosphorylation, which hinders VASP binding to the growing actin filament.

The present finding that phosphorylations at S239 and T278 interfere with actin polymerization (Fig. 20, 21, 24, 25) is in line with several previous studies (Barzik *et al*., 2005; Zhuang *et al*., 2004; Harbeck *et al*., 2000). Both *in vitro*-phosphorylated VASP and phosphomimetic mutants reduce actin polymerization and anti-capping activity *in vitro* (Harbeck *et al*., 2000; Barzik *et al*., 2005). A study in glioma and smooth muscle cells investigated PKG-mediated effects on SRE-activity using arrested and partially arrested VASP mutants (Zhuang *et al*., 2004). They demonstrated that VASP-phosphorylation reduces F-actin formation, as indicated by decreased SRE-activity. Each of the three VASP phosphorylation sites were separately investigated utilizing overexpression of VASP mutants and wild-type PKG. Zhuang and co-workers reported that VASP phosphorylation at S239 by PKG decreased SRE-activity. pS157 has some contribution to this reduced activity, but pT278 shows no influence. T278-phosphorylation was investigated using PKG-activator in living cells without a readout-assay for phosphorylation level at this site. It is tempting to speculate that the SRE-activity was not altered, because the T278 phosphorylation level remained unchanged.

The influence of pS239 and pT278 on actin-based processes in living cells is less understood as compared to pS157. A Mena mutant, which mimicked phosphorylation at S376 (corresponds to S239 in human VASP), did not alter the migration speed of fibroblasts (Loureiro *et al*., 2002). In contrast, the Mena mutant S236D (corresponds to S157 in human VASP) reduced cell migration speed. Interestingly, the Mena double mutant MenaDD (S236D and S276D) showed further reduced cell speed as compared to S236D, indicating a modulation by S376D. Expression of Mena double mutants MenaDD and MenaAA (S236A

and S276A) in Mena- and VASP-deficient fibroblasts influenced the spreading phenotypes of these cells (Applewhite *et al*., 2007). MenaAA led to a ruffling phenotype as compared to wild-type Mena and MenaDD. This ruffling phenotype was described as a wave-like structure undergoing cycles of protrusion and retraction throughout the time of spreading. In contrast, the expression of VASP mutants AST, AAT, and AAA in these fibroblasts increased filopodia formation when compared to each other, but not when compared to wild-type VASP (Applewhite *et al*., 2007). The phosphorylation status of wild-type VASP remains unclear in this study. Therefore, investigation of the spreading phenotype of fibroblasts that express fully arrested VASP mutants would be of interest in order to examine the role of VASP phosphorylation.

Variuos previous studies investigated the role of VASP phosphorylation mediated by kinases in cell migration (Benz *et al*., 2008; Lindsay *et al*., 2007; Howe *et al*., 2002). A comprehensive investigation of pS239 in human epithelial cells showed that pS239 results in a loss of lamellipodial protrusion and cell rounding (Lindsay *et al*., 2007). This study investigated the functional effects of PKG-mediated pS239 using NO and a cGMP synthase inhibitor, as well as phosphomimetic and alanine mutants. They showed that after PKG stimulation, pS239 was increased and VASP was removed from the cell edge, resulting in the withdrawal of the cell edge and rounding of the cell. SDT mutants reduced cell migration speed, as compared to wild-type VASP. A study in fibroblasts, showed that during re-attachment and spreading of fibroblasts S239 phosphorylation is regulated (Howe *et al*., 2002). pS239 was reduced 15 minutes after replating of cells. In contrast, pS239 in endothelial cells was not detectable during spreading, but cells were analyzed for phosphorylation 3, 6, 12, 24, 48, and 72 hours after replating (Benz *et al*., 2008). It can be assumed that the S239 phosphorylation level is altered during re-attachment and spreading, but the pS239 magnitude changes within a short time frame.

All these data of pS239 indicate that phosphorylation at S239 regulates cell movement processes. It is tempting to speculate that pS239 is critical for processes like rounding and detaching, where a withdrawal of the actin cytoskeleton is required.

Due to its implication in the regulation of actin-based processes, VASP is associated with a plenty of basic cellular functions, which are temporally and spatially regulated. Therefore phosphorylation-regulated functions of VASP are and remain an interessing field of investigation.

6.3 Outlook

The first part (section 5.1) of this study identified the AMPK-mediated T278-phosphorylation and demonstrated an implication of pT278 in diabetes. Future studies should investigate VASP phosphorylations and actin dynamics in different metabolic conditions, in order to elucidate the role of AMPK in this context. These studies could address questions like: which actin-based processes are up or down regulated in different energy stages in cells. The VASP T278-phosphorylation extends the list of AMPK-substrates and it is possible that other actin-binding proteins are phosphorylated by AMPK. This phosphorylation may also modulate actin polymerization, or other actin assembly processes such as nucleation, branching, depolymerization, and anti-capping. The analysis of the contribution of a defective actin cytoskeleton in endothelial dysfunction could also be of medical interest. The comparison of pT278 and pS239 in disease like atherosclerosis, hypercholesterolemia, hypertension, and (re)stenosis could further reveal the importance of VASP phosphorylation *in vivo*.

The second part of this work (section 5.2) provides new insights into phosphorylation-regulated VASP functions. To continue this work one might consider investigating cells in different stages of movement (i.e. detaching, re-attaching, and spreading) for i) spatially defined VASP phosphorylations, ii) changes in the F-actin/G-actin equilibrium and iii) VASP protein complex formation and dissociation at defined cellular structures like focal adhesions. Future studies of VASP functions should take into consideration the influence of hetero-tetramerization of VASP with Ena/VASP family members on their functions and examine these effects precisely. In the last two years, proteomic high throughput screenings have identified potential novel phosphorylation sites of VASP besides the three known sites (Rikova *et al*., 2007; Dephoure *et al*., 2008; Zahedi *et al*., 2008). Future studies have to confirm these novel phosphorylation sites and have to verify their physiological role. It is likely that analyses of VASP by mass spectrometry in general will allow the identification of novel sites of modification by phosphorylation and acetylation, as was seen in the case of Cortactin, an actin-binding protein. In the last years, nine sites of acetylations within the F-actin binding region (Zhang *et al*., 2007), and 17 novel phosphorylation sites, besides the known five sites, were identified (Martin *et al*., 2006). Identification and analysis of such possible modifications would open up new ways to understand the regulation of VASP functions.

7 References

Abel, K., Mieskes, G., and Walter, U. (1995). Dephosphorylation of the focal adhesion protein VASP *in vitro* and in intact human platelets. FEBS Lett. 370, 184-188.

Arad, M., Benson, D. W., Perez-Atayde, A. R., McKenna, W. J., Sparks, E. A., Kanter, R. J., McGarry, K., Seidman, J. G., and Seidman, C. E. (2002). Constitutively active AMP kinase mutations cause glycogen storage disease mimicking hypertrophic cardiomyopathy. J. Clin. Invest. 109, 357-362.

Applewhite, D. A., Barzik, M., Kojima, S., Svitkina, T. M., Gertler, F. B., and Borisy, G. G. (2007). Ena/VASP proteins have an anti-capping independent function in filopodia formation. Mol. Biol. Cell 18, 2579-2591.

Aszodi, A., Pfeifer, A., Ahmad, M., Glauner, M., Zhou, X.-H., Ny, L., Andersson, K.-E., Kehrel, B., Offermanns, S., and Fassler, R. (1999). The vasodilator-stimulated phosphoprotein (VASP) is involved in cGMP- and cAMP-mediated inhibition of agonist-induced platelet aggregation, but is dispensable for smooth muscle function. EMBO J. 18, 37-48.

Bachmann, C., Fischer, L., Walter, U., and Reinhard, M. (1999). The EVH2 domain of the vasodilator-stimulated phosphoprotein mediates tetramerization, F-actin binding, and actin bundle formation. J. Biol. Chem. 274, 23549-23557.

Barzik, M., Kotova, T. I., Higgs, H. N., Hazelwood, L., Hanein, D., Gertler, F. B., and Schafer, D. A. (2005). Ena/VASP proteins enhance actin polymerization in the presence of barbed end capping proteins. J. Biol. Chem. 280, 28653-28662.

Bear, J. E., Loureiro, J. J., Libova, I., Fassler, R., Wehland, J., and Gertler, F. B. (2000). Negative regulation of fibroblast motility by Ena/VASP proteins. Cell 101, 717-728.

Bear, J. E., Svitkina, T. M., Krause, M., Schafer, D. A., Loureiro, J. J., Strasser, G. A., Maly, I. V., Chaga, O. Y., Cooper, J. A., Borisy, G. G., and Gertler, F. B. (2002). Antagonism between Ena/VASP proteins and actin filament capping regulates fibroblast motility. Cell 109, 509-521.

Benz, P. M., Blume, C., Moebius, J., Oschatz, C., Schuh, K., Sickmann, A., Walter, U., Feller, S.M., and Renné, T. (2008). Cytoskeleton assembly at endothelial cell-cell contacts is regulated by αII-spectrin-VASP complexes. J. Cell Biol. 180, 205-219.

Brownlee, M. (2001). Biochemistry and molecular cell biology of diabetic complications. Nature 414, 813-820.

Butt, E., Abel, K., Krieger, M., Palm, D., Hoppe, V., Hoppe, J., and Walter, U. (1994). cAMP- and cGMP-dependent protein kinase phosphorylation sites of the focal adhesion vasodilator-stimulated phosphoprotein (VASP) *in vitro* and in intact human platelets. J. Biol. Chem. 269, 14509-14517.

Carling, D. (2004). The AMP-activated protein kinase cascade--a unifying system for energy control. Trends Biochem. Sci. 29, 18-24.

Carling, D., and Hardie, D. G. (1989). The substrate and sequence specificity of the AMP-activated protein kinase. Phosphorylation of glycogen synthase and phosphorylase kinase. Biochim. Biophys. Acta 1012, 81-86.

Chen, L., Daum, G., Chitaley, K., Coats, S. A., Bowen-Pope, D. F., Eigenthaler, M., Thumati, N. R., Walter, U., and Clowes, A. W. (2004). Vasodilator-stimulated phosphoprotein regulates proliferation and growth inhibition by nitric oxide in vascular smooth muscle cells. Arterioscler. Thromb. Vasc. Biol. 24, 1403-1408.

Chen, M. B., McAinch, A. J., Macaulay, S. L., Castelli, L. A., O'Brien P. E., Dixon, J. B., Cameron-Smith, D., Kemp, B. E., and Steinberg, G. R. (2005). Impaired activation of AMP-kinase and fatty acid oxidation by globular adiponectin in cultured human skeletal muscle of obese type 2 diabetics. J. Clin. Endocrinol. Metab. 90, 3665-3672.

Chen, Z., Pheng, I., Sun, W., Su, M., Hsu, P., Fu, Y., Zhu, Y., DeFea, K., Pan, S., Tsai, M., Shyy, J. Y. (2009). AMP-activated protein kinase functionally phosphorylates endothelial nitric oxide synthase Ser633. Circ. Res. 104, 1-10.

Chereau, D., and Dominguez R. (2006). Understanding the role of the G-actin-binding domain of Ena/VASP in actin assembley. J. Struct. Biol. 155, 195-201.

Chitaley, K., Chen, L., Galler, A., Walter, U., Daum, G., and Clowes, A. W. (2004). Vasodilator-stimulated phosphoprotein is a substrate for protein kinase C. FEBS Lett. 556, 211-215.

Comer, A. R., Ahern-Djamali, S. M., Juang, J. L., Jackson, P. D., and Hoffmann, F. M. (1998). Phosphorylation of Enabled by the Drosophila Abelson tryosine kinase regulated

the *in vivo* function and protein-protein interactions of Enabled. Mol. Cell Biol. 18, 152-160

Comerford, K. M., Lawrence, D. W., Synnestvedt, K., Levi, B. P., and Colgan, S. P. (2002). Role of vasodilator-stimulated phosphoprotein in PKA-induced changes in endothelial junctional permeability. FASEB J. 16, 583-585.

Cooper, D. M. F. (2005). Compartmentalization of adenylate cyclase and cAMP signalling. Biochem. Soc. Trans. 33, 1319-1322.

da Silva Xavier, G., Leclerc, I., Salt, I. P., Doiron, B., Hardie, D. G., Kahn, A., and Rutter, G. A. (2000). Role of AMP-activated protein kinase in the regulation by glucose of islet beta cell gene expression. Proc. Natl. Acad. Sci. U S A 97, 4023-4028.

Davies, S. P., Carling, D., and Hardie, D. G. (1989). Tissue distribution of the AMP-activated protein kinase, and lack of activation by cyclic-AMP-dependent protein kinase, studied using a specific and sensitive peptide assay. Eur. J. Biochem. 186, 123-128.

Davis, B. J., Xie, Z., Viollet, B., and Zou, M. H. (2006). Activation of the AMP-activated kinase by antidiabetes drug metformin stimulates nitric oxide synthesis *in vivo* by promoting the association of heat shock protein 90 and endothelial nitric oxide synthase. Diabetes 55, 496-505.

Dent, E. W., Kwiatkowski, A. V., Mebane, L. M., Philippar, U., Barzik, M., Rubinson, D. A., Gupton, S., van Veen, J. E., Furman. C., Zhang, J., Alberts, A. S., Mori, S., and Gertler, F. B. (2007). Filopodia are required for cortial neurite initiation. Nat. Cell Biol. 9, 1347-1359.

Dephoure, N., Zhou, C., Villen, J., Beausoleil, S. A., Bakalarski, C. E., Elledge, A. J., and Gypi, S. P. (2008). A quantitative atlas of mitotic phosphorylation. Proc. Natl. Acad. Sci. U S A 105, 10762-10767.

Disanza, A., Steffen, A., Hertzog, M., Frittoli, E.,. Rottner, K., and Scita, G. (2005). Actin polymerization machinery: the finish line of signaling networks, the starting piont of cellular movement. Cell Mol. Life Sci. 62, 955-970.

Drees, B. E., Andrews, K. M., and Beckerle, M. C. (1999). Molecular dissection of Zyxin function reveals ist involvement in cell motility. J. Cell Biol. 147, 1549-1559.

Engel, K., Schultz, H., Martin, F., Kotlyarov, A., Plath, K., Hahn, M., Heinemann, U., and Gaestel, M. (1995). Constitutive activation of mitogen-activated protein kinase-activated protein kinase 2 by mutation of phosphorylation sites and an A-helix motif. J. Biol. Chem. 270, 27213-27221.

Ermekova, K. S., Zambrano, N., Linn, H., Minopoli, G., Gertler, F., Russo, T., and Sudol, M. (1997). The WW domain of neuronal protein FE65 interacts with proline-rich motifs in Mena, the mammalian homolog of Drosophila Enabled. J. Biol. Chem. 272, 32869-32877.

Ferron, F., Rebowski, G., Lee, S. H., and Dominguez, R. (2007). Structual basis for the recruitment of profilin-actin complexes during filament elongation by Ena/VASP. EMBO J. 26, 4597-4606.

Foretz, M., Ancellin, N., Andreelli, F., Saintillan, Y., Grondin, P., Kahn, A., Thorens, B., Vaulont, S., and Viollet, B. (2005). Short-term overexpression of a constitutively active form of AMP-activated protein kinase in the liver leads to mild hypoglycemia and fatty liver. Diabetes 54, 1331-1339.

Furman, C., Sieminski, A. L., Kwiatkowski, A. V., Rubinson, D., Vasile, E., Bronson, R. T., Fassler, R., and Gertler, F. B. (2007). Ena/VASP is required for endothelial barrier function in vivo. J. Cell Biol. 179, 761-765.

Fradelizi, J., Noireaux, V., Plastino, J., Menichi, B., Louvard, D., Sykes, C., Golsteyn, R. M., and Friederich, E. (2001). ActA and human zyxin habour Arp2/3-independent actin-polymerization activity. Nature Cell Biol. 3, 699-707.

Frank, R. N. (2004). Diabetic retinopathy. N. Engl. J. Med. 350, 48-58.

Fryer, B. H., Wang, C., Vedantam, S., Zhou, G-L., Jin, S., Fletcher, L., Simon, M. C., and Field, J. (2006). cGMP-dependent protein kinase phosphorylates p21-activated kinase (Pak1), inhibiting Pak/Nck binding and stimulating Pak/vasodilator-stimulated phosphoprotein association. J. Biol. Chem. 281, 11487-11495.

Gambaryan, S., Hauser, W., Kobsar, A., Glazova, M., Walter, U. (2001). Distribution, cellular localization, and postnatal development of VASP and Mena expression in mouse tissues. Histochem. Cell Biol. 116, 535-543.

Gertler, F. B., Niebuhr, K., Reinhard, M., Wehland, J., and Soriano, P. (1996). Mena, a

relative of VASP and Drosophila Enabled, is implicated in the control of microfilament dynamics. Cell 87, 227-239.

Golenhofen, N., Ness, W., Wawrousek, E. F., and Drenckhahn, D. (2002). Expression and induction of the stress protein alpha-B-crystallin in vascular endothelial cells. Histochem. Cell Biol. 117, 203-209.

Gourlay, C. W., and Ayscough, K. R. (2005). The actin cytoskeleton: a key regulator of apoptosis and ageing. Nature Rev. Mol. Cell Biol. 6, 583-589.

Grosse, R., Copeland, J. W., Newsome, T. P., Way, M., and Treisman, R. (2003). A role for VASP in RhoA-Diaphanous signalling to actin dynamics and SRF activity. EMBO J. 22, 3050-3061.

Gu, Y. M., Jin, Y. H., Choi, J. K., Baek, K. H., Yeo, C. Y., and Lee, K. Y. (2006). Protein kinase A phosphorylates and regulates dimerization of 14-3-3 epsilon. FEBS Let. 580, 305-310.

Halbrugge, M., Friedrich, C., Eigenthaler, M., Schanzenbacher, P., and Walter, U. (1990). Stoichiometric and reversible phosphorylation of a 46-kDa protein in human platelets in response to cGMP- and cAMP-elevating vasodilators. J. Biol. Chem. 265, 3088-3093.

Han, Y. H., Chung, C. Y., Wessels, D., Stephens, S., Titus, M. A., Soll, D. R., and Firtel, R. A. (2002). Requirement of a vasodilator-stimulated phosphoprotein family member for cell adhesion, the formation of filopodia, and chemotaxis in dictyostelium. J. Biol. Chem. 277, 49877-49887.

Harbeck, B., Huttelmaier, S., Schluter, K., Jockusch, B. M., and Illenberger, S. (2000). Phosphorylation of the vasodilator-stimulated phosphoprotein regulates its interaction with actin. J. Biol. Chem. 275, 30817-30825.

Hardie, D. G. (2003). Minireview: the AMP-activated protein kinase cascade: the key sensor of cellular energy status. Endocrinology 144, 5179-5183.

Hardie, D. G. (2004). The AMP-activated protein kinase pathway--new players upstream and downstream. J. Cell. Sci. 117, 5479-5487.

Hasegawa, Y., Murph, M., Yu, S., Tigyi, G., and Mills, G. B. (2008). Lysophosphatidic acid (LPA)-induced vasodilator-stimulated phosphoprotein mediates lamellipodia formation

to initiate motility in PC-3 prostate cancer cells. Mol. Oncol. 2, 54-69.

Hauser, W., Knobeloch, K. P., Eigenthaler, M., Gambaryan, S., Krenn, V., Geiger, J., Glazova, M., Rohe, E., Horak, I., and Walter, U. (1999). Megakaryocyte hyperplasia and enhanced agonist-induced platelet activation in vasodilator-stimulated phosphoprotein knockout mice. Proc. Natl. Acad. Sci. U S A 96, 8120-8125.

Hernández, S. E., Krishnaswami, M., Miller, A. L., and Koleske, A. J. (2004). How do Abl family regulate cell shape and movement. Trends Cell Biol. 14, 36-44.

Hoffman, L. M., Jensen, C. C., Kloeker, S., Wang, C. L., Yoshigi, M., and Beckerle, M. C. (2006). Genetic ablation of zyxin causes Mena/VASP mislocalization, increased motility, and deficits in actin remodeling. J. Cell Biol. 172, 771-782.

Holt, M. R., Critchley, D. R., and Brindle, N. P. J. (1998). The focal adhesion phosphoprotein VASP. Int. J. Biochem. Cell Biol. 30, 307-311.

Hong, S. P., Momcilovic, M., and Carlson, M. (2005). Function of mammalian LKB1 and Ca2+/calmodulin-dependent protein kinase kinase alpha as Snf1-activating kinases in yeast. J. Biol. Chem. 280, 21804-21809.

Horstrup, K., Jablonka, B., Honig-Liedl, P., Just, M., Kochsiek, K., and Walter, U. (1994). Phosphorylation of focal adhesion vasodilator-stimulated phosphoprotein at Ser157 in intact human platelets correlates with fibrinogen receptor inhibition. Eur. J. Biochem. 225, 21-27.

Howe, A. K., Hogan, B. P., and Juliano, R. L. (2002). Regulation of vasodilator-stimulated phosphoprotein phosphorylation and interaction with Abl by protein kinase A and cell adhesion. J. Biol. Chem. 277, 38121-38126.

Howe, A. K., Baldor, L. C., and Hogan, B. P. (2005). Spatial regulation of the cAMP-dependent protein kinase during chemotactic cell migration. Proc. Natl. Acad. Sci. U S A 102, 14320-14325.

Hurley, R. L., Anderson, K. A., Franzone, J. M., Kemp, B. E., Means, A. R., and Witters, L. A. (2005). The Ca2+/calmodulin-dependent protein kinase kinases are AMP-activated protein kinase kinases. J. Biol. Chem. 280, 29060-29066.

Huttelmaier, S., Harbeck, B., Steffens, O., Messerschmidt, T., Illenberger, S., and Jockusch,

B. M. (1999). Characterization of the actin binding properties of the vasodilator-stimulated phosphoprotein VASP. FEBS Lett. 451, 68-74.

Hwang, J. T., Lee, M., Jung, S. N., Lee, H. J., Kang, I., Kim, S. S., and Ha, J. (2004). AMP-activated protein kinase activity is required for vanadate-induced hypoxia-inducible factor 1alpha expression in DU145 cells. Carcinogenesis 25, 2497-2507.

Kahn, B. B., Alquier, T., Carling, D., and Hardie, D. G. (2005). AMP-activated protein kinase: ancient energy gauge provides clues to modern understanding of metabolism. Cell Metab. 1, 15-25.

Kemp, B. E., Stapleton, D., Campbell, D. J., Chen, Z. P., Murthy, S., Walter, M., Gupta, A., Adams, J. J., Katsis, F., van Denderen, B., et al. (2003). AMP-activated protein kinase, super metabolic regulator. Biochem. Soc. Trans. 31, 162-168.

Kim, J., Ahn, J., Kim, J., Yu, Y., Kim, H., Ha, J., Shinn, S., and Oh, Y. (2007). Fenofibrate regulates retinal endothelial cell survival through the AMPK signal transduction pathway. Exp. Eye Res. 84, 886-893.

Kohler, K., Louvard, D., and Zahraoui, A. (2004). Rab13 regulates PKA signaling during tight junction assembly. J. Cell Biol. 165, 175-180.

Krause, M., Dent, E. W., Bear, J. E., Loureiro, J. J., and Gertler, F. B. (2003). Ena/VASP proteins: regulators of the actin cytoskeleton and cell migration. Annu. Rev. Cell Dev. Biol. 19, 541-564.

Krause, M., Leslie, J. D., Stewart, M., Lafuente, E. M., Valderrama, F., Jagannathan, R., Strasser, G. A., Rubinson, D. A., Liu, H., Way, M., et al. (2004). Lamellipodin, an Ena/VASP ligand, is implicated in the regulation of lamellipodial dynamics. Dev. Cell 7, 571-583.

Kuhnel, K., Jarchau, T., Wolf, E., Schlichting, I., Walter, U., Wittinghofer, A., and Strelkov, S. V. (2004). The VASP tetramerization domain is a right-handed coiled coil based on a 15-residue repeat. Proc. Natl. Acad. Sci. U S A , 17027-17032.

Kwiatkowski, A. V., Gertler, F. B., and Loureiro, J.J. (2003). Function and regulation of Ena/VASP proteins. Trends Cell Biol. 13 (7), 386-392.

Kwiatkowski, A. V., Rubinson, D. A., Dent, E. W., van Veen, J. E., Leslie, J. D., Zhang, J.,

Mebane, L. M., Pinheiro, E. M., Burds, A. A., Bronson, R. T., Mori, S., Fassler, R., and Gertler, F. B. (2007). Ena/VASP is required for neuritogenesis in the developing cortex. Neuron 56, 441-455.

Lage, R., Dieguez, C., Vidal-Puig, A., and Lopez, M. (2008). AMPK: a metabolic gauge regulating whole-body energy homeostasis. Trends Mol. Med. 14, 539-549.

Laurent, V., Loisel, T., Harbeck, B., Wehman, A., Grobe, L., Jockusch, B. M., Wehland, J., Gertler, F. B., and Carlier M.-F. (1999). Role of proteins of the Ena/VASP family in actin-based motility of Listeria monocytogenes. J. Cell Biol. 144, 1245-1258.

Lindsay, S. L., Ramsey, S., Aitchison, M., Renné, T., and Evans, T. J. (2007). Modulation of lamellipodial structure and dynamics by NO-dependent phosphorylation of VASP Ser239. J. Cell Sci. 120, 3011-3021.

Lodish, H., Berk, A., Zipursky, S. L., Matsudaira, P., Baltimore, D., and Darnell, J. (2000). Molecular Cell Biology, 4th Ed., W. H. Freeman and Company, NY.

Loureiro, J. J., Rubinson, D. A., Bear, J. E., Baltus, G. A., Kwiatkowski, A. V., and Gertler, F. B. (2002). Critical roles of phosphorylation and actin binding motifs, but not the central proline-rich region, for Ena/vasodilator-stimulated phosphoprotein (VASP) function during cell migration. Mol. Biol. Cell 13, 2533-2546.

Markert, T., Vaandrager, A. B., Gambaryan, S., Pohler, D., Hausler, C., Walter, U., De Jonge, H. R., Jarchau, T., and Lohmann, S. M. (1995). Endogenous expression of type II cGMP-dependent protein kinase mRNA and protein in rat intestine. Implications for cystic fibrosis transmembrane conductance regulator. J. Clin. Invest. 96, 822-830.

Marsin, A. S., Bouzin, C., Bertrand, L., and Hue, L. (2002). The stimulation of glycolysis by hypoxia in activated monocytes is mediated by AMP-activated protein kinase and inducible 6-phosphofructo-2-kinase. J. Biol. Chem. 277, 30778-30783.

Martin, K. H., Jeffery, E. D., Grigera, P. R., Shabanowitz, J., Hunt, D. F. and Parsons, J. T. (2006). Cortactin phosphorylation sites mapped by mass spectrometry. J. Cell Sci. 119, 2851-2853.

Massberg, S., Grüner, S., Konrad, I., Garcia Arguinzonis, M. I., Eigenthaler, M., Hemler, K., Kersting, J., Schulz, C., Muller, I., Besta, F., et al. (2004). Enhanced *in vivo* platelet

adhesion in vasodilator-stimulated phosphoprotein (VASP)-deficient mice. Blood 103, 136-142.

Menzies, A. S., Aszodi, A., Williams, S. E., Pfeifer, A., Wehmann, A. M., Goh, K. L., Mason, C. A., Fassler, R., and Gertler, F. B.(2004). Mena and Vasodilator-stimulated phosphoprotein are required for multiple actin-dependent processes that shape the vertebrate nervous system. J. Neuosci. 24, 8029-8038.

Minokoshi, Y., Alquier, T., Furukawa, N., Kim, Y. B., Lee, A., Xue, B., Mu, J., Foufelle, F., Ferre, P., Birnbaum, M. J., et al. (2004). AMP-kinase regulates food intake by responding to hormonal and nutrient signals in the hypothalamus. Nature 428, 569-574.

Minokoshi, Y., Kim, Y. B., Peroni, O. D., Fryer, L. G., Muller, C., Carling, D., and Kahn, B. B. (2002). Leptin stimulates fatty-acid oxidation by activating AMP-activated protein kinase. Nature 415, 339-343.

Mulsch, A., Oelze, M., Kloss, S., Mollnau, H., Topfer, A., Smolenski, A., Walter, U., Stasch, J. P., Warnholtz, A., Hink, U., et al. (2001). Effects of *in vivo* nitroglycerin treatment on activity and expression of the guanylyl cyclase and cGMP-dependent protein kinase and their downstream target vasodilator-stimulated phosphoprotein in aorta. Circulation 103, 2188-2194.

Munzel, T., Feil, R., Mulsch, A., Lohmann, S. M., Hofmann, F., and Walter, U. (2003). Physiology and Pathophysiology of vascular signaling controlled by cyclic guanosine 3´,5´-cyclic monophosphate-dependent protein kinase. Circulation 108, 2172-2183.

Munzel, T., Daiber, A., Ullrich, V., and Mulsch, A. (2005). Vascular consequences of endothelial nitric oxide synthase uncoupling for the activity and expression of the soluble guanylyl cyclase and the cGMP-dependent protein kinase. Arterioscler. Thromb. Vasc. Biol. 25, 1551-1557.

Oelze, M., Mollau, H., Hoffmann, N., Warnholtz, A., Bodenschatz, M., Smolenski, A., Walter, U., Skatchkov, M., Meinertz, T., and Munzel, T. (2000). Vasodilator-stimulated phosphoprotein serine 239 phosphorylation as a sensitive monitor of defective nitric oxide/cGMP signaling and endothelial dysfunction. Cir. Res. 87, 999-1005.

Oltman, C. L., Richou, C. L., Davidson, E. P., Coppey, L. J., Lund, D. D., and Yorek, M. A. (2006). Progression of coronary and mesenteric vascular dysfunction in Zucker Obese

and Zucker Diabetic Fatty rats. Am. J. Physiol. Heart Circ. Physiol. 291 (4), 1780-1787.

Parker, P. J., and Murray-Rust, J. (2004). PKC at a glance. J. Cell Sci. 117, 131-132.

Pasic, L., Kotova, T., and Schafer, D. A. (2008). Ena/VASP proteins capture actin filament barbed ends. J. Biol. Chem. 283, 9814-9819.

Profirovic, J., Gorovoy, M., Niu, J., Pavlovic, S., and Voyno-Yasenetskaya, T. (2005). A novel mechanism of G protein-dependent phosphorylation of vasodilator-stimulated phosphoprotein. J. Biol. Chem. 280, 32866-32876.

Ramaekers, F. C. S., and Bosman, F. T. (2004). The cytoskeleton and desease. J. Pathol. 204, 351-354.

Reinhard, M., Halbrugge, M., Scheer, U., Wiegand, C., Jockusch, B. M., and Walter, U. (1992). The 46/50 kDa phosphoprotein VASP purified from human platelets is a novel protein associated with actin filaments and focal contacts. EMBO J. 11, 2063-2070.

Reinhard, M., Giehl, K., Abel, K., Haffner, C., Jarchau, T., Hoppe, V., Jockusch, B. M., and Walter, U. (1995). The proline-rich focal adhesion and microfilament protein VASP is a ligand for profilins. EMBO J. 14, 1583-1589.

Reinhard, M., Jarchau, T., and Walter, U. (2001). Actin-based motility: stop and go with Ena/VASP proteins. Trends Biochem. Sci. 26, 243-249.

Renne, T., Schuh, K., and Muller-Esterl, W. (2005). Local bradykinin formation is controlled by glycosaminoglycans. J. Immunol. 175, 3377-3385.

Rikova, K., Gou, A., Zeng, Q., Possemato, A., Yu, J., Haack, H., Nardone, J., Lee, K., Reeves, C., Li, Y., Hu, Y., Tan, Z., Stokes, M., Sullivan, L., Mitchell, J., Wetzel, R., MacNeill, J., Ren, J. M., Yuan, J., Bakalarski, C. E., Villen, J., Kornhauser, J. M., Smith, B., Li, D., Zhou, X., Gygi, S. P., Gu, T., Polakeiwicz, R. D., Rush, J., and Comb, M. J. (2007). Global survey of phosphotyrosine signaling identifies oncogenic kinases in lung cancer. Cell 131, 1190-1203.

Rottner, K., Behrendt, B., Small, J. V., and Wehland, J. (1999). VASP dynamics during lamellipodia protrusion. Nat. Cell Biol. 1, 321-322.

Ruderman, N., and Prentki, M. (2004). AMP kinase and malonyl-CoA: targets for therapy of the metabolic syndrome. Nat. Rev. Drug Discov. 3, 340-351.

Sandberg, M., Natarajan, V., Ronander, I., Kalderon, D., Walter, U., Lohmann, S. M., and Jahnsen, T. (1989). Molecular cloning and predicted full-length amino acid sequence of the type I beta isozyme of cGMP-dependent protein kinase from human placenta. Tissue distribution and developmental changes in rat. FEBS Lett. 255, 321-329.

Schafer, S., Steioff, K., Linz, W., Bleich, M., Busch, A. E., and Lohn, M. (2004). Chronic vasopeptidase inhibition normalizes diabetic endothelial dysfunction. Eur. J. Pharmacol. 484, 361-362.

Schirenbeck, A., Arasada, R., Bretschneider, T., Stradal, T. E. B., Schleicher, M., and Faix J. (2006). The bundling activity of vasodilator-stimulated phosphoprotein is required for filopodium formation. Proc. Natl. Acad. Sci. U S A 103, 7694-7699.

Schlegel, N., Burger, S., Golenhofen, N., Walter, U., Drenckhahn, D., Waschke, J. (2008). The role of VASP in regulation of cAMP- and Rac 1-mediated endothelial barrier stabilization. Am. J. Physiol. Cell Physiol. 294, C178-C188.

Schmidt, H. H., and Walter, U. (1994). NO at work. Cell 78, 919-925.

Schulz, E., Tsilimingas, N., Rinze, R., Reiter, B., Wendt, M., Oelze, M., Woelken-Weckmüller, S., Walter, U., Reichenpurner, H., Meinertz, M., and Munzel, T. (2002). Functional and biochemical analysis of endothelial (dys)function and NO/cGMP signaling in human blood vessels with and without nitroglycerin pretreatment. Circulation 105, 1170-1175.

Sechi, A. S., and Wehland, J. (2004). ENA/VASP proteins: multifunctional regulators of actin cytoskeleton dynamics. Front. Biosci. 9, 1294-1310.

Skoble, J., Auerbuch, V., Goley, E. D., Welch, M. D., and Portnoy, D. A. (2001). Pivotal role of VASP in Arp2/3 complex-mediated actin nucleation, actin branch-formation, and Listeria monocytogenes motility. J. Cell Biol. 155, 89-100.

Smolenski, A., Bachmann, C., Reinhard, K., Honig-Liedl, P., Jarchau, T., Hoschuetzky, H., and Walter, U. (1998). Analysis and regulation of vasodilator-stimulated phosphoprotein serine 239 phosphorylation *in vitro* and in intact cells using a phosphospecific monoclonal antibody. J. Biol. Chem. 273, 20029-20035.

Smolenski, A., Poller, W., Walter, U., and Lohmann, S. M. (2000). Regulation of human endothelial cell focal adhesion sites and migration by cGMP-dependent protein kinase I. J. Biol. Chem. 275, 25723-25732.

Stein, S. C., Woods, A., Jones, N. A., Davison, M. D., and Carling, D. (2000). The regulation of AMP-activated protein kinase by phosphorylation. Biochem. J. 345 Pt 3, 437-443.

Tani, K., Sato, S., Sukezane, T., Kojima, H., Hirose, H., Hanafusa, H., and Shishido, T. (2003). Abl interator 1 promotes tyrosine 296 phosphorylation of mammalian enabled (Mena) by c-Abl kinase. J. Biol. Chem. 278, 21685-21692.

Trautwein, C., Caelles, C., van der Gerr, P., Hunter, T., Karin, M., and Chojkier, M. (1993). Transactivation by NF-IL6/LAP is enhanced by phosphorylation of its activation domain. Nature 364, 544-547.

Trichet, L., Sykes, C., and Plastino, J. (2008). Relaxing the actin cytoskeleton for adhesion and movement with Ena/VASP. J. Cell Biol. 181, 19-25.

Unger, R. H., and Orci, L. (2001). Diseases of liporegulation: new perspective on obesity and related disorders. FASEB J. 15, 312-321.

Vitriol, E. A., Uetrecht, A. C., Shen, F., Jacobson, K., and Bear, J. E. (2007). Enhanced EGFP-chromophore-assisted laser inactivation using deficient cells rescued with functional EGFP-fusion proteins. Proc. Natl. Acad. Sci. U S A 104, 6702-6707.

Walders-Harbeck, B., Khaitlina, S. Y., Hinssen, H., Jockusch, B. M., and Illenberger, S. (2002). The vasodilator-stimulated phosphoprotein promotes actin polymerisation through direct binding to monomeric actin. FEBS Lett. 529, 275-280.

Wang, M. Y., and Unger, R. H. (2005). Role of PP2C in cardiac lipid accumulation in obese rodents and its prevention by troglitazone. Am. J. Physiol. Endocrinol. Metab. 288, E216-221.

Wentworth, J. K., Pula, G., and Poole, A. W. (2006). Vasodilator-stimulated phosphoprotein (VASP) is phosphorylated on Ser157 by protein kinase C-dependent and -independent mechanisms in thrombin-stimulated human platelets. Biochem. J. 393, 555-564.

Willoughby, D., Wong, W., Schaack, J., Scott, J. D., and Cooper D. M. F. (2006). An anchored PKA and PDE4 complex regulates subplasmalemmal cAMP dynamics. EMBO

J. 25, 2051-2061.

Winder, S. J., and Ayscough K. R. (2005). Actin-binding proteins. J. Cell Sci. 118, 651-654.

Winder, W. W., and Hardie, D. G. (1999). AMP-activated protein kinase, a metabolic master switch: possible roles in type 2 diabetes. Am. J. Physiol. 277, E1-10.

Wong, W., and Scott, J. D. (2004). AKAP signalling complexes: focal points in space and time. Nature Rev. Mol. Cell Biol. 5, 959-970.

Woods, A., Dickerson, K., Heath, R., Hong, S. P., Momcilovic, M., Johnstone, S. R., Carlson, M., and Carling, D. (2005). Ca2+/calmodulin-dependent protein kinase kinase-beta acts upstream of AMP-activated protein kinase in mammalian cells. Cell Metab. 2, 21-33.

Yu, P. K., Yu, D. Y., Cringle, S. J., and Su, E. N. (2005). Endothelial F-actin cytoskeleton in the retinal vasculature of normal and diabetic rats. Curr. Eye Res. 30, 279-290.

Zahedi, R. P., Lewandrowski, U., Wiesner, J., Wortelkamp, S., Moebius, J., Schutz, C., Walter, U., Gambaryan, S., and Sickmann, A. (2008). Phosphoproteome of resting human platelets. J. Proteome Res. 7, 526-534.

Zhang, Y., Tu, Y., Gkretsi, V., and Wu, C. (2006). Migfilin interacts with vasodilator-stimulated phosphoprotein (VASP) and regulates VASP localization to cell-matrix adhesions and migration. J. Biol. Chem. 281, 12397-12407.

Zhang, X., Yuan, Z., Zhang, Y., Yong, S., salas-Burgos, A., Koomen, J., Olashaw, N., Parsons, J. T., Yang, X., Dent, S. R., Yao, T., Lane, W. S., and Seto, E. (2007). HDAC6 modulates cell motility by altering the acetylation level of cortactin. Mol. Cell 27, 197-213.

Zhou, G., Myers, R., Li, Y., Chen, Y., Shen, X., Fenyk-Melody, J., Wu, M., Ventre, J., Doebber, T., Fujii, N., et al. (2001). Role of AMP-activated protein kinase in mechanism of metformin action. J. Clin. Invest. 108, 1167-1174.

Zhuang, S., Nguyen, G. T., Chen, Y., Gudi, T., Eigenthaler, M., Jarchau, T., Walter, U., Boss, G. R., and Pilz, R. B. (2004). Vasodilator-stimulated phosphoprotein activation of serum-response element-dependent transcription occurs downstream of RhoA and is inhibited

by cGMP-dependent protein kinase phosphorylation. J. Biol. Chem. 279, 10397-10407.

Zou, M., Kirkpatrick, S. S., Davis, B. J., nelson, J. S., Wiles, W. G., Schlattner, U., Neumann, D., Brownlee, M., Freeman, M. B., and Goldman, M. H. (2004). Activation of the AMP-activated protein kinase by the anti-diabetic drug metformin in vivo. J. Biol. Chem. 279, 43940-43951.

Zou, M., and Wu, Y. (2008). AMP-activated protein kinase activation as a strategy for protecting vascular endothelial function. Clin. Exp. Pharmacol. Physiol. 35, 535-545.

8 Abbreviations

Abl	Abelson tyrosine kinase
AC	adenylate cyclase
ACC	acetyl coenzym A carboxylase
AMP	Adenosine monophosphate
AMPK	AMP-activated protein kinase
AKAP	A-kinase anchoring protein
Akt	protein kinase B
ATP	Adenosine triphosphate
CA	constitutively active
cAMP	cyclic adenosine-3´,5´-monophosphate
CI	catalytically inactive
cDNA	coding DNA
cGMP	cyclic guanosine-3´,5´-monophosphate
CNBr	cyanogen bromide
DN	dominant negative
DMEM	Dulbecco´s modified eagle´s medium
DTT	Dithiotreitol
E.coli	*Escherichia coli*
ECV304	endothelial cell line, originated from human umbilical vein endothelium
EDTA	Ethylendiamine tetraacetic acid
EGFP	enhanced green fuorescent protein
Ena	Enabled
eNOS	endothelial nitric oxide synthase
EVH1	Ena/vasodilator-stimulated phosphoprotein homology domain 1
EVH2	Ena/vasodilator-stimulated phosphoprotein homology domain 2
Evl	Ena/vasodilator-stimulated phosphoprotein like protein
FACS	fluorescence activated cell sorting
F-actin	filamentous actin
Fig	figure
G-actin	monomeric actin
GAPDH	glyceraldehyde-3-phosphate dehydrogenase
HEK293	human embryonic kidney cells

HeLa	human cervical cancer cells from Henrietta Lacks
HUVEC	human umbilical vein endothelial cells
mAC	membrane-associated adenylate cyclase
Mena	mammalian Ena
NO	nitric oxide
pACC	acetyl coenzyme A carboxylase phosphorylated at T172
PAGE	polyacrylamid gel electrophoresis
PBS	phosphate-buffered saline
PDE	phosphodiesterase
PKA	cAMP-dependent protein kinase
PKB	protein kinase B (also named Akt)
PKC	protein kinase C
PKG	cGMP-dependent protein kinase
PP2B	protein phosphatase 2 B
PPR	poly-proline region
ROS	reactive oxygen species
SD	standard deviation
SDS	Sodiumdodecylsulfate
SH3	Src homology 3 domain
SRE	serum response element
SRF	serum response factor
VASP	vasodilator-stimulated phosphoprotein
w/o	without
wt	wild-type
ZDF	Zucker diabetic fatty

9 Acknowledgments

Firstly, I would like to express my gratitude to Prof. Dr. Ulrich Walter for giving me the opportunity to do my PhD work at his institute. Thank you for always having time to listen to me and for your support in all critical situations.

Furthermore, I thank Prof. Dr. Dr. h.c. Roland Benz for taking the time and being so kind to examine this work as the second examiner.

With hindsight, I underestimated the value of scientific discussion and I would like to have spent more time on them. It was a temptation for me to get stuck in details and to be driven by time pressure.

Special thanks go to Prof. Dr. Dr. Thomas Renné who has coordinated most of my work. I had the pleasure to be his first PhD-student and to join his DGF junior group from scratch, which gave me the opportunity to actively participate in the build-up process.

I especially thank Prof. Dr. Kai Schuh for his commitment and for always having time to listen. I appreciate all the long discussions, good ideas, helpful advice, and pleasant hours in the lab.

I also acknowledge the Deutsche Forschungsgemeinschaft (DFG) for financial support.

A lot of thanks to all members of the DFG junior group, who were very helpful in discussions and made the work in the lab amusing. Thanks to Felicitas Müller, Melanie Ulrich, Dr. Dr. Karin Bundschu, Dr. Julia Johne, Luci Esterl, Monika Kuhn, Birgitta Schinke, Dr. Peter Benz, and Dr. Marco Schwieder. Special thanks to my colleague Robert Untucht for your support in handling ZDF rats, I could not have done these experiments without you.

Moreover, I thank all the members of the Institute of Clinical Biochemistry and Pathochemistry for the pleasant time together.

I also thank the following members of other research groups: PD Dr. Oliver Ritter, Natalie Burkard, Jenny Muck, Prof. Dr. Johann Bauersachs, PD Dr. Andreas Schäfer, Meike Leutke for their help and the cooperation.

Very special thanks are addressed to Tobias, who was extremely patient with me and accepted and supported my work. Further, I would like to thank all my friends and my family, who always showed interest in my work and tried to motivate and support me.

10 Curriculum Vitae

Personal Information

Name	Constanze Blume
Nationality	German
Marital Status	single
Date of birth	25.12.1976
Place of birth	Leipzig, Germany

Experience

2006/10 - to date	Senior Consultant, Binder Associates in Ulm, Germany
2002/12 - 2006/09	Dissertation "Cellular functions of VASP phosphorylations" at the Institute of Biochemisty and Pathobiochemisty in Würzburg, Germany
2001/11 - 2002/08	Junior Consultant, Cell Consulting in Frankfurt, Germany
2001/05 - 2001/10	Practical term, Cell Consulting in Frankfurt, Germany
2000/12 - 2001/02	Travel guide, Pfiff-Reisen in Les Crosets, Switzerland
1999/03 - 2000/04	Employee of the citizens action committee in Basel, Switzerland

Conferences

2005/06/12-10	2nd International Conference on cGMP in Potsdam, Germany
2005/03/17-15	Frühjahrstagung der DGPT in Mainz, Germany
2003/06/16-14	1st International Conference on cGMP in Leipzig, Germany
1999/09/2-08/28	Gap Junction Conference in Gwatt, Switzerland

Education

2000/10/17	Diploma in Molecular Biology, University of Basel, Switzerland
1999/09 - 2000/05	Diploma thesis "Topography of Gap Junction investigated by atomic force microscope", Supervisor Prof. Andreas Engel
1995/10 - 2000/10	Study of molecular biology at University of Basel, Switzerland
1995/06/21	Diploma from German secondary school qualifying for University admission (Abitur) at Uhlandschule Gymnasium in Leipzig
1983/09 - 1995/06	primary and secondary school, Leipzig

04.05.2009, Gaukönigshofen

11 Publications

Benz, P. M., **Blume, C**., Moebius, J., Oschatz, C., Schuh, K., Sickmann, A., Walter, U., Feller, S.M., and Renne, T. (2008). Cytoskeleton assembly at endothelial cell-cell contacts is regulated by aII-spectrin-VASP complexes. J. Cell Biol. 180, 205-219.

Blume, C., Benz, P. M., Walter, U., Ha, J., Kemp, B. E., and Renne, T. (2007). AMP-activated protein kinase impairs endothelial actin cytoskeleton assembly by phosphorylating vasodilator-stimulated phosphoprotein. J. Biol. Chem. 282, 4601-4612.

Johne, J., **Blume, C**., Benz, P. M., Pozgajova, M., Ullrich, M., Schuh, K., Nieswandt, B., Walter, U., and Renne, T. (2006) Platelets promote coagulation factor XII-mediated proteolytic cascade systems in plasma. Biol. Chem. 387, 173-178.

Benz P. M.*, **Blume, C**.*, Seifert, S., Wilhelm, S., Waschke, J., Schuh, K., Gertler, F., Münzel, T., and Renne, T. Differential Ena/VASP phosphorylation controls actin cytoskeleton remodeling. MS submitted; *equal contribution

Abstracts

a) poster presentation

Blume, C., Schuh, K., Benz, P. M., Walter, U., and Renne, T. (2005). *In vivo* modulation of vasodilator stimulated phosphoprotein functions by phosphorylation. International Conference of cGMP Generators, Effectors and Therapeutic Implications, Potsdam, Germany, June 10-12. 2005. Abstract in BMC Pharmacol. 5 (Suppl 1), P4

b) oral presentation

Blume, C., Schuh, K., Benz, P., Walter, U., and Renne, T. (2005). Differential phosphorylations of the vasodilator stimulated phosphoprotein (VASP) regulate actindynamics and subcellular targeting. 46th Spring meeting of the German Society of Experimental and Clinical Pharmacology and Toxicology, Mainz, Germany, March 15-17 2005. Abstract in Naunyn-Schmiedebergs Archives of Pharmacology. 2005; 371, R50